

University of Alberta

**Synthesis and Characterization of Phosphorylcholine-based Polymers and
Nanogels via the Reversible Addition Fragmentation Chain Transfer Process**

by

Neha Bhuchar

A thesis submitted to the Faculty of Graduate Studies and Research
in partial fulfillment of the requirements for the degree of

Master of Science
in
Chemical Engineering

Department of Chemical and Materials Engineering

©Neha Bhuchar

Fall 2011

Edmonton, Alberta

Permission is hereby granted to the University of Alberta Libraries to reproduce single copies of this thesis and to lend or sell such copies for private, scholarly or scientific research purposes only. Where the thesis is converted to, or otherwise made available in digital form, the University of Alberta will advise potential users of the thesis of these terms.

The author reserves all other publication and other rights in association with the copyright in the thesis and, except as herein before provided, neither the thesis nor any substantial portion thereof may be printed or otherwise reproduced in any material form whatsoever without the author's prior written permission.

Abstract

2-Methacryloyloxyethyl Phosphorylcholine is an interesting biocompatible monomer. An improved method for the synthesis of poly(MPC) and its copolymers using Reversible Addition-Fragmentation chain Transfer (RAFT) has been discussed in the first part of the thesis. Previous reports related to the synthesis of MPC homopolymers and copolymers in aqueous medium are found to be less effective because of the hydrolysis of chain transfer agent in water. Hydrolysis of chain transfer agent results in the loss of active chain ends thereby, reducing control over polymerization and increasing the polydispersity of resulting polymers. Therefore, in this work MPC polymers were synthesized by RAFT using methanol as solvent. This method of synthesis produced polymers having controlled molecular weights as well as narrow polydispersities. Di-block and random copolymers of MPC were also synthesized using cationic monomers like 2-aminoethyl methacrylamide hydrochloride (AEMA) and 2-aminopropyl methacrylamide hydrochloride (APMA) and carbohydrate monomers 2-gluconamidoethyl methacrylamide (GAEMA) and 2-lactobionamidoethyl methacrylamide (LAEMA) in various feed ratios. The polymers obtained were well defined and showed polydispersity values close to one.

In the second part of the work, methoxydiethylene glycol methacrylate (MeODEGM)-MPC based thermo-responsive core-shell nanogels were synthesized for use in protein encapsulation and release. The size of the nanogels was controlled by varying the concentration of cross-linker. The nanogels were synthesized using an acid degradable crosslinker which helped in the release of encapsulated protein

at acidic pH. The effect of various parameters on encapsulation efficiency of proteins was studied and it was found that apart from the size of protein, the cross-linker concentration of nanogel also affected the amount of protein encapsulated. AEMA, which was used as a co-monomer in the core, imparted a cationic charge to the nanogel core and hence helped in the encapsulation of oppositely charged proteins. The study of the release profiles of the nanogels at low pH revealed a controlled release scenario.

Acknowledgement

First and foremost, I would like to thank my supervisor Dr Ravin Narain for giving me the wonderful opportunity to work in his group and for all the time he has invested in guiding me through my research. The experiences I have gained through these opportunities have helped me grow academically and more importantly as a person.

I would also like to express my thanks to our collaborator in Japan, Dr Kazuhiko Ishihara who provided the MPC monomer and helped me in reviewing my manuscript.

I would like to thank my lab mates for their guidance through-out my tenure, Marya, Farah, Chen and Rajesh and especially Zhi Cheng who taught me a lot about the work in this lab. I wish them all best of luck in their future endeavours.

I would like to thank my friends for always being there for me: Jignesh, Shishir, Akila, Dipen, Siddhartha, Nitesh, Vishnu and Abhinav for the wonderful time I have had at the University of Alberta.

Last but not the least, I would like to thank my family for their enormous support and love.

Table of Contents

1	Introduction.....	5
1.1	RAFT polymerization:	5
1.1.1	RAFT mechanism:.....	6
1.1.2	Macro-monomers as RAFT agents:.....	10
1.2	Overview of 2-Methacryloyloxyethyl Phosphorylcholine:.....	12
1.3	Thermo-responsive polymers:.....	14
1.4	References:.....	18
2	Instrumentation.....	23
2.1	Gel Permeation Chromatography (GPC):.....	23
2.1.1	Conventional Calibration:.....	26
2.1.2	Universal Calibration:.....	27
2.1.3	Triple Detection:	30
2.2	Dynamic Light Scattering:.....	32
2.3	References.....	35
3	Detailed Study of the Reversible Addition-Fragmentation Chain Transfer Polymerization and Copolymerization of 2-Methacryloyloxyethyl Phosphorylcholine	36
3.1	Introduction.....	36
3.2	Experimental.....	39
3.2.1	Materials	39
3.2.2	Methods	40
3.2.3	Homopolymerization of 2-Methacryloyloxyethyl Phosphorylcholine ..	

.....	41
3.2.4 Synthesis of Diblock Copolymer with Poly (MPC) Segment:	41
3.2.5 Random Copolymerization of 2-Methacryloyloxyethyl phosphorylcholine:.....	43
3.2.6 Synthesis of poly(MPC- <i>b</i> -AEMA- <i>b</i> -MPC) triblock copolymers:.....	44
3.3 Results and Discussion:.....	45
3.3.1 Detailed Kinetic Studies for the Homopolymerization of 2- Methacryloyloxyethyl phosphorylcholine	45
3.3.2 Self-Chain Extension Experiment of MPC:.....	52
3.3.3 Synthesis of Diblock and Random Copolymers of MPC with other Monomers:	54
3.4 References:	60
4 Degradable Thermoresponsive Nanogels for Protein Encapsulation and Controlled Release	64
4.1 Introduction	64
4.2 Experimental:	68
4.2.1 Materials:	68
4.2.2 Synthesis of 2,2-Dimethacroyloxy-1-ethoxypropane (cross-linker):	69
4.2.3 Synthesis of poly(MPC) macroCTA by RAFT polymerization:.....	70
4.2.4 Synthesis of poly(MPC- <i>b</i> -(MeODEGM- <i>stat</i> -CL- <i>stat</i> -AEMA)) nanogel by RAFT polymerization:	70
4.2.5 Protein Encapsulation:	71
4.2.6 Release of Protein from nanogels at acidic pH:.....	71

4.2.7	Activity of protein:.....	72
4.2.8	Characterizations:	72
4.3	Results and Discussion:.....	74
4.3.1	Synthesis of 2,2-Dimethacroyloxy-1-ethoxypropane (cross-linker):	74
4.3.2	Synthesis of nanogels:	75
4.3.3	Protein Encapsulation:	84
4.3.4	Release Profile:	88
4.4	References:	90
5	Conclusion and Future Work	95
5.1	RAFT polymerization of MPC:	95
5.2	Synthesis of acid degradable and thermo-responsive core-crosslinked nanogels:.....	96
	Future Work.....	97
6	Appendix 1.....	98
7	Appendix 2.....	106

List of Tables

Table 3-1 : Effect of two different chain transfer agents, CTP and CTAm on homopolymerizations of poly(MPC) in two different solvents	46
Table 3-2 : Evolution of molecular weight and low PDI shown as the effect of higher CTP/ACVA ratio of 5:1	52
Table 3-3 : Effect of monomer concentration on the molecular weights and polydispersity of the resulting homopolymer	52
Table 3-4 : Molecular weights and molecular weight distribution of statistical copolymers of MPC. Compositions determined by ¹ H NMR and GPC.....	58
Table 4-1: Comparison of hydrodynamic diameter of MPC- <i>b</i> -(MeODEGM - <i>stat</i> -AEMA- <i>stat</i> -CL) nanogel with varying cross-linker concentrations and MeODEGM-AEMA chain length	81
Table 4-2: Study of protein encapsulation efficiencies for nanogels of varying cross-linker concentration and AEMA content. A) Sample A: 15% cross-linker concentration and 5% AEMA feed ratio B) 15% cross-linker concentration and 25% AEMA feed ratio and C) 20% cross-linker concentration and 10% AEMA feed ratio. Each sample was incubated with proteins (Insulin, BSA and β-Gal) of varying molecular weights	87

List of Figures

Figure 1-1 : Mechanism of Reversible Addition Fragmentation Chain Transfer polymerization technique using thiocarbonylthio-based chain transfer agent [1].....	7
Figure 1-2 : Linear kinetic plot indicating first order reaction kinetics w.r.t monomer	9
Figure 1-3 : Linear increase in molecular weight with conversion [3].....	10
Figure 1-4 : Structure of 2-methacryloyloxyethyl Phosphorylcholine	12
Figure 2-1 : Mechanism of GPC separation [1, 3].....	24
Figure 2-2 : Molecular weight calculation by conventional calibration [1, 3]	27
Figure 2-3 : Universal Calibration Curve [1, 3].....	29
Figure 2-4 : Molecular weight calculation by Universal Calibration Curve [1, 3]..	30
Figure 2-5 : Dynamic Light Scattering for measuring sample size distribution [8 B]	34
Figure 3-1: Structures of the monomers: MPC, GAEMA, LAEMA, AEMA and GAMA; initiator ACVA and Chain Transfer agent CTP	40
Figure 3-2 : Homopolymerization of poly(MPC) by RAFT technique in methanol at 60 °C, using ACVA as the thermally degradable initiator and CTP as the chain transfer agent.....	42

Figure 3-3 : Di-block copolymerization of poly(MPC) macroCTA with GAEMA in water at 70 °C in the presence of ACVA as the initiator.....	43
Figure 3-4 : (A) Shifts in GPC peaks with the RAFT homopolymerization of MPC in methanol, using ACVA as the initiator and CTP as the chain transfer agent at 60 °C with a target DP_n of 63 and $CTP/ACVA = 2$, (B) Semi-logarithmic and conversion plot vs. reaction time for RAFT polymerization of poly(MPC) for the above mentioned reaction conditions and, (C) Evolution of molecular weight of poly(MPC) with conversion, confirming living polymerization.	49
Figure 3-5 : Kinetic plot of the homopolymerization reaction of poly(MPC) in methanol at 70 °C, with varying concentrations and CTP/ACVA ratio: (1) CTP/ACVA=2, (2) CTP/ACVA=2 and (3) CTP/ACVA = 5, and varying concentrations, (1) 1.12 M, (2) 0.85 M, (3) 1.12 M	51
Figure 3-6 : Diblock copolymerization of LAEMA with MPC using sequential monomer addition, forming (A) poly(MPC ₅₄ - <i>b</i> -LAEMA ₆₄) and (B) poly(MPC ₁₈ - <i>b</i> -LAEMA ₁₈).	56
Figure 3-7 : Diblock copolymerization of GAEMA with MPC using sequential monomer addition, forming (A) poly(MPC ₅₄ - <i>b</i> -GAEMA ₅₅) and (B) poly(MPC ₁₈ - <i>b</i> -GAEMA ₁₈).....	57
Figure 3-8 : Triblock copolymerization of AEMA with MPC using sequential monomer addition, forming poly(MPC ₄₂ - <i>b</i> -AEMA ₃₆ - <i>b</i> -MPC ₂₅)	59

Figure 4-1: Structures of monomers (MPC, MeODEGM and AEMA), Chain Transfer Agent (CTP) and initiator (ACVA).....	69
Figure 4-2: Schematic representation of core cross-linked micelles with thermo-responsive and degradable core	76
Figure 4-3: RAFT synthesis of poly(MPC- <i>b</i> -(MeODEGM - <i>stat</i> -AEMA- <i>stat</i> -CL)) core cross-linked with thermo-responsive and degradable core	77
Figure 4-4: Evolution of hydrodynamic diameter of reaction mixture of crosslinking nanogel and variation of size with varying cross-linker (CL) concentration	78
Figure 4-5: TEM images of nanogels showing A), B) nanogels with 25% cross-linker concentration; C), D) more monodispersed nanogel solutions with 10% cross-linker concentration and E), F) nanogels with 15% cross-linker concentration	80
Figure 4-6: Decrease in mass-average hydrodynamic diameter with increase in temperature obtained for 0.5 mg/mL aqueous solution of nanogel, for varying cross-linker (CL) concentration.....	82
Figure 4-7: Normalized ratio of ¹ H NMR signal intensity of MeODEGM protons to D ₂ O protons vs. temperature as observed for the methylene group protons of MeODEGM at 3.4 ppm and D ₂ O.....	83
Figure 4-8: Degradation of 10 and 15% cross-linker concentration nanogel at pH 4.5, 5.4 and 6.2. :1) 10% cross-linker concentration at pH 4.5; 2) 10% cross-linker concentration at pH 5.4; 3) 10% cross-linker concentration at pH 6.2; 4) 15% cross-	

linker concentration at pH 4.5; 5) 15% cross-linker concentration at pH 5.4; 6) 15% cross-linker concentration at pH 6.2 84

Figure 4-9: Cumulative release profile of insulin from nanogel solution of varying cross-linker concentrations: 1) 15% cross-linker concentration at pH 4.8; 2) 20% cross-linker concentration at pH 4.8; 3) 15% cross-linker concentration at pH 6.4 and 4) 20% cross-linker concentration at pH 6.4..... 89

Abbreviations

RAFT: Reversible Addition-Fragmentation chain Transfer Polymerization

ATRP: Atom Transfer Radical Polymerization

GPC: Gel Permeation Chromatography

M_n : Number average molecular weight

M_w : Weight average molecular weight

DLS: Dynamic Light Scattering

NMR: Nuclear Magnetic Resonance

TEM: Transmission Electron Microscopy

MPC: 2-Methacryloyloxyethyl Phosphocholine

AEMA: 2-Aminoethyl methacrylamide hydrochloride

APMA: 2-Aminopropyl methacrylamide hydrochloride

GAEMA: 2-Gluconamidoethyl methacrylamide

LAEMA: 2-Lactobionamidoethyl Methacrylamide

GAMA: D-gluconaminoethyl methacrylate

MeODEGM: Methoxydiethylene glycol methacrylate

CL: 2, 2-Dimethacroyloxy-1-ethoxypropane

HEMA: Hydroxyethyl methacrylate

NIPAM: N-isopropylacrylamide

DMP: Di-methoxy Propane

LCST: Lower Critical Solution Temperature

BCA: Bicinchoninic Acid

BSA: Bovine Serum Albumin

ONPG: *o*-Nitrophenyl- β -D-Galactopyranoside

DMF: *N,N'*-dimethyl formaldehyde

ACVA: 4,4'-azobis(4-cyanovaleric acid)

CTA: Chain Transfer Agent

CTP: 4-Cyanopentanoic acid dithiobenzoate

CTAm: *S*-1-dodecyl-*S*-(α,α' -dimethyl- α'' -acetic acid) trithiocarbonate

General Introduction

This thesis is divided into five sections:

Chapter 1 introduces Reversible addition-fragmentation chain transfer polymerization (RAFT) technique. RAFT was chosen, among all the other LRP techniques, for the presented work because of its versatility. It has an ability to polymerize a large variety of monomers (methacrylates, methacryamides, styrene derivatives, acrylates and acrylamides) in varying solvents (including water). Its tolerance to wide variety of functionalities and its ability to synthesize a wide variety of architectures makes it an excellent polymerization technique. Also this technique does not involve the use of any toxic metal catalysts, which makes it an excellent option for bioapplications [1, 4-7].

Chapter 2 introduces the analysis techniques used for characterization of polymers and nanogels. Gel permeation chromatography (GPC) is used to analyze the polymers and copolymers. Another important technique discussed in this chapter is dynamic light scattering (DLS) which is used to analyze the sizes of nanogels.

Chapter 3 deals with the detailed study of the RAFT of 2-methacryloyloxyethyl phosphorylcholine (MPC). The RAFT polymerization conditions were carefully monitored and it was noted that well-defined homopolymers with ideal low polydispersity ($M_w/M_n < 1.2$) could be synthesized in methanol using 4-cyanopentanoic acid dithiobenzoate (CTP) as chain transfer agent and 4,4'-azobis(4-cyanovaleric acid) (ACVA) as initiator. A series of well-defined block copolymers having a range of compositions and molecular weight were prepared using poly(MPC) as the macroCTA. Statistical poly(MPC)-based copolymers of

biological relevance were also synthesized and characterized.

Chapter 4 discusses core cross-linked micelles with thermo-responsive and degradable cores, synthesized using RAFT technique. Well-defined 2-methacryloyloxyethyl phosphorylcholine (MPC) macro RAFT agent was synthesized with a controlled molecular weight and low poly-dispersity (PDI). Core-cross-linked micelles (CCL) with hydrophilic poly(MPC) shell and thermo-responsive core consisting of MeODEGM, AEMA and 2,2-dimethacryloyloxy-1-ethoxypropane (CL) were then obtained by one pot method of copolymerization of MPC macro RAFT agent with the monomers. The size of nanoparticles could be varied by changing the cross-linker concentration. The CCL micelles collapsed at a temperature above the Lower Critical Solution Temperature (LCST) of MeODEGM and the micelles could be disintegrated at low pH. Nanogels were used for the encapsulation of proteins such as insulin, BSA and β -galactosidase and encapsulation efficiencies of each were compared as a function of cross-linker concentration (molar %) and protein molecular weight. The release profile of insulin from nanogel at low pH was studied and the results were analyzed using bicinchoninic acid (BCA) assay. Controlled release of protein was observed over 48 hours.

Chapter 5 summarizes this research work and gives an insight into future work that can be done in the field of thermo-responsive nanogels and protein encapsulation. Shell cross-linked nanogels of NIPAM with MPC in the core have been reported. The application of these nanogels in protein encapsulation and its comparison with the CCL nanogels can constitute an interesting study.

The work described in this thesis concentrates on the polymerization of MPC using RAFT technique. The synthesis of MPC homopolymers using RAFT in aqueous medium has previously been reported by several groups. Water, however, promotes undesirable reactions such as hydrolysis of RAFT agent at high temperatures. Also the dissolution of RAFT agent and initiator in water takes 4-5 hours of mixing time. Therefore, we have suggested that homopolymerization of MPC be carried out in methanol, which suppresses the hydrolysis reactions. We have also synthesized di-block and statistical copolymers of MPC were synthesized with cationic monomer, 2-aminoethyl methacrylamide hydrochloride (AEMA), and carbohydrate moieties, 2-gluconamidoethyl methacrylamide (GAEMA) and 2-lactobionamidoethyl methacrylamide (LAEMA).

Furthermore, MPC was used for the synthesis of core-shell nanogels, where poly(MPC) polymer chains constituted the biocompatible shell and thermoresponsive core of poly(MeODEGM-*stat*-AEMA). Physical self assembly of the amphiphilic MPC polymer and hydrophobic MeODEGM polymer leads to the formation of micelles. These micelles are unstable with respect to solvent concentrations and temperature. They dissociate with change in the critical micelle concentration (CMC) of the micelles with changing conditions. Cross-linking of micelles has been done to stabilize these micelles. Acid degradable cross-linker has been used that leads to the degradation and release of any entrapped macro-molecules at low pH. The encapsulation efficiency and controlled release profile of the proteins of varying sizes were also studied.

Below is a short description of the technique used in the thesis: the RAFT

polymerization and the introduction to thermo-responsive nanogels that have been synthesized for the encapsulation of proteins.

1 Introduction

1.1 RAFT polymerization:

RAFT polymerization was first reported in 1998 by Rizzardo and coworkers. The RAFT process, which has gained significant interest recently, functions on the principle of degenerative chain transfer process [1-6]. One of the important factors that decide the success of RAFT polymerization is the proper selection of chain transfer agent. RAFT agents are thiocarbonylthio compounds belonging to one of the following groups (based on the Z group): dithioesters, xanthates, dithiocarbamates and tri-thiocarbonates [2].

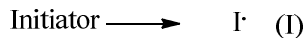
The chain transfer process helps in controlling the molecular weight of the polymer and also, introduces end-functionality [3]. The chain transfer activity is measured by the chain transfer constant, C_{tr} , which is the ratio of rate constant for the chain transfer step to the rate constant for the propagation step. The ideal value for C_{tr} is 1 which means that the relative concentration of chain transfer agent and monomer are constant throughout the polymerization process. RAFT mechanism involves a reversible-addition fragmentation step where the RAFT agents containing $S=C(S)-Z$ moiety is transferred between the active and dormant chains to maintain the living character of the process [4].

1.1.1 RAFT mechanism:

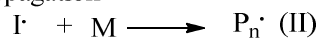
Figure 1-1 outlines the mechanism of the RAFT process, which is as follows: the initiator is decomposed thermally with a half life, $t_{1/2}$ (at a certain temperature). It is the time period within which half the initial concentration of initiator molecules is decomposed. Due to a high monomer concentration, as compared to the chain transfer agent, the initiator radical first reacts with the monomer. The monomer radical which is generated by the initiator, attaches itself to the RAFT chain transfer agent through the reactive thiocarbonyl (C=S) group and forms an intermediate radical (I). The Z group is selected such that it activates the C=S bond and increases the chain transfer constant (C_{tr}) and also stabilizes the resulting intermediate radical I and III by preventing radical coupling. The next stage is the pre-equilibrium stage where the intermediate radical (I) has two possible reaction directions depending upon the nature of R group: either the fragmentation of new radical R^{\bullet} in the forward direction or the regeneration of initiator-generated propagating radical P_n^{\bullet} . For a well-controlled RAFT polymerization, the R group should fragment as fast as possible and re-initiate polymerization quickly. Propagation stage or chain equilibrium is established between the active propagating chains (P_n^{\bullet} and P_m^{\bullet}) and the dormant RAFT agent fragment (fragment 2 and 4). The equilibrium between the dormant chains and the active propagating chains produces an equal probability for all the chains to grow and therefore, the resultant polymer has narrow polydispersity and controlled molecular weight. It has been confirmed that the thiocarbonyl group of the RAFT

agent is present at the end of all polymer chains at the end of polymerization. Therefore, the RAFT technique can be used for the synthesis of various macromolecular architectures like di-block polymers, star polymers and graft polymers.

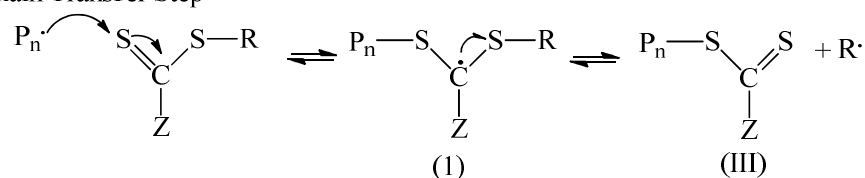
Initiation



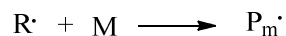
Propagation



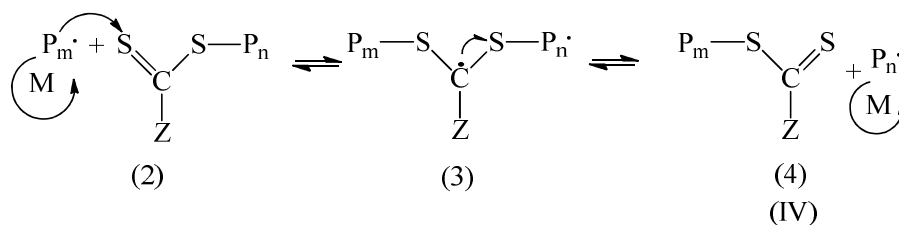
Chain Transfer Step



Re-initiation



Reverse Addition Fragmentation (chain equilibrium)



Termination



Overall Reaction

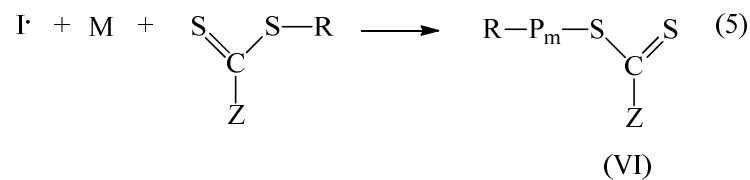


Figure 1-1 : Mechanism of Reversible Addition Fragmentation Chain Transfer polymerization technique using thiocarbonylthio-based chain transfer agent [1]

During the synthesis of di-block copolymers, it is important to consider the following. First of all, the macro CTA synthesis should be stopped at low conversions to avoid dead chains and to retain maximum activity of the thiocarbonylthio functionality. Moreover, to reduce the homopolymer impurity, it is important for the propagating radical of the first block to have a higher propagating rate than the second block [3,5].

The total number of polymer chains obtained at the end of a reaction is the sum of polymer chains resulting from the initiator radical and that from radical R^\bullet . The polymer chains formed from the initiator radical are those which do not have a thiocarbonyl end group. The polymer chains initiated from radical R^\bullet remain living while the number of dead chains is given by the ratio of number of initiator derived chains to the number of RAFT molecules. Therefore, to reduce the termination due to radical coupling and increase the degree of livingness of the RAFT polymerization, the CTA/initiator ratio is kept as high as possible (typically 5/1). The structure, mole ratio and molecular weight of CTA and initiator affect the molecular weight of the resulting polymer. The molecular weight M_n of the polymer can be calculated as follows:

$$M_{n(\text{theory})} = \left(\frac{[Monomer]_0}{[CTA]_0 + 2f[I]_0(1 - e^{-k_d t})} \times MW_{Monomer} \times Conversion \right) + MW_{CTA}$$

Where k_d is the rate coefficient of termination and f is the initiator efficiency.

The R group (radical leaving group) affects the pre-equilibrium stage. It should be a better leaving group than the propagating radical and should be a good reinitiating radical. The Z group, on the other hand, plays an important role in

determining the reactivity and stability of RAFT agent intermediate radicals [5].

A well controlled RAFT system should ensure the following:

- 1) Linear kinetic plot between $\ln([M]_0/[M])$ vs. time (Figure 1-2) indicating first order reaction kinetics with respect to the monomer.
- 2) The evolution of number average molecular weight (M_n) with conversion is linear. The straight line in Figure 1-3 indicates that almost no unimolecular termination is observed.
- 3) Reaction stoichiometry can easily be used to predict the molecular weight of the polymer.
- 4) Low polydispersity is obtained for the resulting polymer.

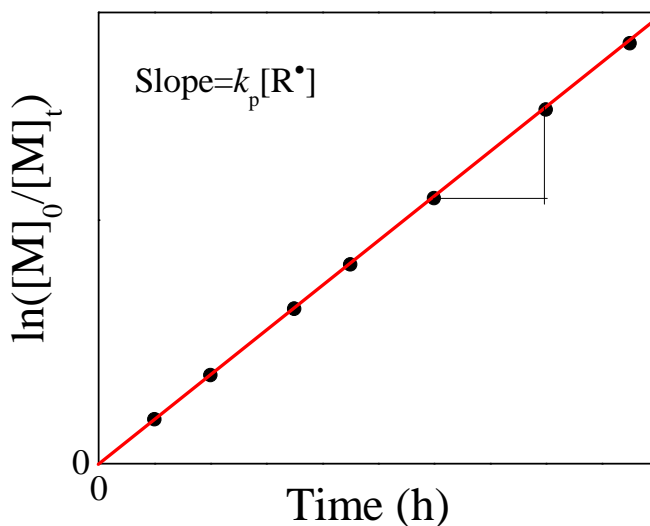


Figure 1-2 : Linear kinetic plot indicating first order reaction kinetics w.r.t monomer

(Semi-logarithmic graph plot)[3]

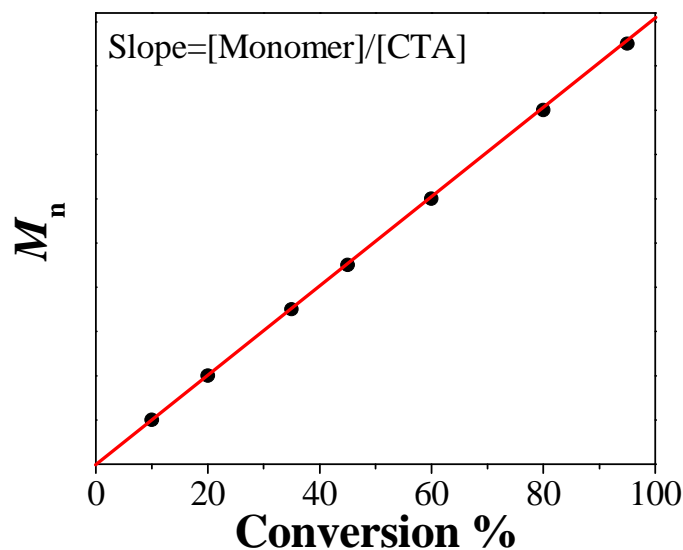


Figure 1-3 : Linear increase in molecular weight with conversion [3]

1.1.2 Macro-monomers as RAFT agents:

Macro-monomers are used in RAFT polymerization to synthesize block copolymers with the macro-monomer as the A block and the co-monomer as the B block. It was observed that the macro-monomers copolymerize more easily with comonomers which are sterically less hindered. The success of block copolymerization depends on the structures of both the macro-monomer and the comonomer [3]. The most important aspects of block copolymerization by RAFT technique is that the fragmentation of adduct radical should dominate over the reaction with monomer (as in the case of RAFT agent and monomer). Sterically bulky monomers offer this advantage naturally. For less sterically hindered monomers, the fragmentation can be sped by increasing the reaction temperature.

RAFT is a great technique that enables the synthesis of well defined, narrow

dispersed polymers. The process is directed by a RAFT chain transfer agent. The main limitation of this technique, however, is the loss of chain transfer agent end group due to hydrolysis or aminolysis when the reaction is carried out in aqueous medium [1,7]. However, water is a preferred solvent for a large number of monomers. RAFT polymerization of Styrene sulphonic acid (sodium salt) was first carried out in aqueous solution by Chiefari *et al.* using sodium 4-cyanopentanoic acid dithiobenzoate (CTPNa) as chain transfer agent [4]. As compared to other living polymerization techniques, like atom transfer radical polymerization (ATRP), which involves the use of metal catalysts, RAFT has great potential for biomedical applications [6].

The advantages that RAFT offers in terms of compatibility with a wide variety of monomers and solvents, controlled polymerization process and narrow polydispersity of polymers obtained are many and the fact that it does not involve the use of any toxic metal catalysts makes it an excellent option for bioapplications. For this reason, the RAFT process has been selected as the method of polymerization for this work.

1.2 Overview of 2-Methacryloyloxyethyl Phosphorylcholine:

2-Methacryloyloxyethyl Phosphorylcholine (MPC) monomer was first synthesized by Nakabayashi *et al.*, to obtain a new biocompatible polymer with a non-thrombogenic surface for artificial organs [8]. Ishihara *et al.* improved the synthesis protocol to obtain pure MPC after recrystallization [9]. The phosphocholine group in the monomer resembles the phospholipid groups on the surface of cell membranes [10-13]. With a polymerizable methacrylate group, MPC can be copolymerized into a range of desired architectures such as graft, di-block, statistical and star copolymers [9,14-17]. These wide varieties of MPC polymers are used for surface modifications.

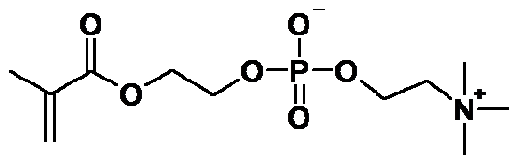


Figure 1-4 : Structure of 2-methacryloyloxyethyl Phosphorylcholine

MPC is a zwitterionic compound and the presence of positive and negative charges can be easily exploited. It has an intrinsic solubility in both organic and polar solvents. These factors together with the fact that it is highly biocompatible and easily polymerizable, makes MPC very useful for bioapplications [10,17-25]. Copolymers of MPC with polysulphone or cellulose hollow fiber membranes increased their thrombogenicity and also retained their permeability. Previous studies have also proved that copolymers of MPC can find applications in

hemodialyzers, oxygenators and glucose sensors [16]. Homopolymers of MPC are also used to stabilize bioactive peptides in their aqueous forms. The copolymers of amphiphilic MPC with hydrophobic polymers make good hydrogels [16].

1.3 Thermo-responsive polymers:

Synthetic polymers are increasingly being used as therapeutic agents for drug delivery. The field of “polymer therapeutics” encompasses polymer gels and polymeric micelles [26-28]. Stimuli-responsive polymers/gels/conjugates are a subclass of such therapeutic systems, which have the ability to undergo changes in size and solubility with changes in the external environment. External stimuli include temperature, pH, electric and magnetic field, concentration of electrolytes and so on [26,29-34]. These “smart systems” act as drug carriers and reduce toxicity and immunogenicity and facilitate organ-specific targeting of the drugs [30]. Our study is based on the use of thermo-responsive core-shell micelles to encapsulate proteins in their cross-linked cores.

Thermo-responsive polymers undergo a volume phase transition which causes a change in their solvation state: Polymers that change from being insoluble at low temperatures to soluble upon heating have a upper critical solution temperature (UCST), for example a system combination of acrylic acid and acrylamide. Contrary to most compounds, some polymers change from a soluble state at lower temperature to an insoluble aggregated state at higher temperature and are known to have a lower critical solution temperature (LCST), for example, N-isopropylacrylamide (NIPAM), *N,N'*-diethylacrylamide (DEAM) and methoxydiethylene glycol methacrylate (MeODEGM) [2,20,26,35-42]. The change in hydration state is the effect of change in hydrogen bonding properties, depending upon whether intra-hydrogen bonding between polymers is favored

over the inter-hydrogen bonding of polymer molecules with water [28].

Nanogels are swollen cross-linked networks of hydrophilic or amphiphilic polymers [26,28,29,43-45]. They offer many advantages as polymer therapeutics with their tunable size (nanoscale to micro-scale), large surface area (for multivalent bio-conjugation) and a cross-linked network for the incorporation of macro-molecules [29,46-48]. Biocompatibility and biodegradability are also essential characteristics of these nanogels.

The size of nanogels depends upon the nature of polymer and the amount of cross-linker used. The size of particles increases with the increase in cross-linker concentration. Parameters such as size, swelling ratio and pore size along with the chemical properties (presence of ionizable groups) determine the amount of drug loading in a nanogel [49].

Surface charge of nanogels makes them vulnerable to non-specific interactions. To prevent this, nanogels can be functionalized with receptor-recognizing ligands. For example the functionalization of poly(NIPAM) nanogels with folic acid resulted in vectorization by receptor-mediated endocytosis with much higher efficiency as compared to non-functionalized nanogels [30].

As mentioned above, thermosensitive nanogels are increasingly being used for the immobilization of “hydrolytically sensitive” proteins and peptides. The physically entrapped proteins are released on thermal stimulus. Two different methods namely physical entrapment and direct addition method can be used for protein encapsulation in nanogels. Physical entrapment can be carried out by incubating the nanogel solutions with the drugs for a period of 24 hours. For example,

cholesterol can be encapsulated in the cores of nanogels owing to the hydrophobic interactions between them. Another method of protein encapsulation by physical entrapment is by dialysis. It is carried out in the same way except the drug is incubated with the nanogel solution in a dialysis membrane which is followed by washing away any unbound drug. On the other hand, in the direct addition method, drugs or proteins are dissolved in the reaction solution of monomers during the synthesis of nanogels. This method is used in the preparation of aspirin-loaded gels. During the process, aspirin salt solution is dissolved in azo-dextran solution to initiate photo-polymerization. Some proteins are first chemically modified by N-hydroxysuccinimidoacrylate (NHS) or α -chymotrypsin followed by polymerization with the desired monomers. Nanogels that contain chemically conjugated proteins tend to increase the thermo-stability and shelf-life of the proteins [26,44].

There are two major concerns when a drug/protein is loaded into a nanogel. First of all, it is very important to have an efficient encapsulation of the protein in the polymer matrix. Secondly, one must ensure that the release of drug/protein by any applied/local trigger occurs in a controlled fashion [20,21,26,37,50-56].

Different kinds of protein-nanogel interactions result in different kind of release profiles. Polymeric nanogels can be used to encapsulate biological agents within them and also deliver them in response to changes in the environment. The release profile of drugs or proteins is dependent upon the type of release mechanism taking place, which can be one of the following [44].

- 1) Diffusion controlled mechanism: The drug release occurs by the diffusion of

drug through the nanogel pores/mesh. For example, the release of doxorubicin from pluronic based nanogels occurs via diffusion controlled mechanism [20,26,52-54].

- 2) Chemically controlled mechanism: Drug release occurs due to degradation/hydrolysis or dissolution of the nanogels. The rate of drug release depends upon the polymer erosion or cross-linker degradation by hydrolysis or enzymatic degradation [57-62].
- 3) Swelling controlled mechanism: This happens when certain polymers swell upon contact with biological fluids. The drug diffuses out due to increase in the pore size of the nanogel [63].
- 4) Environmentally responsive mechanism: Environmentally responsive polymers show changes in their swelling ratio with changes in temperature, pH or magnetic stimulus. The encapsulated molecules are released due to an increase in porosity of the nanogels [48,64-67].

Core-cross-linked nanogels with MeODEGM in the core and an amphiphilic MPC corona have been synthesized using acid degradable cross-linker. The thermo-responsive nanogel was used for encapsulation of proteins and the release profile of these proteins was studied at varying pH.

1.4 References:

- [1] Thomas, D. B.; Convertine, A. J.; Hester, R. D.; Lowe, A. B.; McCormick, C. L. *Macromolecules*. **2004**, *37*, 1735-1741
- [2] Lowe, A.; McCormick, C. *Prog. Polym. Sci.* **2007**, *32*, 283-351
- [3] Matyjaszewski, K.; Davis, T. P. *Handbook of Radical Polymerization*; Wiley Interscience, 2002; Vol. 125
- [4] Chiefari, J.; Chong, Y. K. B.; Ercole, F.; Krstina, J.; Jeffery, J.; Le, T. P. T.; Mayadunne, R. T. A.; Meijs, G. F.; Moad, C. L.; Moad, G.; Rizzardo, E.; Thang, S. H.; South, C. *Macromolecules*. **1998**, *9297*, 5559-5562
- [5] Boyer, C.; Bulmus, V.; Davis, T. P.; Ladmiral, V.; Liu, J.; Perrier, S. *Chem. Rev.* **2009**, *109*, 5402-36
- [6] Moad, G.; Chiefari, J.; Chong, (Bill) Y.; Krstina, J.; Mayadunne, R. T.; Postma, A.; Rizzardo, E.; Thang, S. H. *Polym Int.* **2000**, *49*, 993-1001
- [7] Levesque, G.; Arsène, P.; Fanneau-Bellenger, V.; Pham, T. N. *Biomacromolecules*. **2000**, *1*, 400-6
- [8] Ishihara, K.; Ueda, T.; Nakabayashi, N. *Polymer J.* **1990**, *22*, 355-360
- [9] Iwasaki, Y.; Ishihara, K. *Anal Bioanal Chem.* **2005**, *381*, 534-546
- [10] Yuan, J.-J.; Armes, S. P.; Takabayashi, Y.; Prassides, K.; Leite, C. a P.; Galembeck, F.; Lewis, a L. *Langmuir*. **2006**, *22*, 10989-10993
- [11] Matsuno, R.; Ishihara, K. *Macromol. Symp.* **2009**, *279*, 125-131
- [12] Yan, L.; Ishihara, K. *J Poly. Sci.: Part A: Poly. Chem.* **2008**, *46*, 3306–3313

- [13] Iwasaki, Y.; Ishihara, K. *Anal Bioanal Chem.* **2005**, *381*, 534-46
- [14] Yu, B.; Lowe, A. B.; Ishihara, K. *Biomacromolecules.* **2009**, *10*, 950-958
- [15] Ma, Y.; Tang, Y.; Billingham, N. C.; Armes, S. P.; Lewis, A. L.; Lloyd, A. W.; Salvage, J. P. *Macromolecules.* **2003**, *36*, 3475-3484
- [16] Nakabayashi, N.; Iwasaki, Y. *Biomed Mater Eng.* **2004**, *14*, 345-354
- [17] Yusa, S.I.; Fukuda, K.; Yamamoto, T.; Ishihara, K.; Morishima, Y. *Biomacromolecules.* **2005**, *6*, 663-70
- [18] Katakura, O.; Morimoto, N.; Iwasaki, Y.; Akiyoshi, K.; Kasugai, S. *J. Med. Dent. Sci.*, **2005**, *52*, 115-121.
- [19] Goda, T.; Matsuno, R.; Konno, T.; Takai, M.; Ishihara, K., *Colloid Surf. B-Biointerfaces*, **2008**, *63*, 64-72
- [20] York, A.W.; Kirkland, S.E.; McCormick, C.L., *Adv. Drug Delivery Rev.*, **2008**, *60*, 1018-1036
- [21] Ishihara, K.; Takai, M., *J. R. Soc. Interface*, **2009**, *6*, S279-S291
- [22] Clarke, S.; Davies, M.C.; Roberts, C.J.; Tendler, S.J.B.; Williams, P.M.; O'Byrne, V.; Lewis, A.L; Russell, J.; *Langmuir*, **2000**, *16*, 5116-5122.
- [23] Kyomoto, M.; Moro, M.; Takatori, Y.; Kawaguchi, H.; Nakamura, K.; Ishihara, K., *Biomaterials*, **2010**, *31*, 1017-1024.
- [24] Jiang, W.; Fischer, G.; Girmay, Y.; Irgum, K., *J. Chromatogr. A*, **2006**, *1127*, 82-91.
- [25] Tsarevsky, N.V.; Matyjaszewski, K., *Chem. Rev.*, **2007**, *107*, 2270-2299
- [26] Kabanov, A. V.; Vinogradov, S. V. *Angew. Chem. Int. Ed.* **2009**, *48*, 5418-5429

- [27] Sisson, A. L.; Haag, R. *Soft Matter*. **2010**, *6*, 4968-4975
- [28] Schmaljohann, D. *Adv. Drug Delivery Rev.* **2006**, *58*, 1655-70
- [29] Oh, J.; Drumright, R.; Siegwart, D.; Matyjaszewski, K. *Prog. Polym. Sci.* **2008**, *33*, 448-477
- [30] Hidalgo-Alvarez, R. *Structure and Functional Properties of Colloidal Systems*; 2009; pp. 367-386
- [31] Okano T, Bae YH, Jacobs H, K. S. *J Control Release*. **1990**, *11*, 255-265
- [32] Feil H, Bae YH, Feijen J, K. S. *Macromolecules*. **1992**, *25*, 5528-5530
- [33] Matsukuma D, Yamamoto K, Ayoyagi, T. *Langmuir*. **2006**, *22*, 5911-5915
- [34] Ho E, Lowman A, M. M. *Biomacromolecules*. **2006**, *7*, 3223-3228
- [35] Doherty, E.S.; Kan, C.W.; Barron, A. E. *Electrophoresis*. **2003**, *24*, 4170-4180.
- [36] Fournier, D.; Hoogenboom, R.; Thijs, H. M. L.; Paulus, R. M.; Schubert, U. S. *Macromolecules*. **2007**, *40*, 915-920
- [37] Oh, J.; Drumright, R.; Siegwart, D.; Matyjaszewski, K. *Prog. Polym. Sci.* **2008**, *33*, 448-477
- [38] Andersson, M.; Hietala, S.; Tenhu, H.; Maunu, S. L. *Colloid Polym Sci.* **2006**, *284*, 1255-1263
- [39] Lyon, N. S. and L. A. *Colloid & Polymer Science*. **2006**, *286*, 1061-1069.
- [40] Vasilieva, Y.; Thomas, D. B.; Scales, C. W.; McCormick, C. L. *Macromolecules*. **2004**, *37*, 2728-2737

- [41] Hu, T.; You, Y.; Pan, C.; Wu, C. *J. Phys. Chem. B.* **2002**, *106*, 6659-6662
- [42] Prevot, M.; Déjugnat, C.; Möhwald, H.; Sukhorukov, G. B. *ChemPhysChem.* **2006**, *7*, 2497–2502
- [43] Matzelle, T.; Reichelt, R. *Acta Microscopica.* **2008**, *17*, 45-61
- [44] Shidhaye, S.; Lotlikar, V.; Malke, S.; Kadam, V. *Curr Drug Therapy.* **2008**, *3*, 209-217
- [45] Vinogradov, S. V.; Bronich, T. K.; Kabanov, A. V. *Adv. Drug Delivery Rev.* **2002**, *54*, 135-47
- [46] Singh, N.; Lyon, L. A. *Colloid Polym Sci.* **2008**, *286*, 1061-1069
- [47] Tan, J.; Tan, M.; Tam, M. *Local Reg Anesth.* **2010**, 93
- [48] Smith, M. H.; South, A. B.; Gaulding, J. C.; Lyon, L. A. *Anal.Chem.* **2010**, *82*, 523-530
- [49] He, J.; Yan, B.; Tremblay, L.; Zhao, Y. *Langmuir.* **2011**, *27*, 436-444
- [50] Arotçaréna, M.; Heise, B.; Ishaya, S.; Laschewsky, A. *J. Am. Chem. Soc.* **2002**, *124*, 3787-3793
- [51] Naeye, B.; Raemdonck, K.; Remaut, K.; Sproat, B.; Demeester, J.; De Smedt, S. C. *Eur. J. Pharm. Sci.* **2010**, *40*, 342-351
- [52] Shi, L.; Berkland, C. *Macromolecules.* **2007**, *40*, 4635–4643
- [53] Oh, J. K. *Can. J. Chem.* **2010**, *88*, 173-184
- [54] Kabanov, A. V.; Vinogradov, S. V. *Angew. Chem. Int. Ed.* **2009**, *48*, 5418-5429.

- [55] Risbud, M. V.; Hardikar, A. A.; Bhat, S. V.; Bhonde, R. R. *J. Control Release*. **2000**, *68*, 23-30
- [56] Panyam, J.; Labhasetwar, V., *Adv. Drug Delivery Rev.* **2003**, *55*, 329-347
- [57] Cadée, J.; Groot, C. J. de; Jiskoot, W.; Otter, W. den; Hennink, W. E. *J. Control Release*. **2002**, *78*, 1-13
- [58] Cai, C.; Bakowsky, U.; Rytting, E.; Schaper, A. K.; Kissel, T. *Eur. J. Pharm. Biopharm.* **2008**, *69*, 31-42
- [59] Las Heras Alarcon, C. de; Pennadam, S.; Alexander, C. *Chem. Soc. Rev.* **2005**, *34*, 276-285
- [60] Goh, E. C. C.; Stöver, H. D. H. *Macromolecules*. **2002**, *35*, 9983-9989
- [61] Kim, Y.; Thapa, M.; Hua, D. H.; Chang, K.-O. *Antiviral Res.* **2011**, *89*, 165-173
- [62] Zhang, L.; Bernard, J.; Davis, T.P.; Barner-Kowollik, C.; Stenzel, M.H., *Macromol. Rapid Commun.* **2008**, *28*, 123-129
- [63] Kim, B.; La Flamme, K.; Peppas, N. *J. Appl. Polym. Sci.* **2003**, *89*, 1606-1613
- [64] Kuckling, D.; Vo, C. D.; Wohlrab, S. E. *Langmuir*. **2002**, *18*, 4263-4269
- [65] Hamidi, M.; Azadi, A.; Rafiei, P. *Adv. Drug Delivery Rev.* **2008**, *60*, 1638-1649
- [66] Smulders, W.; Monteiro, M. J. *Macromolecules*. **2004**, *37*, 4474-4483
- [67] Wu, W.; Shen, J.; Banerjee, P.; Zhou, S. *Biomaterials*. **2010**, *31*, 8371-8381

2 Instrumentation

2.1 Gel Permeation Chromatography (GPC):

Gel permeation chromatography (GPC) or Size Exclusion Chromatography (SEC) is a common technique for determining the molecular weights and molecular weight distribution of the polymers. When equipped with different kinds of detectors, such as Deflection RI Detector, UV/Vis Detector, Viscometer Detector and Light Scattering Detector, different data can be analyzed *via* various calibration methods (Conventional Calibration, Universal Calibration, and Triple Detection) [1].

When a sample is injected in the apparatus, the polymer molecules are separated with respect to their hydrodynamic volumes (V_h). Separation occurs in columns with porous packings. The choice of columns depends upon the solvent and range of molecular weights. For example, Viscotek column for aqueous GPC is packed with porous hydroxymethacrylate polymer. The maximum pore size increases for a higher exclusion limit of M_w . For best chromatographic separation, the right selection of solvent and column should be made for a sample. The solubility of the sample dictates the use of column and solvent [1, 2].

Larger molecules cannot enter the column pores and are therefore eluted faster at interstitial volume (V_i). However, smaller particles get captured in the pores and elute later at sum of interstitial and pore volume ($V_i + V_p$). Molecules with sizes between the two mentioned elute at an elution volume V_e given by:

$$V_e = V_i + K_{\text{sec}} \cdot V_p$$

K_{sec} is the equilibrium constant [3].

Figure 2-1 shows the process flow of gel permeation chromatography, with the continuous flow of a mobile phase through the system through a solvent delivery device. Unwanted vapor or gas bubbles in the line causes signal instability and noise. To get rid of any air bubbles, the solvents are degassed before being put on-line. After the sample is injected in-line, the sample is carried through the GPC columns, where separation occurs based on size difference [1, 2]. After eluting out of the column, the sample passes through detectors and the output is analyzed in data processing system.

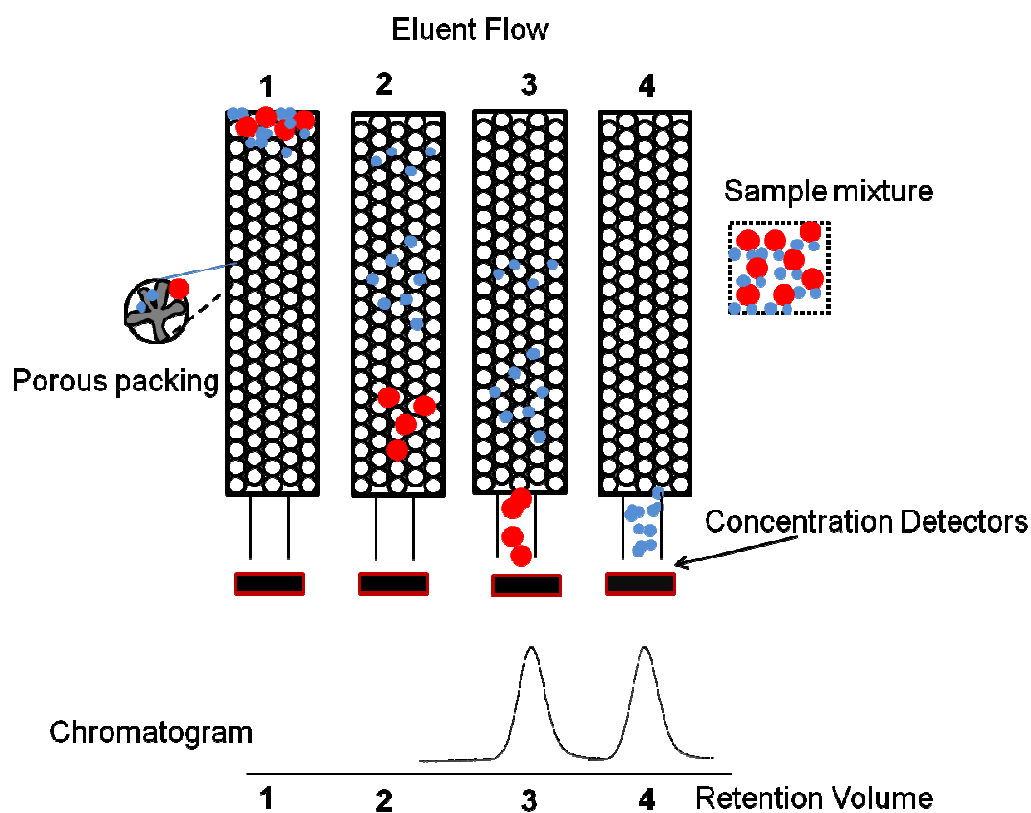


Figure 2-1 : Mechanism of GPC separation [1, 3]

The extent of GPC analysis depends on the number of detectors. Molecular weight, molecular weight distribution, radius of gyration and hydrodynamic radius are a few parameters that can be analyzed depending on the choice of detectors and calibrations. Moreover, additional information on macromolecular structure, conformation, branching, copolymer composition and aggregation can also be obtained. The most commonly used detectors in GPC are [3 A, 3 B]:

- 1) Refractive Index Detectors (RI): It measures the change in refractive index of the effluent passing through the flow cell as compared to the eluent. These detectors are used to calculate molar mass and concentration profiles.
- 2) UV/Vis detectors: UV/Vis adsorption is measured at a fixed wavelength. Based on the calibration curve, UV detectors are used to measure the concentration profiles and molecular masses of copolymer samples. The use of this type of detectors is limited because the chromophore group is not present in a wide range of monomers. The detector can however be used for the same function as RI i.e., measuring molar mass and concentration profiles using the calibrated standards.
- 3) Online Light Scattering Detectors (Low Angle Laser Light Scattering (LALLS), Right Angle Laser Light Scattering (RALLS) or Multi Angle Laser Light Scattering (MALLS)): These detectors measure the scattering light intensity at one or many scattering angles. These can be used to measure absolute molar mass and to determine structure in solution.

Depending on various types of detectors, different calibrations are used. The calibration methods have been discussed below in detail.

2.1.1 Conventional Calibration:

Conventional calibration is the most popular calibration technique for the analysis of relative molecular weight. It involves the use of a concentration detector, a Refractive Index (RI) or UV/Vis detector and a calibrated column. Standards of known molecular weight and molecular weight distribution are used to create a calibration curve (log Molecular weight (M_w) vs Retention Volume (RV)). The relative molecular weight of polymer samples is calculated using the same calibration curve. However, this calculation is based on an assumption that the samples and standards have the same density and structure. This is the reason that the molecular weights obtained are referred to as relative molecular weight. The technique is simple and cost-effective, but has some limitations which are described as follows.

- 1) There is a difference between the relative molecular weight and true molecular weight.
- 2) The process overlooks any structural and conformational differences.
- 3) It involves a lengthy process of column calibration.

In order to get as close as possible to the true molecular weights, almost mono-dispersed polymer standards of nearly similar structures are used for calibration [1]. Molecular weight calculation by conventional calibration is shown in Figure 2-2. The calibration curve is created by fitting the data into a simple polynomial equation:

$$\text{Log } M_w = A_0 + A_1V + A_2V^2 + A_3V^3 + \dots + A_nV^n$$

The unknown samples are analyzed for their number and weight average

molecular weights as obtained by their definitions:

$$M_n = \frac{\sum N_i \cdot M_i}{\sum N_i}$$

$$M_w = \frac{\sum N_i \cdot M_i^2}{\sum N_i \cdot M_i}$$

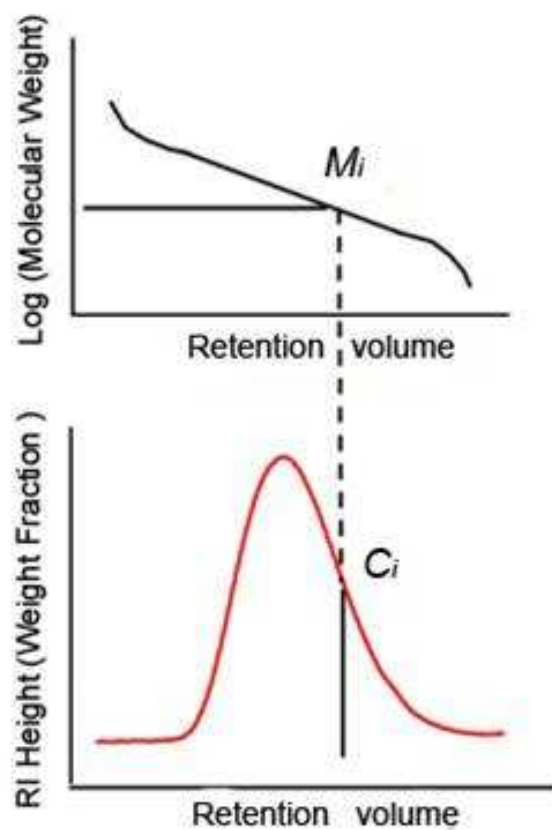


Figure 2-2 : Molecular weight calculation by conventional calibration [1, 3]

(Note: M_i = molecular weight of the i th polymer chain and c_i is the concentration/weight fraction of the i th polymer chain)

2.1.2 Universal Calibration:

This calibration method was created to overcome the assumption of same

chemical structures of calibration and polymer samples. It uses an extra detector called the viscometer, which can be used to determine the intrinsic viscosity and hydrodynamic radius along with the molecular weight of the sample. The most common viscometer is the Four Capillary Viscometer, which consists of four capillary tubes arranged in a balanced bridge arrangement, analogous to the wheatstone bridge. It measures the differential pressure caused by movement of the sample solution through these tubes and calculates the intrinsic viscosity (IV). The molecular weight (M_w), intrinsic viscosity (IV) and hydrodynamic volume (V_h) are related through the equation:

$$M_w \cdot IV = 5/2 \cdot N_A \cdot V_h$$

Where, N_A is Avogadro's Constant.

When combined with a concentration detector (RI or UV/Vis), a calibration curve can be created between $\log V_h$ vs. Retention Volume. The universal calibration curve indicating that different standards fit in the same calibration curve is shown in Figure 2-3. This reduces the difference between the analyte and standards. The M_n and M_w calculated by universal calibration were found to perform well particularly with samples having low molecular weights. However, column calibration by standards was still required by this method [1, 5].

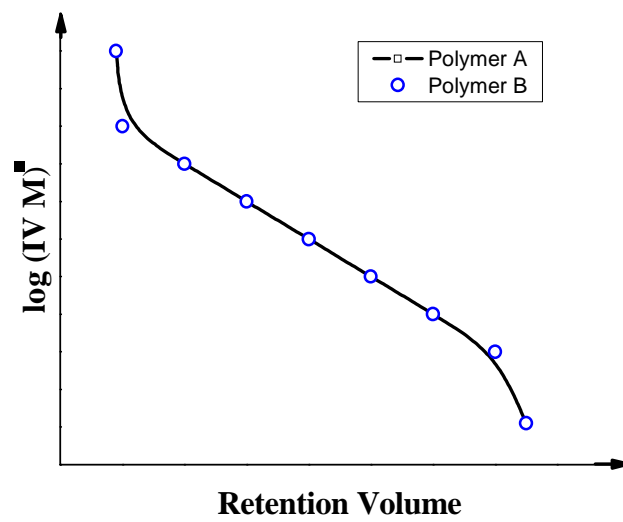


Figure 2-3 : Universal Calibration Curve [1, 3]

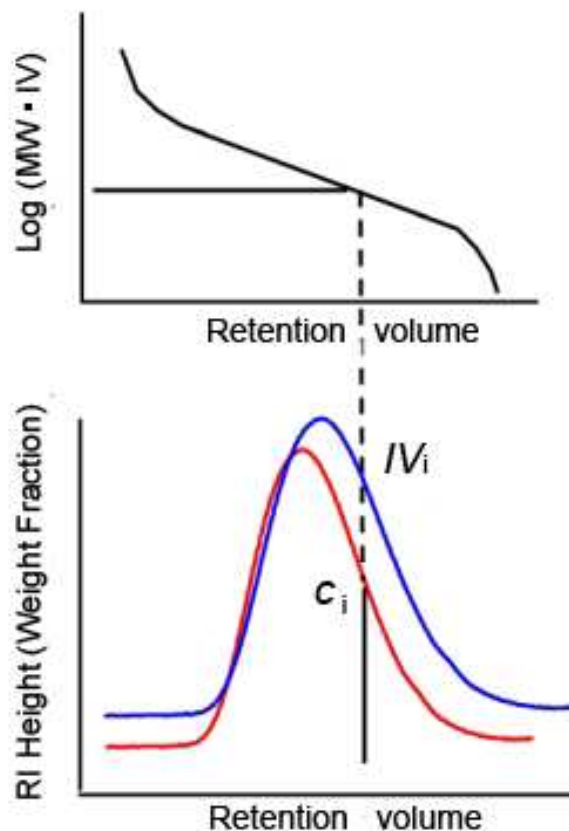


Figure 2-4 : Molecular weight calculation by Universal Calibration Curve [1, 3]

2.1.3 Triple Detection:

Triple detection is the most accurate calibration technique available to determine the absolute molecular weight of the polymer. It consists of the concentration detector (RI/ UV/Vis), the viscometer and the light scattering detector. Because of the light scattering detector, only a single standard is required to calibrate the system. The absolute molecular weight is calculated by the Rayleigh's equation:

$$R(\theta)|_{\theta \rightarrow 0} \cong KCM$$

Where R is the intensity, θ is the angle of scattered light, K is the optical constant,

C is the concentration and M is molecular weight [1].

The relationship between M_w (or M_n) and the signal peaks is as

$$\text{follows: } M_w \propto \frac{\text{LALS Peak Area}}{\text{RI Peak Area}} \text{ and } M_n \propto \frac{\text{RI Peak Area}}{\text{Molar Conc. Peak Area}}$$

The polarity of the polymer sample determines the polarity of the stationary phase and the continuous phase in chromatography. While the use of aqueous GPC is inevitable for analysis of water soluble polymers, it also brings challenges to solve. High performance column packings are prepared from methacrylate gels, which contain residual carboxylate groups imparting an overall negative charge to the packing. This gives rise to ion-exclusion (sample polyelectrolyte and packing material having the same charge lead to early elution) or ion-inclusion (sample polyelectrolyte and packing material having opposite charges leads to interaction between the two and hence delayed elution) [2 A, 2 B, 6]. A buffer solution with a certain pH is used to prevent any absorption or precipitation of the water soluble polymer and small amount of salt is added to acquire the random coil of the polymer. Organic eluent that are miscible in water can also be added in small quantities. However, non-neutral eluents and salts can damage the equipment.

2.2 Dynamic Light Scattering:

A dynamic light scattering instrument uses the principle of light scattering to determine the hydrodynamic size of a particle as shown in Figure 2-5. Light can be treated as an electromagnetic wave. The electrons of a particle start oscillating when this oscillating electromagnetic wave strikes them. If the light source is monochromatic and coherent, for example a laser source, we can observe a time dependent fluctuation in scattering intensity. This is because the particles themselves undergo Brownian motion and therefore the distance between the scatterers keeps changing with time. The larger the particle, the slower is its Brownian motion [7, 8 A].

An accurately known temperature is also important for DLS for the viscosity calculations. Fluctuations in temperature also causes convection currents to flow which causes non-random movements which may affect the size interpretation [8 A].

In Quasi Elastic Light Scattering (QELS), the total time over which a measurement is made, is divided into small time intervals called time delays. The fluctuating signal is measured by the autocorrelation $C(t)$, t being the time delay. As the time delay increases, the correlation is lost and the function approaches a constant value B .

$$C(t) = Ae^{-2\gamma t} + B$$

Where, A is the optical constant determined by instrument design and

$$\gamma = Dq^2 \text{ rad/sec}$$

“q” is calculated from scattering angle θ , wavelength of laser light λ_0 and refractive index η of the liquid:

$$q = \frac{2\pi\eta}{\lambda_0} 2\sin(\theta/2)$$

The translational diffusion coefficient, D , is the quantity measured by QELS. Particle shape is assumed to be globular unless needle/rod shaped particles are specifically mentioned, with aspect ratio greater than 5. Particle size is related to D by equation:

$$D = \frac{K_b}{3\pi\eta(t)d} T$$

Where, K_b is the Boltzmann constant (1.38×10^{16} ergs/deg), T is temperature in K, $\eta(t)$ is viscosity in centipoises and d is the particle diameter. Another important assumption is that the particle movement is independent of one another.

When a size distribution is broad, effective diameter is the average diameter measured by the intensity of light scattered by each particle. Hydrodynamic diameter (D_h) measured by Photon correlation spectroscopy technique is the sum of particle diameter and the double layer thickness. It is defined as the diameter a sphere would have in order to diffuse at the same rate as the particle. It can also be referred to as the Equivalent Sphere Diameter [7].

When a broad range of particle diameters is present, the effective diameter is measured as the average diameter subjective to the intensity of light scattered by each particle [7, 8 A].

The polydispersity of particles has no units. It is close to zero (0.000 to 0.020) for monodispersed particles or nearly monodispersed particles, small (0.020-0.080)

for narrow dispersed particles and larger for broader distributions.

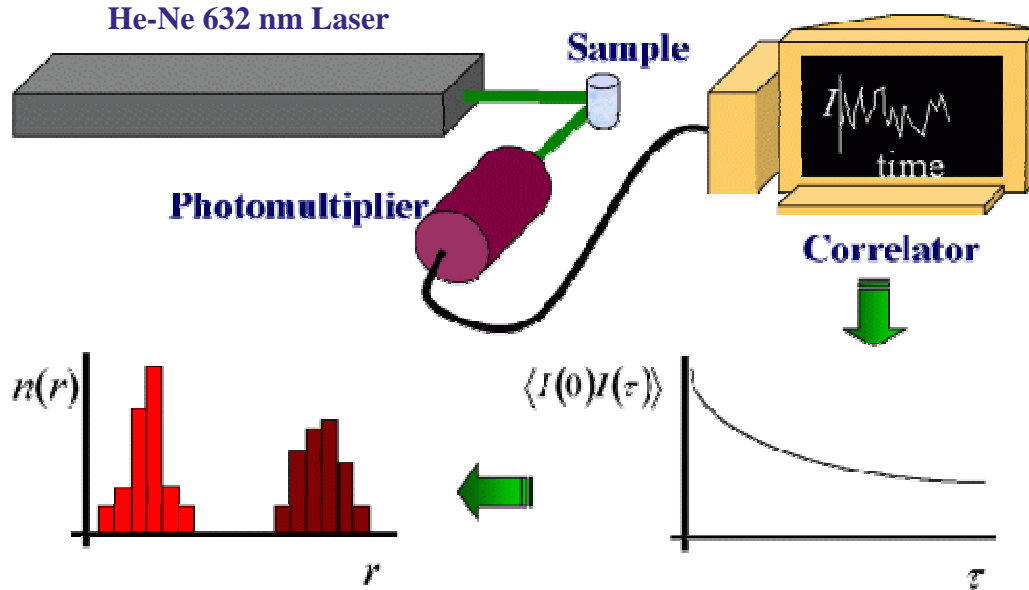


Figure 2-5 : Dynamic Light Scattering for measuring sample size distribution [8 B]

2.3 References

- [1] Complete Guide for GPC / SEC / GFC Instrumentation and Detection Technologies; Viscotek Corporation; 2006
- [2] A) Striegel, A.M.; Kirkland, J.J.; Wallace, W.Y.; Donald, D.B, *Modern Size Exclusion Liquid Chromatography*, Wiley Interscience, 2009.
- B) http://www.waters.com/waters/nav.htm?cid=10167894&locale=en_US
- [3] A) http://www.malvern.com/LabEng/products/viscotek/viscotek_gpc_sec/components/columns_aqueous.htm.
- B) <http://academic.sun.ac.za/polymer/gpectref.htm>
- [4] Held, D., Kilz, P. *The Column*. 2008, pp. 17-20.
- [5] Benoit, H., *J Chem Phys.*, **1966**, 63, 1507
- [6] Cazes, J., *J. Chem. Educ.*, **1970**, 47, A461-A471
- [7] DLS instruction manual, Brookhaven Instrument Corporation
- [8] A) B.Chu, *Laser Light Scattering : Basic Principles and Practice*, Academic Press, Boston, 1991.
- B) http://www.ecs.umass.edu/che/henson_group/research/emul.html

3 Detailed Study of the Reversible Addition-Fragmentation Chain Transfer Polymerization and Copolymerization of 2-Methacryloyloxyethyl Phosphorylcholine

3.1 Introduction

Zwitterionic compounds draw considerable attention in industry and research. Due to their polar nature, they are soluble in water. The presence of positive and negative charges on these ions can be easily exploited. We have studied the polymerization of 2-methacryloyloxyethyl phosphorylcholine (MPC), an amphiphilic zwitterionic monomer [1]. The MPC is methacrylate with a phosphorylcholine group, which is one of the representative phospholipid polar groups on the cell membrane [2],[3]. The MPC polymers showed excellent blood compatibility due to reduction of protein adsorption even when they contact with whole blood without anticoagulant [4]-[8]. Based on the functionality of the MPC polymers, they have been used in various blood contacting medical devices such as oxygenator, catheter, cardiovascular stent, implantable blood pump to prevent blood coagulation at these surfaces [9]-[18]. Also, the grafting of the poly(MPC) on artificial hip joints improves lubrication and reduces wear of polyethylene liner of the hip joint [19]. A range of MPC polymers (di-block, tri-block, random, graft copolymers) and hydrogels, have been synthesized for surface modifications [14],[20],[21].

Due to the significant interest of MPC polymers, different controlled radical polymerization techniques have been used for the synthesis of well-defined MPC polymers. Controlled polymerization of MPC by atom transfer radical

polymerization (ATRP) was reported by Armes *et al.* [22]. The ATRP is a type of living radical polymerization (LRP) which is carried out using transition metal catalysts [23]. The advantage of aqueous ATRP for MPC is the small time frame in which the reaction is completed. More than 96 % yields were obtained within 10 min of the start of reaction. However, the copolymers with other vinyl compounds were obtained with extremely high polydispersities [22]. Also, metal catalyst residues make ATRP ineffective for biomedical applications [23]. Very recently, poly(MPC) copolymers have been prepared using soap free heterogeneous polymerization [24]. With the development of reversible addition-fragmentation chain transfer polymerization (RAFT) technique [25],[26],[27], an increasing number of polymers for biomedical devices were prepared via RAFT due to its compatibility with various solvents, ideal tolerance to a wide range of conditions and monomers, as well as no metal catalyst involvement [27]. The RAFT was employed in the synthesis of well-defined MPC polymers. Firstly, Yusa *et al.* [28] reported RAFT polymerization of MPC in water using a combination of 4,4'-azobis(4-cyanopentanoic acid) (ACVA) and 4-cyanopentanoic acid dithiobenzoate (CTP). The polymerization of MPC in water was found to be very fast. The reaction time was reported to be around 2 h. However, the polydispersity of resulting MPC polymer was relatively high ($M_w/M_n \sim 1.27$). Another factor is that the dissolution of solid phase ACVA and CTP in pure water was difficult, which may have directly affected the initial stages of the polymerization. Yu *et al.* [29] improved the protocol by adding 5 wt% NaHCO_3 . However, at least 4 h stirring in an ice-bath was still required for

the dissolution of ACVA and CTP.

Considering the above reasons as well as the significance of MPC polymers in the biomedical field, a detailed study of the RAFT polymerization of MPC in methanol has been carried out and its copolymerization with primary amine and sugar-based monomers is described.

The diblock copolymers of MPC unit with other monomer unit can be used to increase the specificity of a surface towards cell interaction. We have synthesized diblock copolymers of MPC with 2-aminoethyl methacrylamide hydrochloride (AEMA), 2-gluconamidoethyl methacrylamide (GAEMA), D-gluconaminoethyl methacrylate (GAMA) and 2-lactobionamidoethyl methacrylamide (LAEMA). AEMA is a cationic polymer and hence its copolymer with MPC can be used for DNA complexation [30]. GAEMA, GAMA and LAEMA are synthetic glycopolymers. Glycopolymers containing pendant saccharide groups are known to interact with proteins via multivalent interactions [31]. Depending upon the pendant saccharide groups, these monomers may be specific to particular biomolecules [32].

3.2 Experimental

3.2.1 Materials

The MPC with 7.0 ppm inhibitor was obtained from NOF, Co (Tokyo, Japan), which was synthesized by the method reported previously [1]. 2-Aminoethyl methacrylamide hydrochloride (AEMA) [33], 2-gluconamidoethyl methacrylamide (GAEMA) [32], D-gluconaminoethyl methacrylate (GAMA) [34], 2-lactobionamidoethyl methacrylamide (LAEMA) [35], were synthesized according to previous reports. The CTA, cyanopentanoic acid dithiobenzoate (CTP), was synthesized as previously described [36],[37]. 4,4'-Azobis(4-cyanovaleric acid) (ACVA) was purchased from Sigma Aldrich (Canada) and used as received. Methanol and HPLC grade water were purchased from Caledon Laboratory Chemicals (Canada). The structure of monomers, initiator and chain transfer agent used for the polymerization of MPC are shown in Figure 3-1.

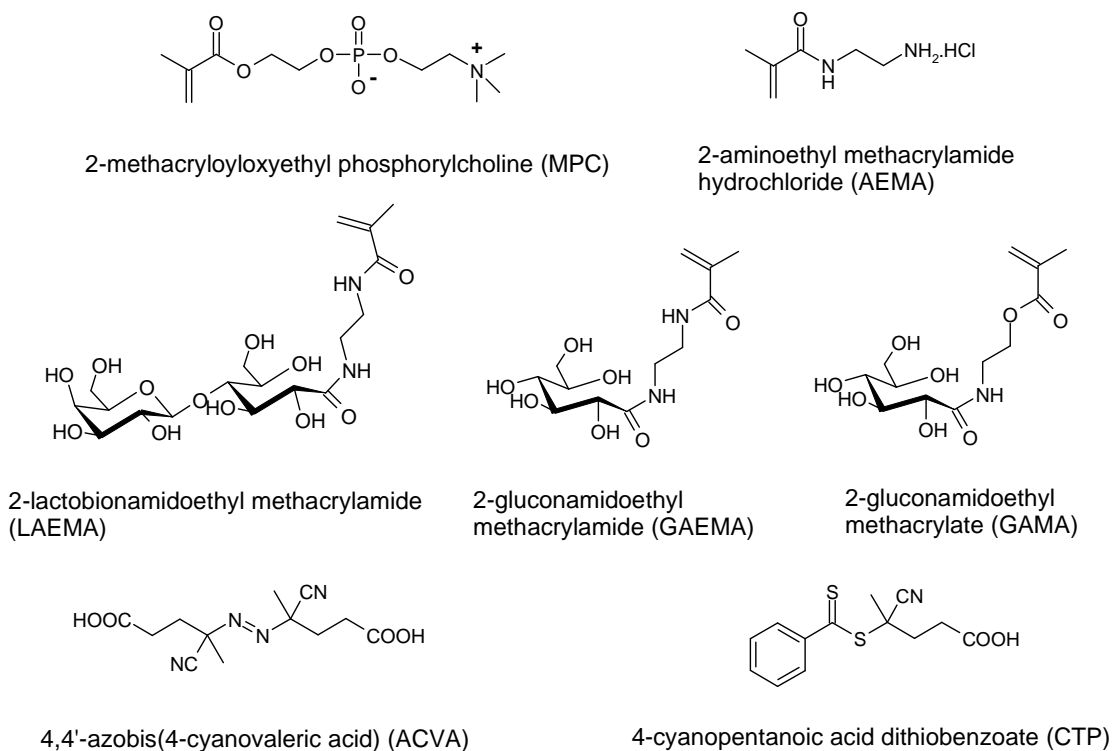


Figure 3-1: Structures of the monomers: MPC, GAEMA, LAEMA, AEMA and GAMA; initiator ACVA and Chain Transfer agent CTP

3.2.2 Methods

Number average molecular weight (M_n) and polydispersity (M_w/M_n) of the polymer samples were determined at a flow rate of 1.0 mL/min using Viscotek conventional GPC system equipped with two Waters Ultrahydrogel linear WAT011545 columns (pore size: blend, exclusion limit = 7.0×10^6) and Viscotek model 250 dual detector. 0.50 M sodium acetate/0.50 M acetic acid buffer was used as eluent. The GPC was calibrated by six near-monodispersed poly(ethylene oxide) (PEO) standards ($M_p - 1.01 \times 10^3 - 1.01 \times 10^5 \text{ g mol}^{-1}$). $^1\text{H-NMR}$ spectra of the polymers were recorded on a *Varian* 400 or 500 MHz instrument.

3.2.3 Homopolymerization of 2-Methacryloyloxyethyl Phosphorylcholine

Homopolymerization of MPC was conducted using RAFT technique, at 60 °C, The ACVA as the initiator and CTP as the CTA. In a typical protocol, in a 10 mL Schlenk tube, MPC (2.0 g, 6.8 mmol), CTP (0.030 g, 0.10 mmol, target $DP_n = 63$) and ACVA (1.5×10^{-2} g, 0.052 mmol) were dissolved in 6 mL methanol. The solution was then degassed via four freeze-vacuum-thaw cycles and placed in the 60 °C oil bath for 11 h. The conversion was determined by ^1H NMR spectroscopy using D_2O as solvent and by comparing the vinyl resonance of the monomer (appearing between 5.3 and 5.8 ppm) to the methyl resonance of the polymer (appearing between 0.5 and 1.4 ppm). The polymer was obtained by precipitating in a large quantity of acetone. The molecular weight and polydispersity were obtained from aqueous GPC after the methanol solution of polymer samples were dried in air. The resulting polymer molecular weight M_n was 1.4×10^4 g/mol, indicating more than 80 % conversion. The polydispersity (M_w/M_n) was around 1.1. The reaction scheme for homopolymerization of MPC in methanol is shown in Figure 3-2.

3.2.4 Synthesis of Diblock Copolymer with Poly (MPC) Segment:

The chain extension reaction was carried out using various monomers initiated from poly(MPC)-based macro-CTA. The synthesis of poly(MPC)-based macro-CTAs was carried out use the above mentioned procedure, employing 2:1 ratio of CTP/ACVA and quenched at ~ 60% conversion. A typical procedure for block copolymerization of MPC with GAEMA is as follows: the poly(MPC)-based

macro-CTA (0.20 g, 1.2×10^{-2} mmol, $M_n=1.6 \times 10^4$ g/mol; $M_w/M_n = 1.1$), GAEMA (0.22 g, 0.70 mmol) and ACVA (1.7×10^{-3} g, 5.8×10^{-3} mmol) were dissolved in 1.5 mL water. After degassing via four freeze-vacuum-thaw cycles, the solution was kept in 70 °C oil bath for polymerization. The polymers were obtained by precipitating in acetone. The residual GAEMA was removed by washing with *N,N'*-dimethyl formaldehyde (DMF). (In the case of AEMA and GAMA, the residual monomer was removed by washing with methanol.) Molecular weight from the typical polymerization reaction for the synthesis of poly(MPC₅₄-*b*-GAEMA₅₅) was 3.3×10^4 g/mol with a polydispersity of 1.3. The reaction scheme for di-block copolymerization of MPC with GAEMA is shown in Figure 3-3.

Note: In the synthesis of poly(MPC₅₄-*b*-AEMA₅₄), the polymerization can be also conducted at 60 °C in 1.5 mL methanol.

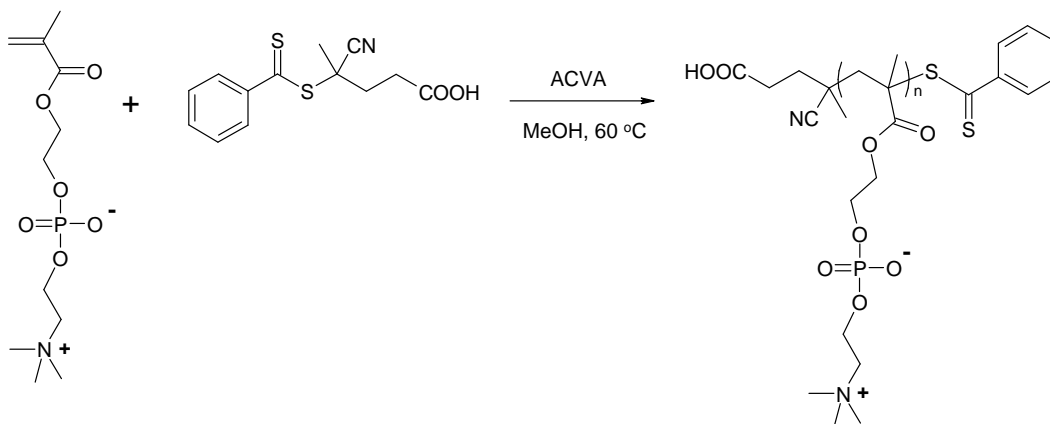


Figure 3-2 : Homopolymerization of poly(MPC) by RAFT technique in methanol at 60 °C, using ACVA as the thermally degradable initiator and CTP as the chain transfer agent.

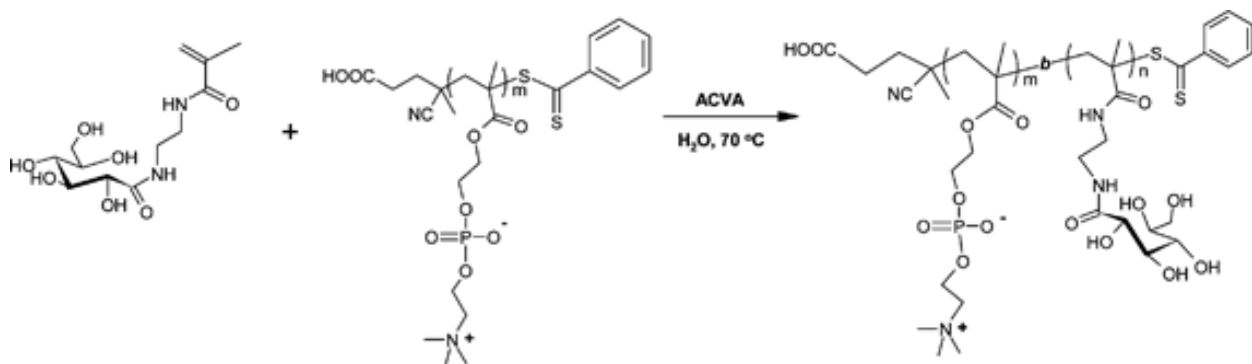


Figure 3-3 : Di-block copolymerization of poly(MPC) macroCTA with GAEMA in water at 70 °C in the presence of ACVA as the initiator.

3.2.5 Random Copolymerization of 2-Methacryloyloxyethyl phosphorylcholine:

The random polymers of MPC with LAEMA, GAEMA, GAMA or AEMA were made by adding the monomers in 1:1 molar ratio. A typical polymerization process for the copolymerization of GAEMA and MPC is given, MPC (0.19 g, 0.65 mmol) and GAEMA (0.20 g, 0.65 mmole) were dissolved in 2 mL water, followed by the addition of 0.30 mL 2-propanol stock solution of CTP (2×10^{-3} g, 8.0×10^{-3} mmol) and ACVA (1.0×10^{-3} g, 4.0×10^{-3} mmol). Acetic acid (0.2 mL) were added to prevent the hydrolysis of CTP in the aqueous solution [38]. The solution was kept in a 70 °C oil bath for polymerization. The reaction was stopped after 20 h by quenching in liquid nitrogen. The molecular weight was analysed in GPC and the composition was confirmed using $^1\text{H-NMR}$. The random copolymerization of poly(MPC-*stat*-AEMA) was carried out in methanol at 60 °C, as the AEMA is soluble in methanol. The molar weight (M_n) of the resulting

polymer, poly(MPC₅₀-stat-GAEMA₄₅), for the above procedure was 2.8×10^4 and the PDI was 1.19.

3.2.6 Synthesis of poly(MPC-*b*-AEMA-*b*-MPC) triblock copolymers:

The chain extension process was initiated by using poly(MPC) macroCTA. The synthesis was carried out in methanol using the above mentioned procedure. Triblock copolymers were synthesized using a typical protocol: poly(MPC) macroCTA (0.2 g, 1.6×10^{-2} mmol, $M_n = 12,469$ g/mol, M_w/M_n 1.19) and AEMA (0.21 g, 1.2 mmol) were dissolved in water. ACVA (2.2 mg, 8×10^{-3} mmol) stock solution in 2-propanol was mixed in the reaction mixture. This mixture was purged with nitrogen gas for 30 min. for degassing and the reaction was initiated by heating at 70 °C for 2 hours. Reaction was stopped by quenching in liquid nitrogen and the polymer was obtained by precipitating the final solution in acetone. The monomer was removed by washing the precipitate with methanol. The powder was then freeze dried to remove traces of acetone. The poly(MPC-*b*-AEMA) macroCTA was further used for the synthesis of tri-block copolymer. Poly(MPC-*b*-AEMA) macroCTA(0.1 g, 5.2×10^{-3} mmol, $M_n=18,455$ g/mol, $M_w/M_n = 1.26$) and MPC(0.125 g, 0.4 mmol) were dissolved in water and mixed with stock solution of ACVA (0.7 mg, 2.7×10^{-3} mmol) in 2-propanol. The reaction mixture was degassed by purging with nitrogen and the reaction was started by heating the solution at 70 °C. The final polymer was retrieved by precipitating in acetone. Any residual monomer was removed by washing the solution with water/acetone (1/7). The polymer was freeze dried and a pink powder was retained. The resultant polymer poly(MPC₄₂-*b*-AEMA₃₆-*b*-MPC₂₅)

was found to have a molecular weight of 36,000 g/mol and PDI 1.32.

3.3 Results and Discussion:

3.3.1 Detailed Kinetic Studies for the Homopolymerization of 2-Methacryloyloxyethyl phosphorylcholine

The RAFT technique was used for the homopolymerization of MPC. RAFT polymerization enables access to “site specific functionality” concurrently providing a control over molecular weight and molecular weight distribution [27]. As mentioned already, there have been studies on the polymerization of MPC using living polymerization techniques such as ATRP and RAFT. ATRP of MPC was extensively studied in methanol as solvent. However, a detailed study for the RAFT polymerization of MPC in methanol is still lacking. Therefore, in this work, the RAFT polymerization of MPC was conducted in methanol instead of water as solvent. Methanol provides a low viscosity solution for the preparation of high molecular weight polymers [39].

Synthesis of controlled molecular weight and low polydispersity polymers depends on several parameters. The choice of RAFT agent in the polymerization procedure largely affects these parameters. The use of CTP for this reaction was determined by comparing the polymer samples prepared without chain transfer agent and in the presence of two different CTAs, *S*-1-dodecyl-*S*-(α,α' -dimethyl- α'' -acetic acid) trithiocarbonate (CTAm) and CTP.

Table 3-1 shows a comparison of the results of various polymerization reactions carried out using CTP, CTAm or without CTA.

Table 3-1 : Effect of two different chain transfer agents, CTP and CTAm on homopolymerizations of poly(MPC) in two different solvents

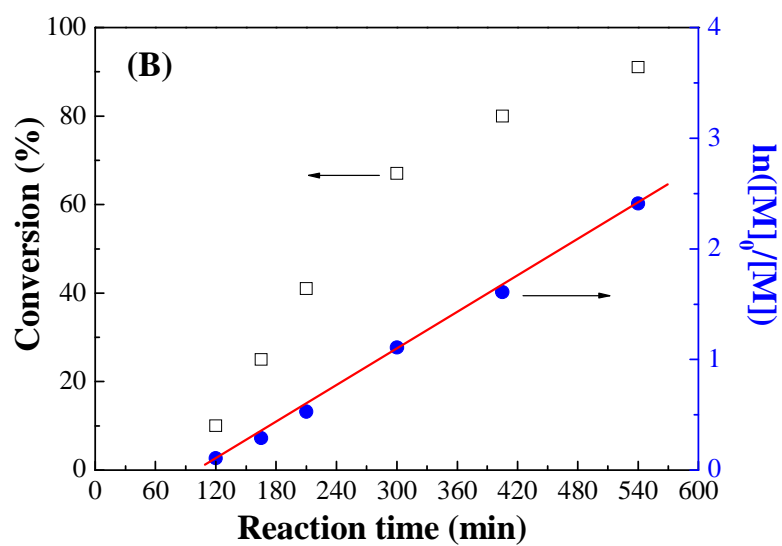
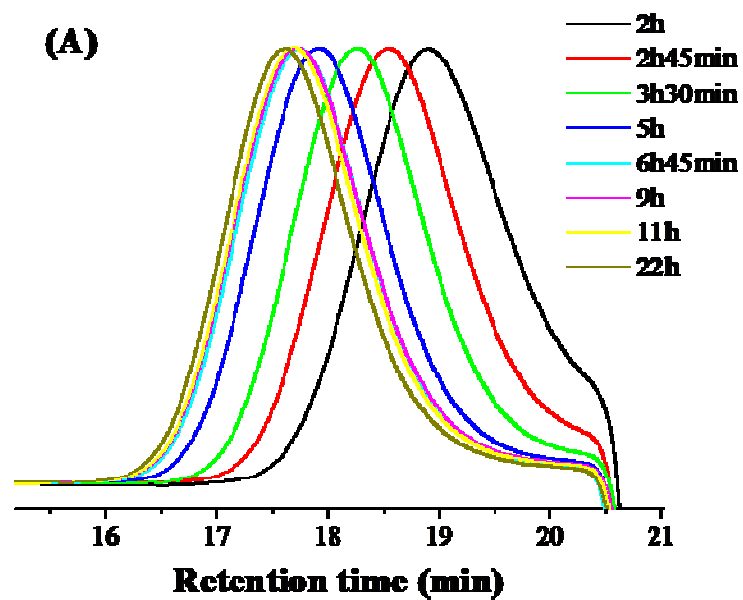
Code	CTA	Solvents	Target DPn	M_n (GPC) g/mol ($\times 10^4$)	M_w/M_n (GPC)
1.1	N/A	EtOH	-	3.89	1.66
1.2	CTAm	EtOH	60	1.81	1.57
1.3	CTAm	MeOH	60	2.18	1.72
1.4	CTP	MeOH	63	1.29	1.08

It was observed that without the addition of chain transfer agent, the molecular weight was about double than the target molecular weight. The molecular weight was found to be controlled when either the dithio-based CTP or trithio-based CTAm was employed. The polydispersity, however, was better controlled by using CTP as chain transfer agent. Similar results were also observed in the previous study of the RAFT polymerizations of LAEMA [35]. Moreover, CTP, as the chain transfer reagent, is compatible with a wide variety of monomers. Therefore, CTP was selected as the chain transfer agent for the RAFT polymerizations of the MPC.

Compared to the previous reports [28],[29] in which the polymerization of the MPC was conducted in water, methanol was chosen as solvent in this work to firstly eliminate the requirement for a long time of the dissolution of CTP and ACVA or any addition of salt. Moreover, water (if not acidified) can cause unwanted side reactions for example, hydrolysis of CTP, which can reduce the control over polymerization [38]. The rate of hydrolysis of CTP is found to be strongly temperature dependent. As reported by Levesque *et al.* [40], for a 24 h-

polymerization reaction in water, around 5.0-25% hydrolysis occurs at 20 °C. With the increase in temperature, this rate increases exponentially. For example, at 35 °C, 40-60% hydrolysis occurs over 24 h in pH range 7.5-8.5 [40]. To avoid this and to facilitate ease of dissolution of CTP in the solvent, methanol was preferred. Methanol, being a volatile solvent, the polymerizations was conducted at 60 °C and Schlenk tube was used to reduce the loss of solvent during the polymerization process.

Another important aspect in RAFT is the ratio of chain transfer agent to initiator. This ratio may affect the control of the polymerization. It turns out, in a fixed amount of CTA, the less initiator, the fewer radicals are generated and hence termination reactions and dead chains can be reduced. However, there is no obvious difference of the polydispersities was observed in our case (Table S1, Trail 1 (Appendix 1)). On the other hand, using less initiator usually slows down the pace of polymerization reaction. Considering the lower decomposition rate of ACVA in methanol [39], a CTP/ACVA ratio of 2.0 has been used in the polymerization unless otherwise mentioned. This was done to override the effect of organic solvent on the speed of polymerization reaction [41].



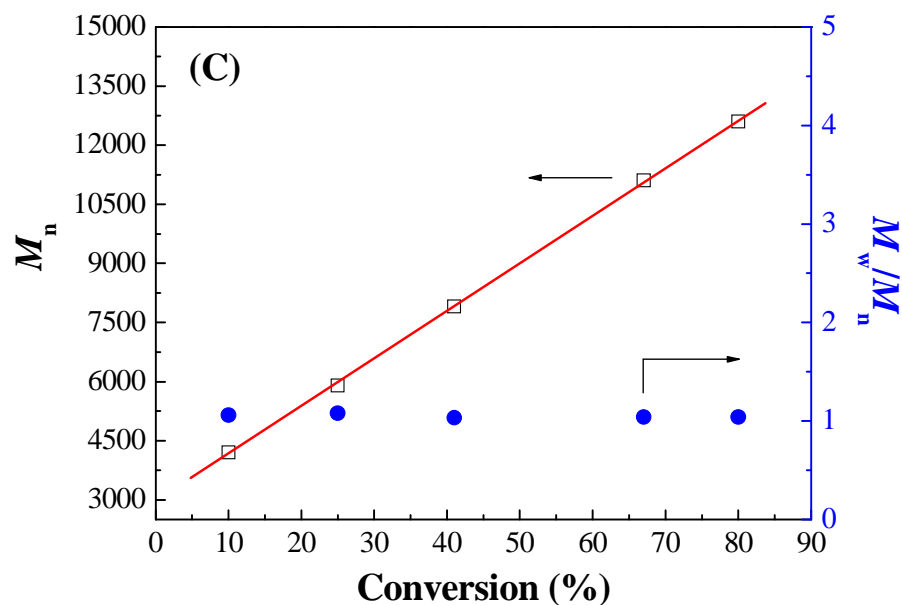


Figure 3-4 : (A) Shifts in GPC peaks with the RAFT homopolymerization of MPC in methanol, using ACVA as the initiator and CTP as the chain transfer agent at 60 °C with a target DP_n of 63 and CTP/ACVA = 2, (B) Semi-logarithmic and conversion plot vs. reaction time for RAFT polymerization of poly(MPC) for the above mentioned reaction conditions and, (C) Evolution of molecular weight of poly(MPC) with conversion, confirming living polymerization.

Figure 3-4 illustrates the kinetics of homopolymerization of MPC at the conditions described above. In the GPC trace (Figure 3-4 (A)), the shift in peaks to a shorter elution time indicates a gradual increase in the molar mass of the polymer with reaction time. Figure 3-4 (B) and (C) show the increase in conversion with time and the linear increase in molecular weight with conversion, respectively. $\ln([M_0]/[M])$ vs. reaction time is a straight line indicating a first order reaction with respect to the monomer concentration. Low polydispersities were also observed even in the high molecular weight polymer (e.g. $M_n = 1.26 \times 10^4$ g/mol, $M_w/M_n = 1.04$; $M_n = 2.18 \times 10^4$ g/mol, $M_w/M_n = 1.13$). Comparing to

previous reports ($M_n = 1.21 \times 10^4$ g/mol, $M_w/M_n = 1.12$ [28]; $M_n = 2.18 \times 10^4$ g/mol, $M_w/M_n = 1.27$ [28]), lower polydispersity may be due to the well dissolution of CTP and ACVA at the very beginning of the polymerization. All these factors showed that the polymerization of the MPC in methanol was carried out in a controlled manner. For a target degree of polymerization (DP_n) of 60, a high monomer conversion (>80%) was achieved after 10 h of reaction. Table S1 (Appendix 1) shows the synthetic parameters, molecular weights, and molecular weight distributions for the RAFT homopolymerization of the MPC.

Molecular weight was found to increase up to ~ 80 %. The slow increase of the molecular weight after 80% conversion in the kinetic study experiment may be due to the high viscosity of the solution. It should be noted that poly(MPC) with different (higher) DP_n as well as narrow-molecular weight distribution were also successfully synthesized (Figure S1 in Appendix 1).

A summary of polymerization kinetics is shown in Table 3-2. The results show that for higher CTP/ACVA ratio (of 5:1), the reaction is slower and takes almost twice the amount of time to complete the reaction as compared to CTP/ACVA ratio of 2. We noted that there was no difference between the polydispersities of the two polymers (with different CTP/ACVA ratios).

With a fixed mole ratio of monomer to chain transfer agent, the solution concentrations and amount of initiator were varied to study the kinetics of the reaction. The results showed that the rate of the polymerizations strongly depended on the concentration of initiator: the higher concentration of the initiator used, the faster polymerization obtained (Figure 3-5). For the same CTP/ACVA

ratio with higher concentration of monomer (1.12 M), a faster rate of polymerization was observed (Table 3-3).

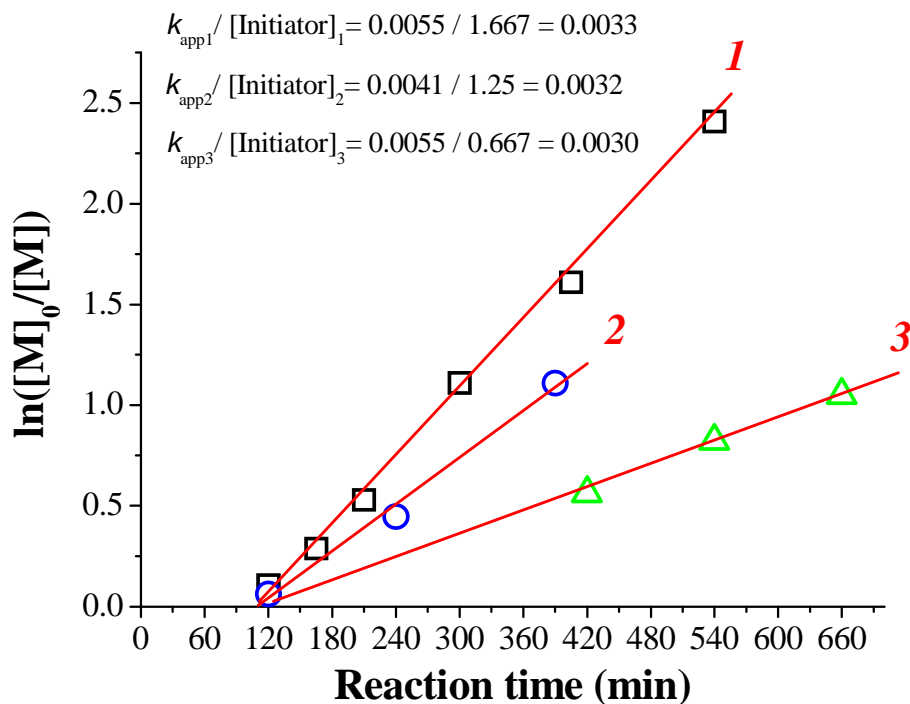


Figure 3-5 : Kinetic plot of the homopolymerization reaction of poly(MPC) in methanol at 70 °C, with varying concentrations and CTP/ACVA ratio: (1) CTP/ACVA=2, (2) CTP/ACVA=2 and (3) CTP/ACVA = 5, and varying concentrations, (1) 1.12 M, (2) 0.85 M, (3) 1.12 M

Table 3-2 : Evolution of molecular weight and low PDI shown as the effect of higher CTP/ACVA ratio of 5:1

Code	Reaction Time (h)	Conv.% (NMR)	M_n (Theory) g/mol ($\times 10^4$)	M_n (GPC) g/mol ($\times 10^4$)	M_w/M_n (GPC)
3.1	7	43	1.03	8.4	1.08
3.2	9	56	1.33	1.01	1.11
3.3	11	65	1.54	1.12	1.10
3.4	23	78	1.84	1.34	1.13

Table 3-3 : Effect of monomer concentration on the molecular weights and polydispersity of the resulting homopolymer

Code	[Monomer] (M)	Conv.% (NMR)	M_n (Theory) g/mol ($\times 10^4$)	M_n (GPC) g/mol ($\times 10^4$)	M_w/M_n (GPC)
2.1a	1.12	97	3.04	2.87	1.16
2.2a	0.84	98	3.08	2.81	1.17
2.2b	0.56	92	2.88	1.83	1.11
2.1b	0.42	69	2.17	2.18	1.13

All kinetics also brought out a similar inhibition time of 2.0 h in the polymerization process. This may be due to the fact that the monomer contains around 70 ppm of inhibitor. MPC monomer is highly hygroscopic, attempt to remove the inhibitor prior to the polymerization was unsuccessful.

3.3.2 Self-Chain Extension Experiment of MPC:

Poly(MPC)-based macro-CTA was obtained/purified by precipitating the polymer in acetone. Compared to the dialysis method, precipitation can effectively prevent

the hydrolysis of the macroCTA [42]. The accessibility of poly(MPC)-based macro-CTA was investigated in the self-chain extension experiments. The shift in the GPC peak after the sequential monomer addition confirmed the success of self-chain extension experiments. This formed the basis for the di-block copolymerization of MPC with other monomers.

From previous discussions, for the synthesis of the first block, the monomer concentration of 1.1 M proved to be the most effective. Subsequently, the effect of monomer concentration on the synthesis of the second block was studied (Figure S3 in Appendix 1). The results have been summarized in Table S2 (Appendix 1). The results indicated that higher monomer concentration helps in the better control of molecular weight distribution (Table S1, Trial 2 (Appendix 1)). Also, the lower monomer concentration was used in order to prevent an overly high viscosity of the solution during polymerization reaction. Another factor that was studied for the self-chain extension of MPC was the CTP/ACVA ratio. Interestingly, when comparing the polymerizations with various ratios of CTP/ACVA (Table S2, Trial 2 and 3 (Appendix 1)), no obvious difference of polydispersities was observed in the homopolymerizations (1.07 against 1.09), but the difference was significant in their corresponding self-chain experiments (1.16 against 1.21). Figure S2 (Appendix 1) shows the self chain extension of MPC using CTP/ACVA ratio of 5.0.

Similar results were also found in the self-chain experiments of LAEMA [35]. Probing into the classic RAFT mechanism the answer may be found in the main equilibrium stage. The chains generated from initiator ACVA and the chains

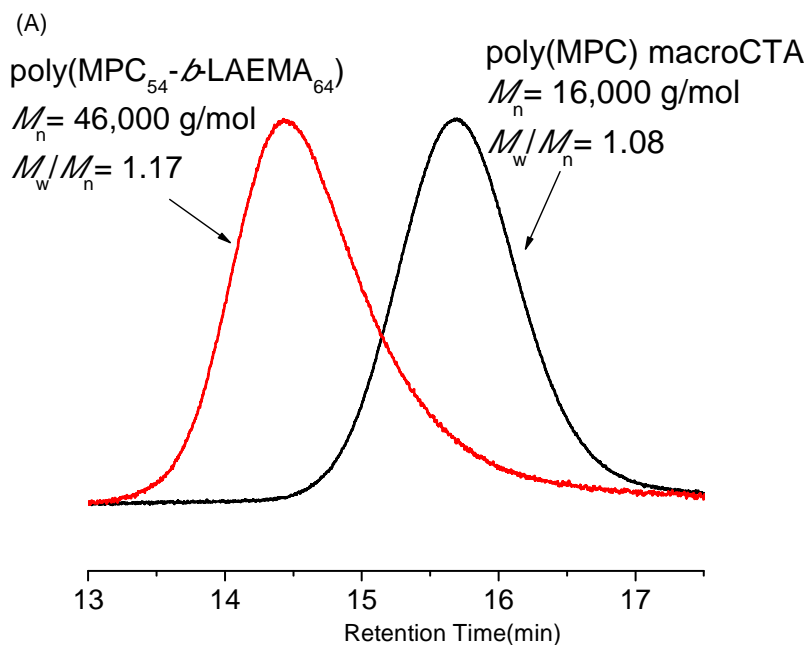
generated from the CTP leaving group have similar or even the same activity because of the same chemical structures. This maintained the equilibrium during the reaction. However, when the reaction was quenched, the “extra” (compared to the number of CTP mercapt groups) polymeric radicals became dead chains which could not be activated again. Therefore the difference in polydispersity was higher in the self-chain experiments.

3.3.3 Synthesis of Diblock and Random Copolymers of MPC with other Monomers:

The MPC was copolymerized with various monomers. The AEMA bearing primary amino group has been copolymerized with MPC in the past by Sakaki *et al.* [30]. The AEMA unit in the polymer has been used for the DNA complexation while, the second block, the poly(MPC) may increase the water solubility and biocompatibility of the copolymer. It was observed that the biocompatibility, water solubility and nuclear resistance of the poly(MPC-*stat*-AEMA) was better than those of the conventional cationic DNA carrier poly(L-lysine). Similarly, the motivation behind copolymerization of MPC with the synthetic glycopolymers is that these polymers contain saccharide moieties and thus entail various biological functions such as cell growth regulation, adhesion to specific biomolecules etc. The biological applications of these polymers have been well studied by Narain *et al.* [32].

Generally, the copolymerizations were conducted in a mixture of H₂O and water miscible organic solvent because of the poor solubility of the second monomers and corresponding polymers in pure organic solvents. H₂O was acidified by the

addition of small amount of acetic acid to reduce the hydrolysis of CTA [38]. As shown in Figure 3-6 and Figure 3-7 and S4 (a),(b) and S5 (a),(b) (Appendix 1) in the diblock copolymerization experiments, a clear shift to high molecular weight in the GPC traces was observed in all cases indicating the success in blocking of these monomers on MPC.



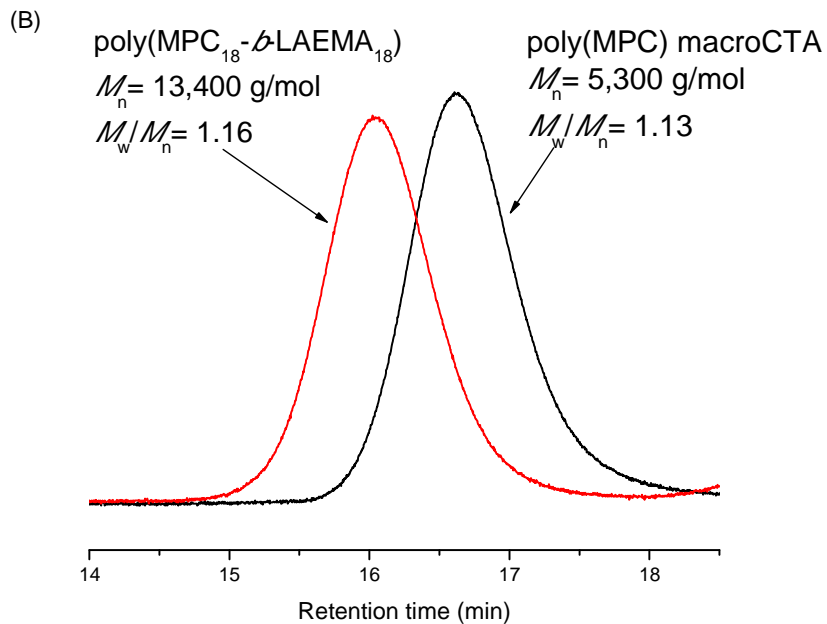
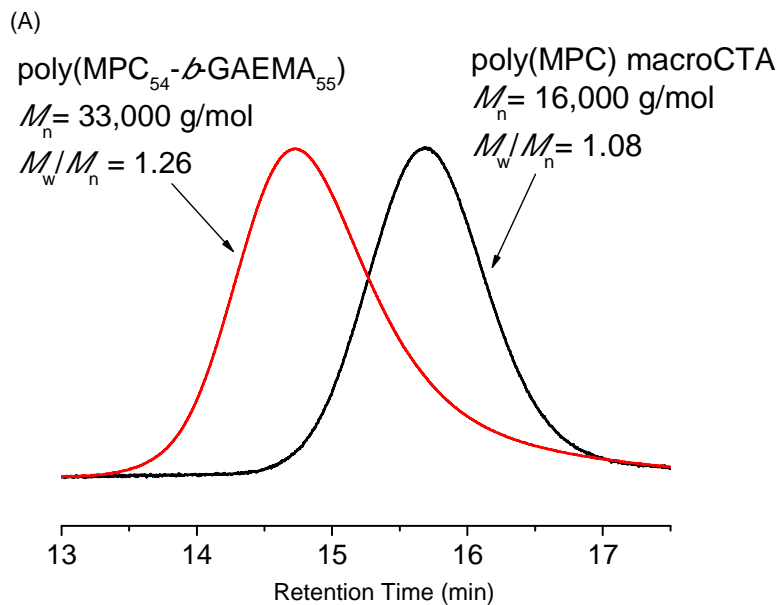


Figure 3-6 : Diblock copolymerization of LAEMA with MPC using sequential monomer addition, forming (A) poly(MPC₅₄-*b*-LAEMA₆₄) and (B) poly(MPC₁₈-*b*-LAEMA₁₈).



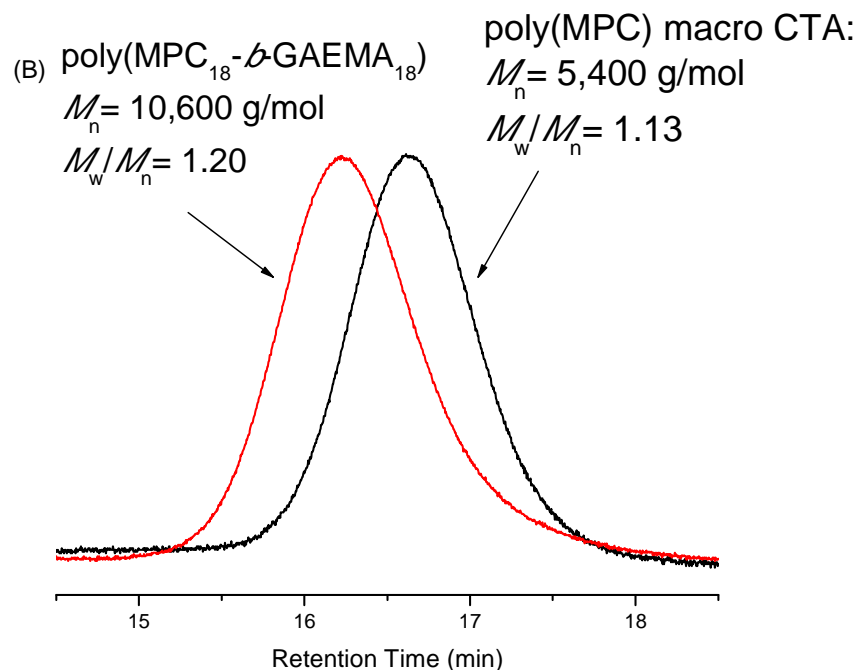


Figure 3-7 : Diblock copolymerization of GAEMA with MPC using sequential monomer addition, forming (A) poly(MPC₅₄-*b*-GAEMA₅₅) and (B) poly(MPC₁₈-*b*-GAEMA₁₈)

Different DP_n values were also targeted in the diblock copolymerizations. A slight broadening of GPC traces were found in the samples with higher DP_n (Figure 3-6 (a) and Figure 3-7 (a), S4(a) and S5(a) (Appendix 1)) which may be due to the lower reactivity or the flexibility of the leaving group for the longer polymer chains (See also Table S3 (Appendix 1)). Another interesting observation was that poly (MPC)-based macroCTA, which is an ester, was compatible with all amide monomers used in this work. For instance, copolymers with low PDI were successfully synthesized in the diblock copolymerization of MPC with GAEMA (amide) and GAMA (ester). The DP of the resulting copolymer was found to be

slightly higher than what was actually targeted. This may have happened due to the termination of primary radicals before their addition to the monomer. This results in lower initiator efficiency [23]. Similar to the synthesis of diblock copolymers, triblock copolymers were synthesized as shown in Figure 3-8 with low polydispersities. The graph shows the shifting of peaks with the addition of each block.

Random copolymerization of MPC, on the other hand, yielded 80% conversion (Table 3-4). NMR was used to determine the ratio of monomer ratios in statistical copolymers (Figure S6 (Appendix 1)).

Table 3-4 : Molecular weights and molecular weight distribution of statistical copolymers of MPC. Compositions determined by ^1H NMR and GPC

Code	Statistical Copolymers of MPC	M_n (Theory) g/mol ($\times 10^4$)	M_n (GPC) g/mol ($\times 10^4$)	M_w/M_n (GPC)
4.1	Poly(MPC _{42-stat} -LAEMA ₄₂)	4.5	3.2	1.25
4.2	Poly(MPC _{50-stat} -GAEMA ₄₅)	3.6	2.8	1.19
4.3	Poly(MPC _{58-stat} -GAMA ₄₈)	3.61	3.2	1.20
4.4	Poly(MPC _{52-stat} -AEMA ₄₃)	2.7	2.2	1.25

Diblock copolymerization of MPC with AEMA can be carried out in pure methanol as solvent. AEMA concentration of 0.25 M was recommended because the high viscosity of the reaction solution at the end of the polymerization. The polydispersity of the resulting diblock copolymer was observed as low as 1.2 while similar experiment conducted in H₂O resulted in a copolymer $M_w/M_n = 1.3$.

This result also indicted the advantage of using methanol as solvent. But higher

target molecular weights of poly(MPC-*stat*-AEMA) cannot be synthesized in methanol. It has been observed that the copolymer formed precipitates out before the reaction can complete, hence, giving low molecular weight polymers. This can be explained by the fact that poly (MPC) segment increases the solubility in methanol. But as the reaction proceeds and the poly(MPC-*b*-AEMA) chain length increases, the solubility of the copolymer decreases due to incompatibility with the solvent.

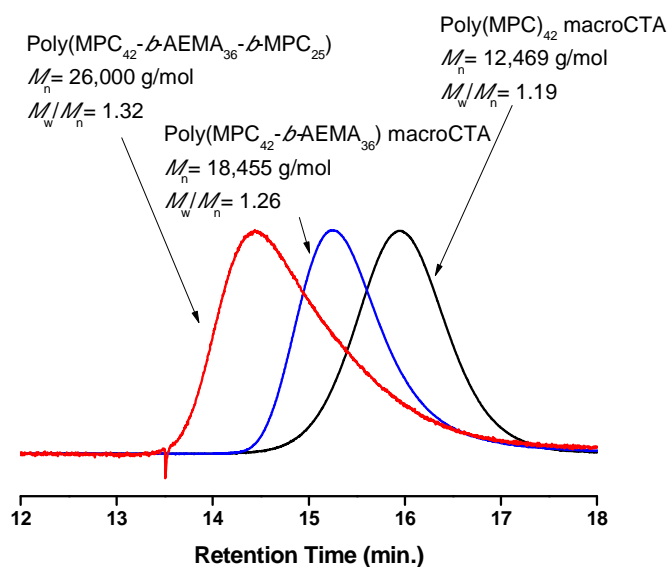


Figure 3-8 : Triblock copolymerization of AEMA with MPC using sequential monomer addition, forming poly(MPC₄₂-*b*-AEMA₃₆-*b*-MPC₂₅)

3.4 References:

- [1] Ishihara, K., Ueda, T., Nakabayashi, N.; *Polym. J.*, **1990**, *22*, 355-360
- [2] Yuan J., Armes S., Takabayashi Y, Prassides K., Leite C., Galembeck F., Lewis A; *Langmuir*, **2006**, *22*, 10989-93
- [3] Iwasaki Y., Ishihara K.; *Anal Bioanal. Chem.* , **2005** , *381*, 534–546
- [4] Ishihara, K., Aragaki, R., Ueda, T., Watanabe, A., Nakabayashi, N.; *J Biomed Mater Res*, **1990**, *24*, 1069-1077
- [5] Ishihara, K., Ziats, N., Tierney, B., Nakabayashi, N., Anderson, J.; *J Biomed Mater Res*, **1991**, *25*, 1397-1407
- [6] Ishihara, K., Arai, K., Nakabayashi, N., Morita, S., Furuya, K.; *J Biomed Mater Res*, **1992**, *26*, 937-945
- [7] Ishihara, K., Nomura, H., Mihara, T., Kurita, K., Iwasaki, Y., Nakabayashi, N.; *J Biomed Mater Res*, **1998**, *39*, 323-330
- [8] Yan L., Ishihara K., *J Poly. Sci.: Part A: Poly. Chem.*, **2008**, *46*, 3306–3313
- [9] Enomoto K., Hasebe T., Asakawa R., Kamijo A., Yoshimoto Y., Suzuki T., Takahashi K., Hotta A.; *Diam and Rel Mat* ,**2010**, *19*, 806-813
- [10] Lomas H., Du J., Canton I., Madsen J., Warren N., Armes S., Lewis A., Battaglia G; *Macromol Biosci* ,**2010**, *10*, 513-530
- [11] Nam K., Kimura T., Funamoto Seiichi., Kishida A.; *Acta Biomat* , **2010**, *6*, 403-408
- [12] Xu Y., Takai M., Ishihara K.; *Ann Biomed Eng*, **2010** , *38*, 1938-53

- [13] Kyomoto M., Moro T., Takatori Y., Kawaguchi H., Nakamura K., Ishihara K.; *Biomaterials* , **2010**, *31*, 1017-24
- [14] Shimizu T., Goda T., Minoura N., Takai M., Ishihara K.; *Biomaterials* ,**2010**, *31*, 3274-80
- [15] Lewis L.; *Colloids Surf., B: Biointerfaces* **2000**, *18*, 261-275.
- [16] Lewis L., Hughes P., Kirkwood L.; Leppard S.; Redman, Tolhurst, L., Stratford, P. ; *Biomaterials*, **2000**, *21*, 1847-1859
- [17] Moro, T.; Takatori, Y.; Ishihara, K.; Konno, T.; Takigawa, Y.; Matsushita, T.; Chung, U. I.; Nakamura, K.; Kawaguchi, H. *Nat. Mater.* **2004**, *3*, 829-836
- [18] Katakura O., Morimoto N., Iwasaki Y., Akiyoshi K., Kasugai S.; *J Med Dent Sci*, **2005** , *52*, 115-121
- [19] Kyomoto, M.; Moro, T.; Saiga, K.; Miyaji, F.; Kawaguchi, H.; Takatori, Y.; Nakamura, K.; Ishihara, K. *Biomaterials*, **2010**, *31*, 658-668
- [20] Wang C., Javadi A., Ghaffari M., Gong S.; *Biomaterials*, **2010**, *31*, 4944-4951
- [21] Iwasaki, Y.; Takamiya, M.; Iwata, R.; Yusa, S.; Akiyoshi, K.; *Coll and Surf B: Bioint* **2007**, *57*, 226–236
- [22] Lobb E., Ma Y., Billingham N., and Armes S.; *J. Am. Chem. Soc.* **2001**, *123*, 7913-7914
- [23] Matyjaszewski K., Davis T.P., *Handbook of Radical Polymerization*, **2002**, Wiley Interscience.

- [24] Kojima, R.; Kasuya, M C Z.; Ishihara, K.; Hatanaka, K.; *Polym J* **2009**, *41*, 370–373.
- [25] Chiefari, J.; Chong, Y. K.; Ercole, F.; Krstina, J.; Jeffery, J.; Le, T. P. T.; Mayadunne, R. T. A.; Meijs, G. F.; Moad, C. L.; Moad, G.; Rizzardo, E.; Thang, S. H. *Macromolecules* **1998**, *31*, 5559–5562.
- [26] Moad G; Rizzardo E.; Thang H.; *Acc. Chem. Res.* **2008**, *41*, 1133–1142.
- [27] Boyer, C.; Bulmus, V.; Davis, T. P.; Ladmiral, V.; Liu, J.; Perrier, S. *Chem. Rev.*, **2009**, *109*, 5402–5436.
- [28] Yusa S.; Fukuda K.; Yamamoto T.; Ishihara K.; Morishima Y. *Biomacromolecules*, **2005**, *6*, 663-670
- [29] Yu B., Lowe A., Ishihara K.; *Biomacromolecules* **2009**, *10*, 950–958.
- [30] Sakaki S., Tsuchida M., Iwasaki Y., Ishihara K.;, *Bull Chem Soc Jan*, **2004**, *77*, 2283-2288
- [31] Miura Y.; *J. Polym. Sci.: Part A: Polym. Chem.* **2007**, *45*, 5031–5036
- [32] Deng, Z., Ahmed, M., Narain, R.; *J. Polym. Sci.: Part A: Polym. Chem.* **2009**, *47*, 614–627.
- [33] Deng, Z., Bouchékif, H., Babooram, K., Housni, A, Choytun, N., Narain, R.; *J. Polym. Sci.: Part A: Polym. Chem.* **2008**, *46*, 4984–4996.
- [34] Narain R.; Armes S.; *Biomacromolecules*. **2003**, *4*, 1746–1758.
- [35] Deng Z., Li S., Jiang X., Narain R.; *Macromolecules* **2009**, *42*, 6393–6405.

- [36] Mitsukami Y., Donovan M. S., Lowe A. B., McCormick, C. L. 831, *Macromolecules* **2001**, *34*, 2248–2256.
- [37] Lai, J. T.; Filla, D.; Shea, R., *Macromolecules* **2002**, *35*, 6754–6756
- [38] Thomas D., Convertine A., Hester R., Lowe A., and McCormick C., *Macromolecules* **2004**, *37*, 1735-1741
- [39] Lyoo W., Song D, Lee W., Han S. , Noh S., *J Appl Polym Sc.*, **2006**, *102*, 4831 – 4834
- [40] Levesque G., Arse`ne P., Fanneau-Bellenger V., Pham T.; *Biomacromolecules* **2000**, *1*, 400-406.
- [41] Ma Y., Tang Y., Billingham N., and Armes S.P, Lewis A, Lloyd A and Salvage J.P., *Macromolecules* **2003**, *36*, 3475-3484
- [42] Vasilieva Y., Thomas, D., Scales, C., McCormick, C.; *Macromolecules* **2004**, *37*, 2728-273

4 Degradable Thermo-responsive Nanogels for Protein Encapsulation and Controlled Release

4.1 Introduction

Nanogels are nano-sized networks of swollen cross-linked polymers. These systems are increasingly being studied for their attractive properties in medicine and pharmacy [1-6]. Nano-sized particles have the advantage of “Enhanced permeation and retention” owing to their small size which also facilitates easy renal clearance [7]. Apart from their small size, extra stability in aqueous medium and high water retention, they can also be made to respond to the changes in the external environment, for example, temperature and pH. These so called “smart” nanogels are increasingly being considered for Drug Delivery Systems (DDS) [1, 8]. For example, change in size of pH controlled systems helps in controlled release of encapsulated drugs [9, 10]. Similarly, temperature sensitive nanogels undergo a phase change from hydrophilic to hydrophobic at a transition temperature. This temperature is called the Lower Critical Solution Temperature (LCST). Methoxydiethylene glycol methacrylate (poly(MeODEGM)) and poly(N-isopropylacrylamide) (poly(NIPAM)) are examples of thermo-responsive polymer. NIPAM has a LCST of 34 °C (very close to body temperature) [9, 11]. However, its use in biological studies is discouraged because of its toxicity. MeODEGM, on the other hand, is widely used in medicine and pharmacy because of its excellent biocompatibility. The LCST of MeODEGM is 24 °C [12, 14].

In order to be used as DDS, surface functionalization of nanogels with organ

specific ligands can be done to target specific tissues or organs. Nanocarriers have known to show very high drug loading capacity (sometimes as high as 800%) [15]. The success of using such nanocarriers relies on their ability for a controlled release of encapsulated drugs.

Nanogels have been synthesized using various approaches: physical self assembly, covalent cross-linking of pre-formed polymers and template supported nanofabrication [16]. Free emulsion or precipitation polymerization is an easy way to produce nano-micelles where ionic surfactants are used to stabilize these nanoparticles in water. Whereas emulsion polymerization is carried out in an aqueous medium and the core consists of the hydrophobic monomer, inverse mini-emulsion polymerization technique is used for hydrophilic monomers like N-vinyl caprolactam [17, 18]. The presence of surfactants at the critical micelle concentration (CMC) induces toxicity to the nanogel and hence is not viable for in vivo studies. Also, removal of surfactants from the nanogel is not easy. Self assembly of amphiphilic polymers is another approach which eliminates the need of surfactants for the synthesis.

Wooley *et al.* have synthesized tri-block crosslinked micelles forming stabilized nanogels [19-22]. Multi-responsive polymeric micelles which respond to changes in both pH and temperature have been synthesized by Kuckling *et al.* [3].

Various living polymerization techniques are used for the synthesis of nanogels to maintain control over molecular weights and polydispersity of the polymer units [7]. These techniques include Ring opening polymerization, Ring opening metathesis polymerization, Cyanoxyl-mediated free radical polymerization, Atom

transfer radical polymerization (ATRP), and Nitroxide-mediated polymerization (NMP) [23, 24]. Reversible Addition-Fragmentation Chain Transfer Polymerization (RAFT) is a suitable technique for polymerization and is very popular for biological applications [25, 26]. Micelles containing RAFT agents are easy to crosslink and thus form core cross-linked [27-29], shell cross-linked [30, 31] or nexus between both [32, 33].

Self assembly of the amphiphilic copolymers in water leads to the formation of micelles. But under special conditions, like low concentration or high ionic environment, these micellar structures may not exhibit a strong amphiphilic character and hence be unstable in aqueous solution, exist as unimers [32, 34]. Crosslinking of polymers can play a significant role in imparting the required stability. This technique combines self-assembly and crosslinking and provides excellent control over the “spatial distribution of polymeric chains” in an aqueous solution [16].

Cross-linkers that degrade or hydrolyze under special conditions, for example, low pH, reductive environment or presence of DTT are conducive for drug delivery as their degradation causes the release of encapsulated macro-molecules. Encapsulation of a drug prevents its fast clearance from body [32]. Responsive nanogel systems have shown to control the activity of biopolymers and at the same time, controlling the release of a therapeutic [22, 35, 36]. Previous reports have shown that nanoparticles and nanogels increase the stability of trapped enzymes/proteins against degradation and denaturation and modulated release of these biomolecules at specific or targeted sites [37-40]. Protein encapsulation in

nanogels, microgels, nanotubes and nanoparticles is being intensively studied and these systems have shown immense potential in drug delivery systems [37, 41-43]. Protein encapsulation in hydrogel systems and controlled release of insulin, lysozyme, calcitonin, interleukin-2 has been studied intensively [22, 44-46].

The present study entails the synthesis, characterization and application of thermo responsive, acid degradable core-crosslinked nanogels. Solubility of the nanogels is attributed to the hydrophilic MPC shell. 2-methacryloyloxyethyl phosphorylcholine (MPC) is a well-known amphiphilic compound. The phosphorylcholine group on the methacrylate monomer well resembles the polar phospholipid group present on the cell membrane. Hence, MPC polymers show very high biocompatibility and various copolymers of MPC are popularly used for bio-medical applications [47-49]. The core comprises of MeODEGM and AEMA cross-linked with an acid degradable cross-linker. The thermo-responsive MeODEGM core swells and shrinks with the change in temperature which helps the entrapment of drug. A cationic monomer, AEMA can be used for an oppositely charged oligomer or protein.

A range of pH domains is found in human body. For example, while physiological pH is 7.5, pH in endosomes and lysosomes are 5.5-6 and 4-5 respectively. The cross-linker is acid degradable and the release of encapsulated protein was evaluated as a function of pH. Size trends and polydispersities of various nanogels synthesized by RAFT polymerization method have been analyzed. Protein encapsulation and release from such nanogels has been evaluated and compared for different cross-linker concentrations.

4.2 Experimental:

4.2.1 Materials:

2-Methacryloyloxyethyl phosphorylcholine (MPC) was obtained from NOF, Co (Tokyo, Japan), which was synthesized by a method reported previously [50]. Hydroxyethyl methacrylate (HEMA), di-methoxy propane , p-toluene sulphonic acid, methoxydiethylene glycol methacrylate (MeODEGM) and 4,4'-azobis-(cyanovaleric acid) (ACVA) were ordered from Sigma Aldrich (Canada) and were used as obtained. 2-Aminoethyl methacrylamide Hydrochloride (AEMA) [51] and 4-cyanopentanoic acid dithiobenzoate (CTP) [52, 53] was synthesized as described according to previous reports. 2-propanol, HPLC grade water and acetone were purchased from Caledon Laboratories (Canada).

Micro BCA assay kit was obtained from Fisher Scientific. Gwiz β -galactosidase was purchased from Aldevron. Bovine serum albumin (BSA) was purchased from Promega Corporation. Insulin was obtained from Sigma Aldrich.

The structures of monomers, initiator and chain transfer agent are shown in Figure 4-1.

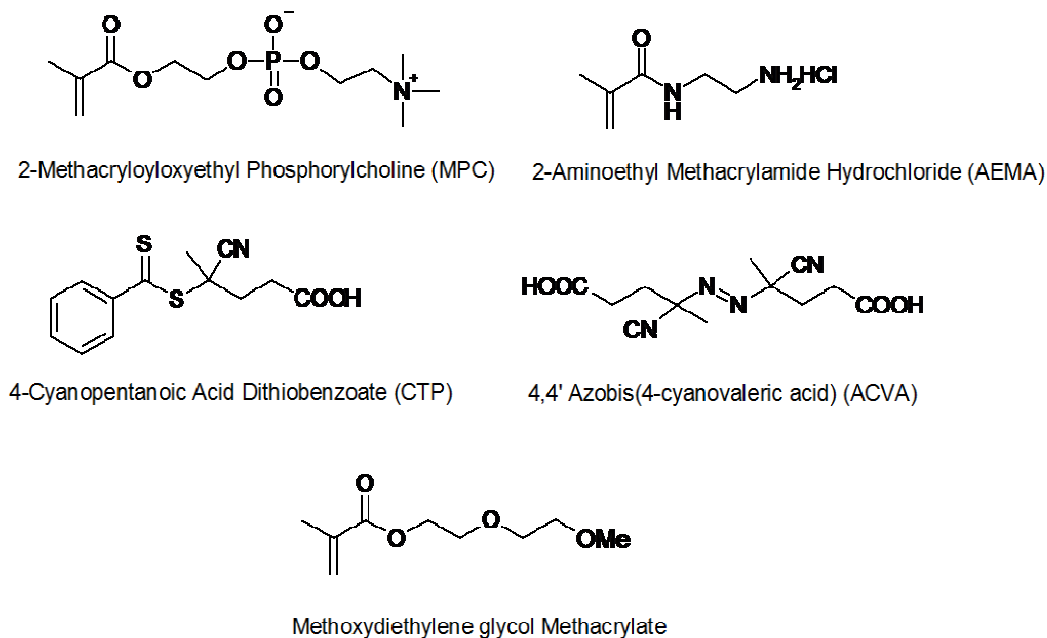


Figure 4-1: Structures of monomers (MPC, MeODEGM and AEMA), Chain Transfer Agent (CTP) and initiator (ACVA)

4.2.2 Synthesis of 2,2-Dimethacroyloxy-1-ethoxypropane (cross-linker):

The cross-linker has been reported by Aspinwall and coworkers [54]. However, the synthesis has been carried out at different conditions. HEMA (2-Hydroxyethyl methacrylate) (10 g, 76.8 mmol) and Di-methoxy propane (4.0 g, 38.4 mmol) were mixed together in a 25 mL reactor. Toluene Sulfonic Acid (p-TSA) (66 mg, 0.34 mmol) was added as catalyst. Hydroquinone (50 mg, 0.45 mmol) was added to the reaction mixture to avoid self-polymerization of the resulting cross-linker. The reaction was carried out at 20 °C for 6 hours. The reaction was not run for a longer period to avoid the occurrence of possible side reactions. A pale yellow oil was recovered at the end of the reaction. The cross-linker was purified by column chromatography using mobile phase of hexane, ethyl acetate and Tri-ethyl Amine.

The product was kept under vacuum line for 4 hours to remove any traces of low boiling HEMA. The cross-linker was stored at 4-8 °C.

4.2.3 Synthesis of poly(MPC) macroCTA by RAFT polymerization:

MPC macroCTA was synthesized as previously reported [55]. MPC (3 g, 10.2 mmol), CTP (2.8×10^{-2} g, 0.1 mmol) and ACVA (1.4×10^{-2} g, 0.051 mmol) were dissolved in 9 mL methanol in a 25 mL reactor. The solution was degassed by purging nitrogen for 30 minutes and then placed for stirring at a temperature of 60 °C for 6 hours. The polymer was obtained by precipitating the mixture in acetone. Any remaining traces of monomer were removed by washing the solution in water-acetone (1:7). The precipitate was again washed with acetone for 3-4 times and the final powder was freeze dried. The poly(MPC) macroCTA molecular weight and PDI were found to be 1.2×10^4 g/mol and 1.21, respectively.

4.2.4 Synthesis of poly(MPC-*b*-(MeODEGM-*stat*-CL-*stat*-AEMA)) nanogel by RAFT polymerization:

Poly(MPC) macroCTA (3.9×10^{-2} g, 3.3×10^{-3} mmol), MeODEGM (0.2 g, 1.1 mmol), AEMA (4.4×10^{-2} g, 0.26 mmol), CL (6.0×10^{-2} g, 0.19 mmol) (15% monomer concentration) were dissolved in 4 mL water and sonicated. ACVA (4.0×10^{-4} g, 1.6×10^{-3} mmol) was dissolved in 1 mL 2-propanol and added to the reaction mixture. The solution was degassed by purging with Nitrogen for 30 minutes and the reaction was carried out at 70 °C for 24 hours. Reaction was stopped by quenching in liquid nitrogen. Nanogel was centrifuged at 14000 rpm and 40 °C. The supernatant was discarded and the precipitate was washed with

distilled water 3-4 times. The final precipitate was dissolved in water and freeze dried overnight. A white powder was recovered and stored in refrigerator.

4.2.5 Protein Encapsulation:

Drug loading was done using incubation method. Aqueous solutions of nanogels were prepared in 10 mg/mL concentrations. The nanogel solution was mixed with 3.0×10^2 μ L solution of 1mg/mL BSA solution and left to incubate for 24 hours at 4 °C.

The total amount of protein encapsulated was calculated after centrifuging the sample at 40 °C in Beckmann Coulter Centrifuge (Microfuge 22R) (14000 rpm, 15 minutes). The solution was separated into a white precipitate and supernatant. The amount of protein encapsulated in the nanogel was measured by incubating with Bicinchoninic acid (BCA assay) for 2 hours at 37 °C and reading the absorbance at 570 nm using TECAN Genios Pro microplate reader. The plate reader was pre-calibrated using varying concentrations of protein and data was analyzed using Boltzmann function to give the best sigmoidal fit.

The amount of protein encapsulated (D) was calculated as follows:

$$D = \frac{\text{Total protein} - \text{Free protein}}{\text{Total protein}}$$

Where *free protein* is the protein in supernatant.

4.2.6 Release of Protein from nanogels at acidic pH:

In order to study the release of encapsulated protein, the nanogel was precipitated and re-dispersed in a citrate buffer solution of pH 4.8 and 6.4. The solution was

divided into 7 aliquots. At regular intervals, the nanogel aliquots were precipitated and total protein content in the supernatant (released protein) was determined using BCA assay.

4.2.7 Activity of protein:

The activity of β -galactosidase protein encapsulated in nanogel was studied by β -galactosidase assay. The nanogel was precipitated and separated from the supernatant (solution 1). The precipitate was redispersed in 100 μ L sodium phosphate buffer solution (solution 2). 150 μ L o-nitrophenyl- β -D-galactopyranoside (ONPG) (4 mg/mL) was added to 100 μ L solution 1 and 2 in the presence of 4.5 μ L 100X Mg solution (0.64 μ L of β -Mercaptoethanol in 100 μ L of 0.1M MgCl₂) in a 96 well plate and was incubated for 4 hours at 37 °C. The yellow colour developed was detected using the TECAN Genios pro microplate reader at 420 nm.

4.2.8 Characterizations:

Nuclear Magnetic Resonance: ¹H and ¹³C -NMR spectra of the cross-linker were recorded on a Varian 500 MHz instrument. The sample was prepared using CDCl₃ as solvent.

MeODEGM shows thermo-responsive behaviour and undergoes coil to globule transition at a lower critical solution temperature (LCST) of 24 °C. This transition was also studied at a molecular level by NMR spectroscopy in D₂O. The signal intensities of MeODEGM protons vs. that of solvent protons were compared at various temperatures (below and above the LCST). To account for the chemical

shift of signal intensities at elevated temperatures, 1% 4,4-dimethyl-4-silapentane-1-sulfonic acid (DSS) solution was added as a reference at 0 ppm.

Mass Spectroscopy: Mass spectroscopy was carried out in Agilent Technologies 6220 orthogonal acceleration TOF (oaTOF) (Santa Clara California, USA).

Gel Permeation Chromatography: The number average molecular weight (M_n) and polydispersity (M_w/M_n) of the macro CTA was studied using Viscotek conventional GPC connected to two Waters Ultrahydrogel linear WAT011545 columns (pore size: blend; exclusion limit= 7.0×10^6) and has a Viscotek model 250 dual detector. An acidic buffer of 0.50M sodium acetate /0.50M acetic acid was used as eluent. Calibration of GPC was done by six monodispersed poly(ethylene oxide) (PEO) standards ($M_p - 1.01 \times 10^3 - 1.01 \times 10^5 \text{ g mol}^{-1}$).

Dynamic Light Scattering: Size of MeODEGM nanogels was analyzed using Viscotek DLS 802 instrument which is equipped with a He-Ne laser at a wavelength of 632 nm and a Peltier temperature controller. The aqueous nanogel solution was filtered through a 0.045 μm pore size Millipore membrane. Data were obtained at an angle of 90° within a temperature range on 25-50 $^\circ\text{C}$. Omnisize software was used to record the DLS size data. 0.5 mL aliquots were drawn at 0 min, 30 min, 1 h, 2 h, 5 h, 18 h and 24 h of reaction time.

Transmission Electron Microscopy: Size and morphology of the nanogels were analyzed by Transmission Electron Microscopy (TEM) on Philips Transmission Electron Microscope fitted with CCD camera. The nanogel samples were coated on the TEM grid and Phospho-tungstic Acid (PTA) was used as a contrast agent.

4.3 Results and Discussion:

MeODEGM based core- cross-linked nanogels were successfully synthesized with an amphiphilic shell and a thermo-responsive core using RAFT polymerization method. These nanogels, degrade under acidic pH and the rate of degradation was dependent on both pH and cross-linker concentration. These acid degradable nanogels were used to study the encapsulation efficiency and the release profile of proteins.

4.3.1 Synthesis of 2,2-Dimethacroyloxy-1-ethoxypropane (cross-linker):

The pH in human body varies from 7.4 (physiological pH) to 5.5-6 in endosomes and 4-5 in lysosomes. Acid degradable crosslinker was synthesized for this study, to facilitate release of encapsulated proteins at low pH. The reaction of HEMA and 2-dimethoxy propane yields acid degradable cross-linker as shown in Figure S1(Appendix 2). Mole ratio 2:1 was used for the reaction. A pale yellow oil that was recovered after 6 hours of reaction was kept under vacuum line for 4 hours to get rid of any remaining traces of HEMA. It was observed that if the reaction was continued for more than the specified time of 6 hours, the product turned dark brown, which is possibly due to side reactions that start simultaneously. The cross-linker was stored in refrigerator at 4 °C to avoid these side reactions to take place. The ^1H and ^{13}C NMR of the purified cross-linker is shown in Figure S2 and Figure S3 (Appendix 2). ^1H NMR (ppm) : δ 1.27 (6H, $\text{C}(\text{CH}_3)_2$), 2.01 (6H, $\text{OCOCCH}_3\text{CH}_2$), 3.65 (4H, $\text{C}(\text{CH}_3)_2(\text{OCH}_2\text{CH}_2\text{O})_2$), 4.27 (4H, $\text{C}(\text{CH}_3)_2(\text{OCH}_2\text{CH}_2\text{O})_2$); 5.60 (2H, $\text{OCOCCH}_3\text{CH}_2$); 6.48(2H, $\text{OCOCCH}_3\text{CH}_2$).

^{13}C NMR (ppm): δ 17.9 (OCOCCH₃CH₂), 26.5 (C(CH₃)₂), 60.7 (C(CH₃)₂(OCH₂CH₂O)₂), 65.7 (C(CH₃)₂(OCH₂CH₂O)₂), 113.0 (C(CH₃)₂), 125.2 (OCOCCH₃CH₂), 136.0 (OCOCCH₃CH₂), 167.2 (OCOCCH₃CH₂).

MS: The calculated molecular weight of the cross-linker is 323.1465, found 323.1464, corresponding to the molecular formula C₁₅H₂₄NaO₆.

4.3.2 Synthesis of nanogels:

Core-shell nanogels were synthesized using acid degradable cross-linker, by RAFT polymerization technique. A one pot synthesis method developed by Pan et al. (56), which involves the polymerization of cross-linker with the monomer to get stabilized core cross-linked micelles, was followed for synthesizing nanogels. Therefore, in this RAFT polymerization process, cross-linking and polymerization happened simultaneously.

The core shell nanogel comprised of a temperature sensitive MeODEGM core along with a primary amine monomer AEMA, imparting an additional functionality to the core, crosslinked by an acid degradable cross-linker CL and an amphiphilic shell of MPC polymer chains (Figure 4-3) MPC macro CTA (M_n 1.2 $\times 10^4$ g/mol) was synthesized in methanol as discussed in previous protocol [55]. The conversion was kept low (60%) to prevent the formation of dead chains as a result of the termination reactions that set in towards the end of the reaction. The macro CTA was further used to copolymerize MeODEGM and AEMA in the presence of the cross-linker CL in water using ACVA as initiator. The use of ACVA as initiator is driven by two factors. First, it can be thermally decomposed and has a half life of 10 hours in aqueous solution at 69 °C and secondly, it is

slightly more hydrophilic than other thermally sensitive initiators like Azobisisobutyronitrile (AIBN). Tao *et al.* observed that a hydrophobic initiator interferes with the hydrophobic core and hence produces unstable micelles. On the contrary, ACVA, which is more hydrophilic, yields controlled and more stable nanogels [57].

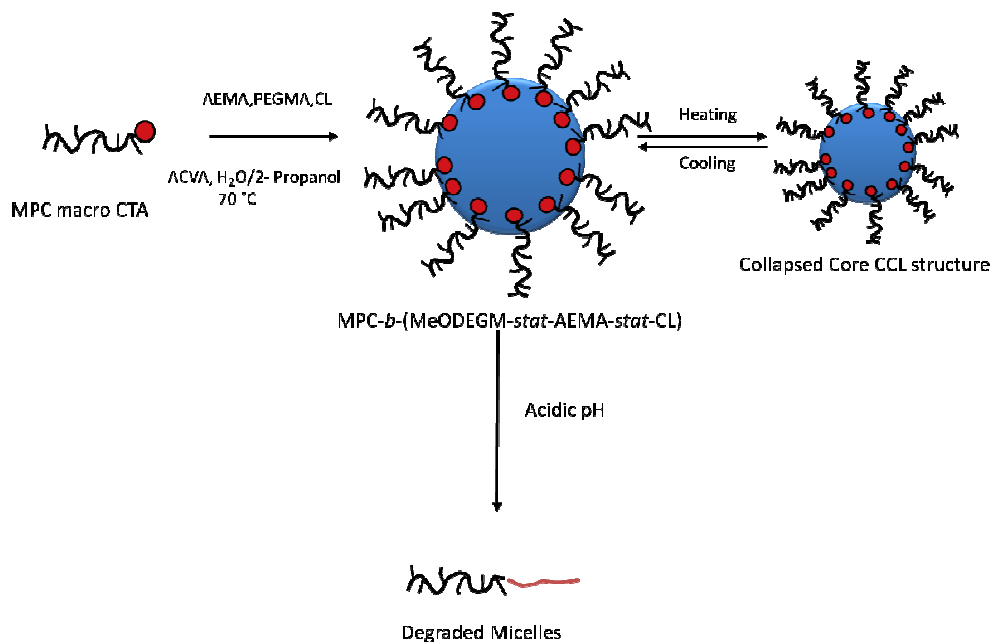


Figure 4-2: Schematic representation of core cross-linked micelles with thermo-responsive and degradable core

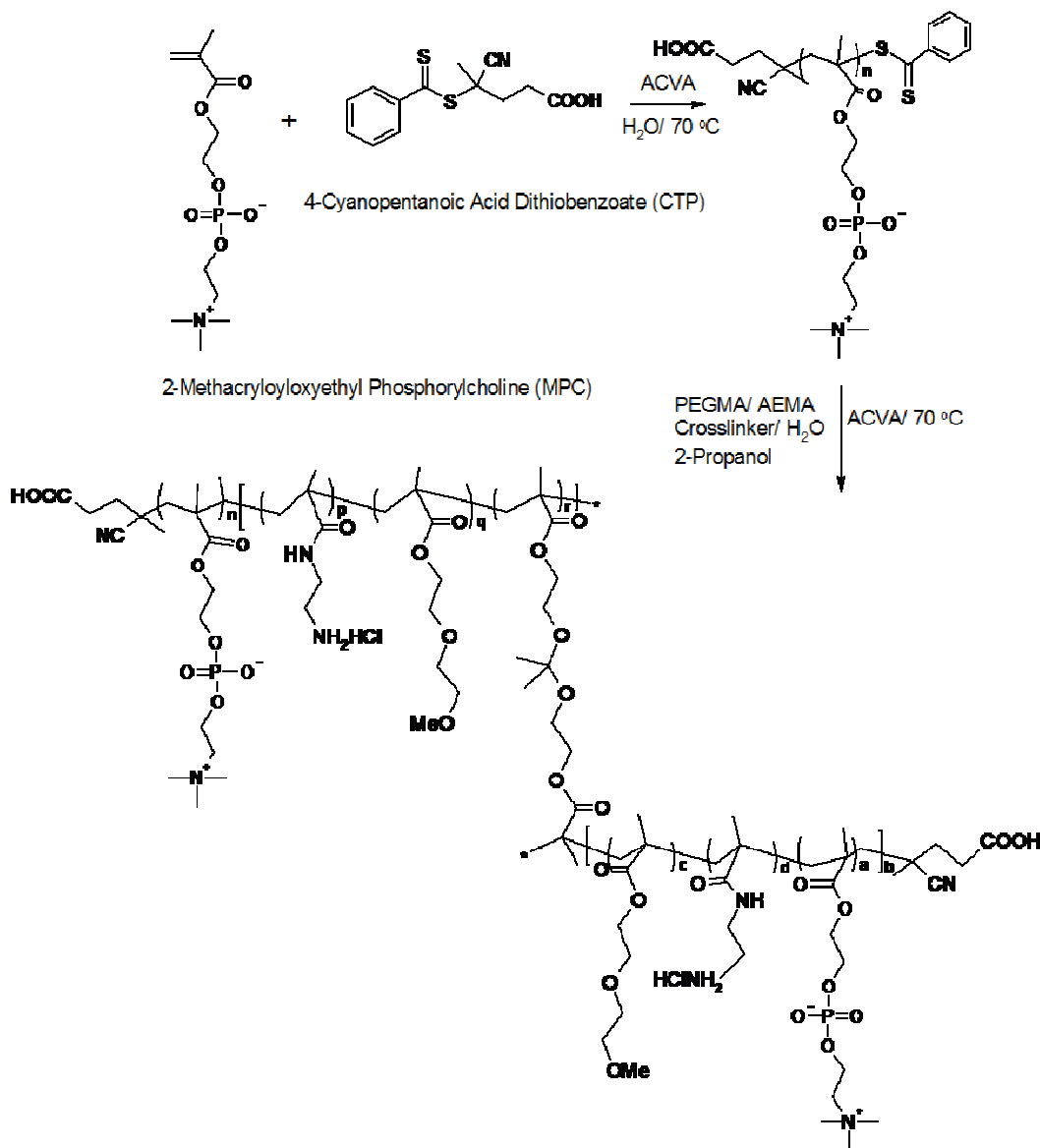


Figure 4-3: RAFT synthesis of poly(MPC-*b*-(MeODEGM -*stat*-AEMA-*stat*-CL)) core cross-linked with thermo-responsive and degradable core

Micelle structures can easily dissociate after dilution. To prevent dissociation of micelle structures of di-block copolymers, they are stabilized by cross-linking [58]. The size and stability of nanogels depend on cross-linker concentration (molar ratio with respect to the total molar monomer concentration) (expressed in

percentage). For the synthesis of uniform, fixed micelles, it is necessary to have a suitable amount of cross-linker. Branched copolymers and unstable nanostructures can be formed as a result of low cross-linker concentration [12]. On the other hand, very high cross-linker concentration can result in the formation of microgel or hydrogel networks [59]. To confirm this effect, cross-linker concentration was varied from 7, 10, 15 and 20%. The particle size and their polydispersities were determined using DLS instrument as shown in Figure 4-4.

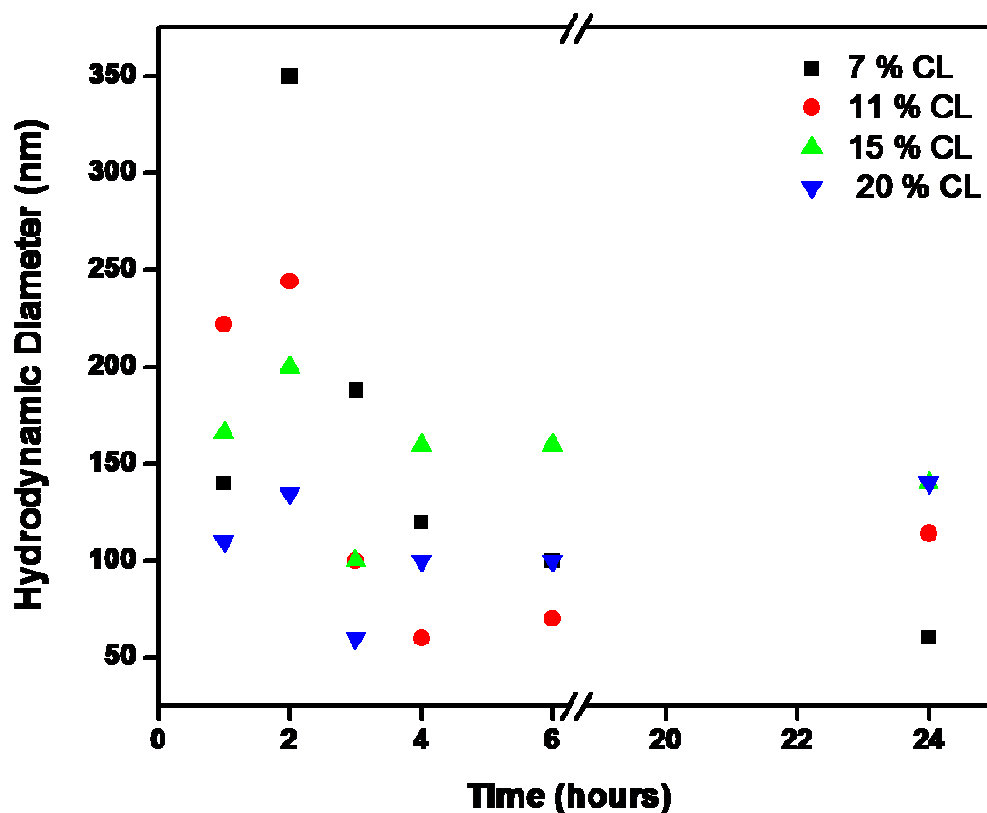


Figure 4-4: Evolution of hydrodynamic diameter of reaction mixture of crosslinking nanogel and variation of size with varying cross-linker (CL) concentration

The evolution of hydrodynamic size of the nanogel with time was studied for varying amounts of cross-linker. It was observed that the nanogels attained a

stable size within 5-6 hours of reaction time and with increasing cross-linker concentration, the hydrodynamic size and poly-dispersity also increased. It was observed that for low cross-linker concentrations (7-10%), the sizes were small (35-50 nm) and increased with temperature. This may be due to the unstable micelle structures and formation of aggregates of MeODEGM polymers. On the other hand, for a high concentration of cross-linker (35%), a very turbid solution was obtained. Particle precipitation was observed when the solution was left undisturbed for some time. Thus, the size of particles formed was in micrometer range and hence were unstable in solution. Stable nanogels were obtained at an optimum cross-linker concentration of 15-20%. Particle size of 130 nm and low polydispersity (0.08-0.2) were determined by DLS. TEM images of these nanogels are shown in Figure 4-5.

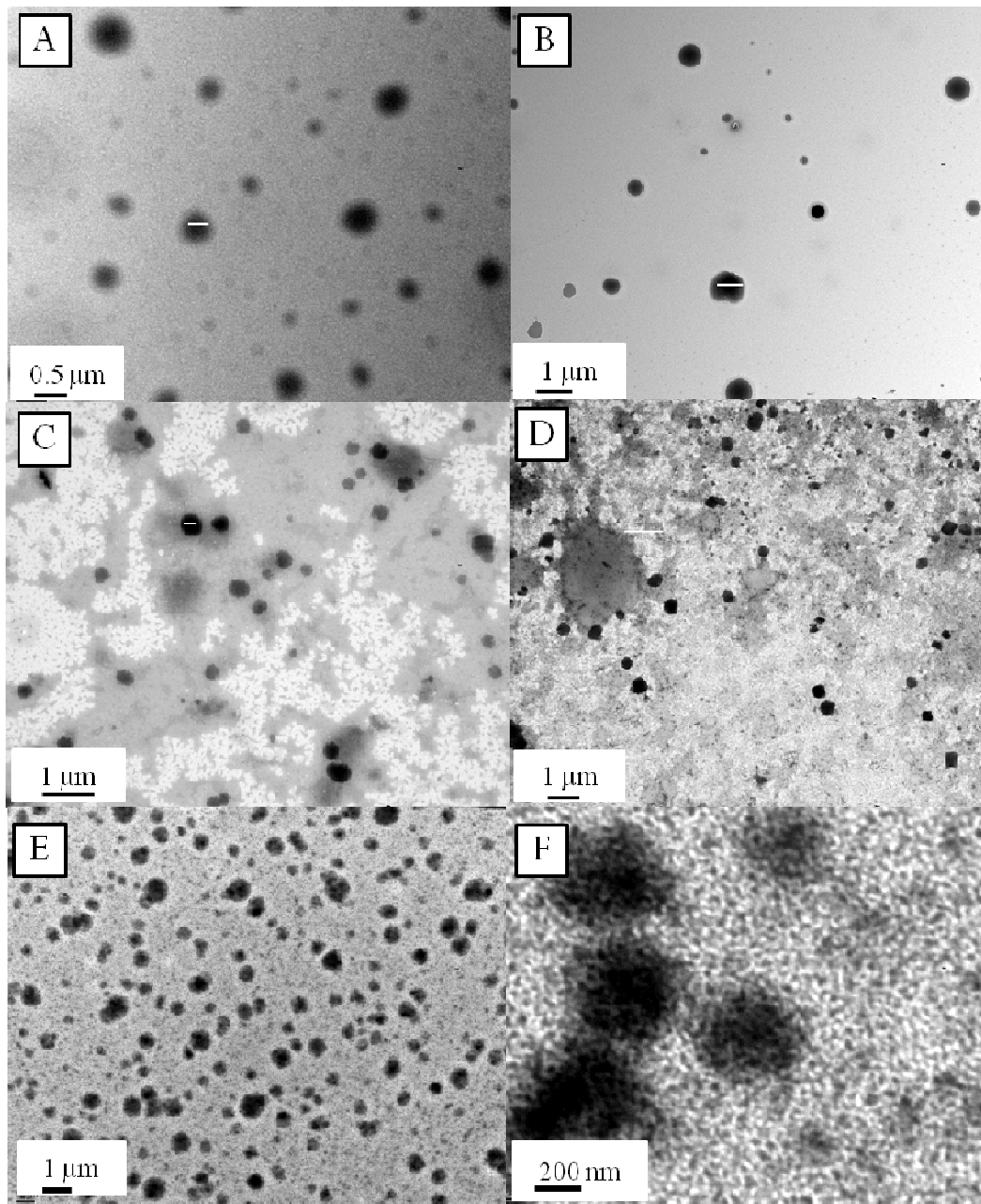


Figure 4-5: TEM images of nanogels showing A), B) nanogels with 25% cross-linker concentration; C), D) more monodispersed nanogel solutions with 10% cross-linker concentration and E), F) nanogels with 15% cross-linker concentration

MeODEGM is a thermo-responsive polymer and experiences a phase-change from being hydrophilic at low temperatures (24 °C) to hydrophobic at high

temperatures. The MeODEGM core of the micelle, therefore, collapses at high temperatures, which is indicated by a notable decrease in size above 24 °C. Table 4-1 shows the variation in size of nanogels with change in MeODEGM chain length and cross-linker concentration. MeODEGM chain length has little effect on the size of nanogels but it affects the LCST of the nanogel.

Table 4-1: Comparison of hydrodynamic diameter of MPC-*b*-(MeODEGM -*stat*-AEMA-*stat*-CL) nanogel with varying cross-linker concentrations and MeODEGM-AEMA chain length

Sample	Nanogel	Cross-linker	Hydrodynamic Diameter (nm)	Poly-dispersity
1.1	MPC ₇₀ - <i>b</i> -(MeODEGM- <i>stat</i> -AEMA- <i>stat</i> -CL) ₅₀₀	7	45	0.092
1.2	MPC ₇₀ - <i>b</i> -(MeODEGM- <i>stat</i> -AEMA- <i>stat</i> -CL) ₃₀₀	10	60	0.298
1.3	MPC ₇₀ - <i>b</i> -(MeODEGM- <i>stat</i> -AEMA- <i>stat</i> -CL) ₄₀₀	10	114	0.069
1.4	MPC ₄₃ - <i>b</i> -(MeODEGM- <i>stat</i> -AEMA- <i>stat</i> -CL) ₄₀₀	15	140	0.24
1.5	MPC ₄₃ - <i>b</i> -(MeODEGM- <i>stat</i> -AEMA- <i>stat</i> -CL) ₄₀₀	20	150	0.14
1.6	MPC ₄₃ - <i>b</i> -(MeODEGM- <i>stat</i> -AEMA- <i>stat</i> -CL) ₄₀₀	25	200	0.14

Lutz *et al.* observed that increase in MeODEGM levels in the nanogel increased LCST from 24 °C to as high as 84 °C [13, 60]. Temperature dependent DLS studies showed that nano-particles shrunk from 147 to 115 nm at 30 °C (as shown in Figure 4-6), The phase transition of MeODEGM from hydrophilic to hydrophobic state could be seen as the solution immediately turned milky white from transparent as the temperature was raised. The nanogels were found to be quite stable at 50 °C (Figure S5 (Appendix 2)).

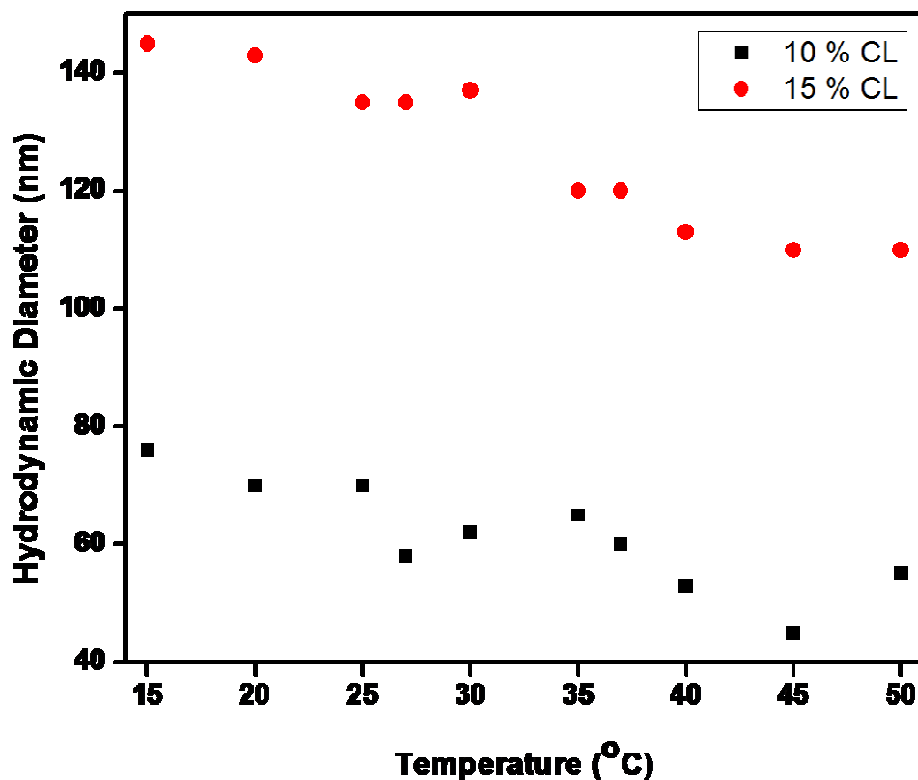


Figure 4-6: Decrease in mass-average hydrodynamic diameter with increase in temperature obtained for 0.5 mg/mL aqueous solution of nanogel, for varying cross-linker (CL) concentration

The phase transition behavior of nanogel core was studied using *VTNMR* (Variable Temperature NMR). It was observed that peak intensity of the thermo-responsive polymer reduces after phase transition. Schönhoff *et al.* have attributed this reduction in NMR signal intensity of poly(NIPAM) to the decrease in polymer segmental mobility which further decreases the relaxation time T [61]. The ^1H NMR peak intensity of methylene group of poly(MeODEGM) at 3.4 ppm was compared with normalized solvent (D_2O) peak intensity. The reduction in polymer signal intensity above phase transition is shown in Figure 4-7. The *VTNMR* (Variable Temperature NMR) of nanogel is shown in Figure S4 (Appendix 2).

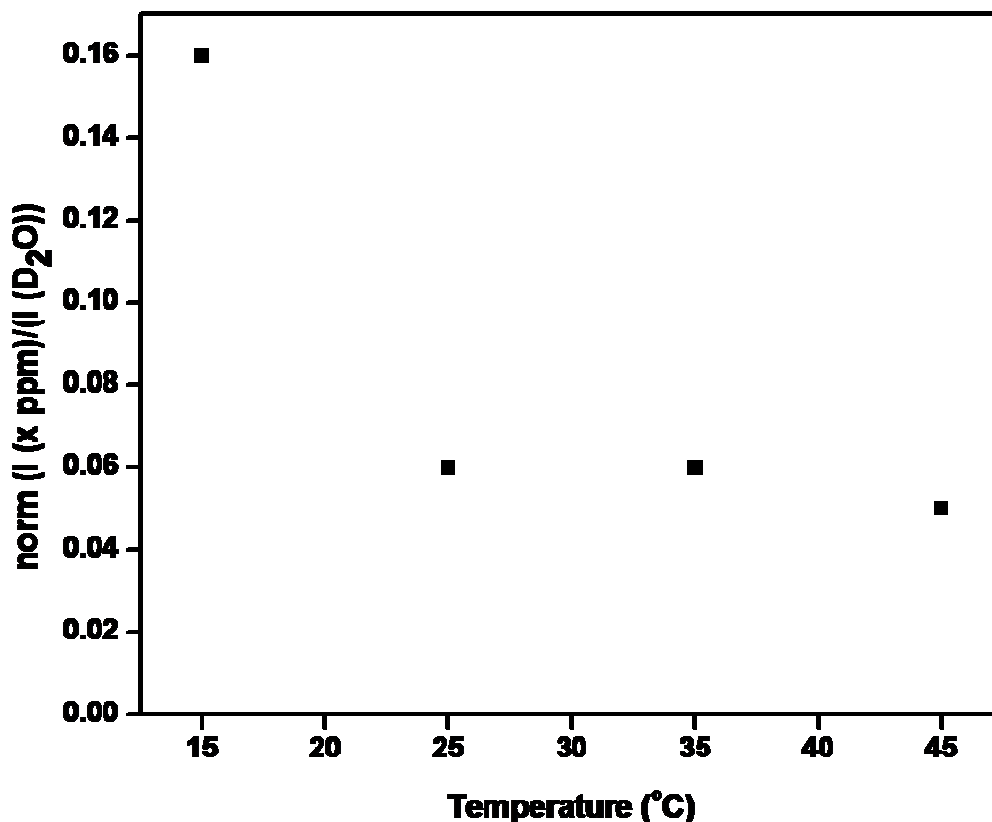


Figure 4-7: Normalized ratio of ^1H NMR signal intensity of MeODEGM protons to D_2O protons vs. temperature as observed for the methylene group protons of MeODEGM at 3.4 ppm and D_2O .

The effect of pH on the nanogel was studied to find the rate of degradation of the cross-linker at low pH. The pH of distilled water is slightly acidic (pH 6.7). Nanogels in distilled water could be stored for 2-3 days without degradation. A comparative study of the rate of degradation at different pH (pH 4.5, 5.2 and 6.4) and varying cross-linker concentration (10 and 15%) was carried out. As expected, the nanogels were found to be unstable and degrade under acidic conditions (Figure 4-8). Also, the rate of degradation of the nanogels is more pronounced for low cross-linker concentration (10 %), which degraded within 2

hours at pH 4.5 and 5.2. The nanogels were found to be very stable under neutral and alkaline pH. For higher cross-linker concentrations however, the degradation curve shifted to the right, indicating higher stability at low pH for a longer time.

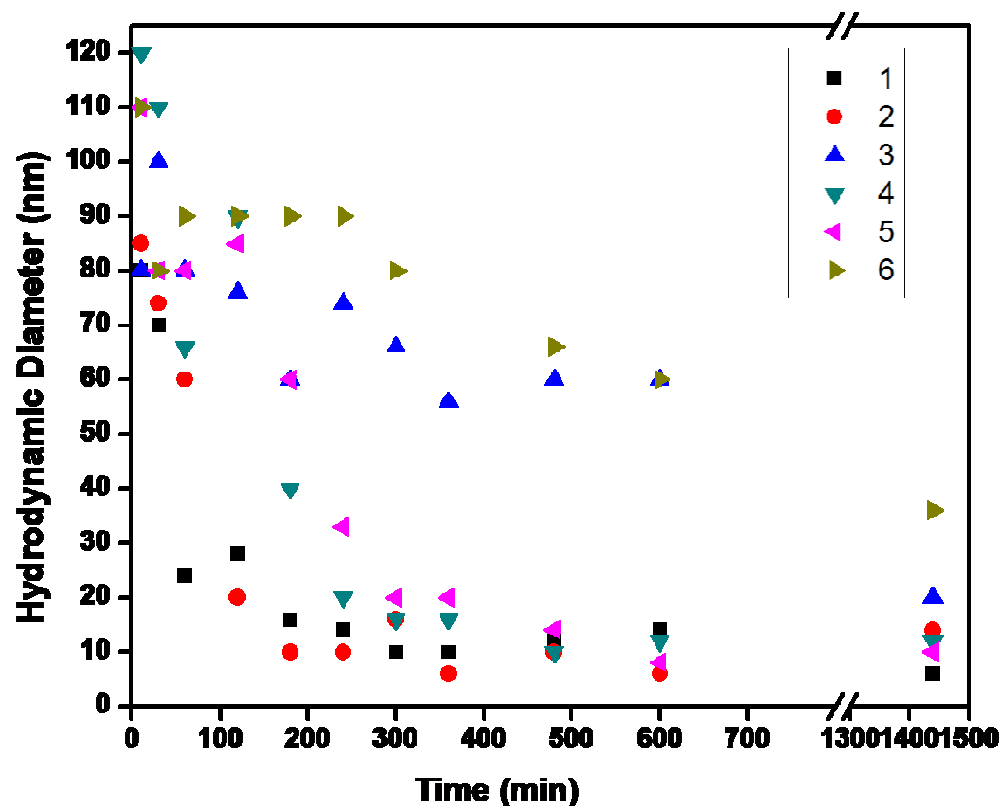


Figure 4-8: Degradation of 10 and 15% cross-linker concentration nanogel at pH 4.5, 5.4 and 6.2. :1) 10% cross-linker concentration at pH 4.5; 2) 10% cross-linker concentration at pH 5.4; 3) 10% cross-linker concentration at pH 6.2; 4) 15% cross-linker concentration at pH 4.5; 5) 15% cross-linker concentration at pH 5.4; 6) 15% cross-linker concentration at pH 6.2

4.3.3 Protein Encapsulation:

An important application of stimuli-responsive nanogels is the encapsulation of macromolecules in their core or coronas. Crosslinking of polymers provides a

stable micelle structure which can be exploited to trap macromolecules of various sizes. However, the release of trapped drugs is only possible by the degradation of cross-linker under physiological conditions. We have used acid degradable cross-linker which degrades at low pH, thereby releasing the encapsulated proteins.

The protein was loaded using the incubation method. Insulin, BSA and β -galactosidase were incubated overnight in aqueous nanogel solutions (5 mg/mL) at 4 °C. The three proteins vary largely in their sizes. Insulin is the smallest protein with size 5.80 kDa, while BSA has a molecular weight of 66.7 kDa and β -galactosidase is the largest protein of size 125 kDa. MeODEGM nanogels are hydrophobic at room temperature. The proteins were incubated at low temperature (7 °C) to ensure maximum encapsulation. The incubation method is reported to be less efficient than the encapsulation method, as per previous reports [62]. However, these nanogels showed high loading probably due to the additional functionality of the core of the nanogels (presence of protonated amino groups). The cationic nature of the core has (poly(AEMA) - pK_a 8.8) has facilitated the encapsulation of negatively charged macromolecules. For example, BSA has a pI (Isoelectric point or the point of zero charge) of 4.6 and therefore has a negative surface charge at neutral pH.

The nanogel was precipitated at 14000 rpm and 40 °C. Before precipitating, the gels were collapsed to trap the protein within the core. The amount of entrapped protein was estimated by calculating the difference between the amount of protein added and the amount of non-encapsulated protein in the aqueous phase of precipitated protein. It was observed that two factors that dictated the amount of

protein encapsulated were the cross-linker concentration and the percentage of AEMA in the core.

A comparative study of three samples is shown in Table 4-2. The analysis showed that 92.4 % of insulin was encapsulated for nanogel with 15% feed cross-linker concentration and 25% feed ratio AEMA (Sample B). For higher cross-linker concentration, the encapsulation reduced to 80%. A possible explanation for the strong dependence of encapsulation efficiency on the cross-linker concentration may be due to its effect on pore size of the cross-linked nanogel. A higher cross-linker concentration is expected to produce a tighter network, therefore providing a smaller pore size. Encapsulation of macromolecules is easier for a larger pore size network. While lower cross-linker concentration fails to cross-link stably, higher amounts decrease the pore size leading to reduced loading capacity. To study the effect of AEMA, nanogels with varying amount of cationic components were studied and compared. For the same amount of cross-linker, the AEMA component also affects the encapsulation efficiency. This may be due to the electrostatic interaction between the protein and cationic nanogel due to opposite charges of protein and MeODEGM-AEMA nanogel at neutral pH. Thus we observe that Sample B is the optimum cross-linker concentration and AEMA concentration for the encapsulation of proteins.

Table 4-2: Study of protein encapsulation efficiencies for nanogels of varying cross-linker concentration and AEMA content. A) Sample A: 15% cross-linker concentration and 5% AEMA feed ratio B) 15% cross-linker concentration and 25% AEMA feed ratio and C) 20% cross-linker concentration and 10% AEMA feed ratio. Each sample was incubated with proteins (Insulin, BSA and β -Gal) of varying molecular weights

Sample	Protein	Amount of Encapsulation (μg)	Percentage Encapsulation
Sample A	Insulin	45.8	91.6
	BSA	54	36
	β -Gal	-	-
Sample B	Insulin	46.2	92.4
	BSA	90	59.9
	β -Gal	0.7	35
Sample C	Insulin	40	80
	BSA	40	26.6
	β -Gal	-	-

A careful analysis of data indicates that the size and properties of macromolecules also play an important role in determining the total encapsulation. Insulin showed highest percentage encapsulation in agreement with its smallest size and lowest molecular weight (5.5×10^3). β -galactosidase, on the other hand has a molecular weight of 5.4×10^5 , and consequently the lowest encapsulation efficiency. The encapsulation efficiency decreased from 92% for insulin to 35% for β -galactosidase.

4.3.4 Release Profile:

The release profile of nanogels was studied at varying pH. The nanogel solution was incubated overnight with 50 μL Insulin protein (1mg/mL). Nanogels with 15 and 20% cross-linker concentration were incubated overnight with 50 μL Insulin protein (1mg/mL). The nanogels were precipitated and the amount of protein encapsulated was determined by BCA assay to be 29 μL . The precipitated nanogel was re-dispersed in buffer solutions of pH 4.8 and 6.4. Aliquots from buffer solution were taken at regular intervals and the amount of protein released was calculated. Almost 90% protein was released over a period of 48 hours at pH 4.8. Thus, the release profile of insulin from MeODEGM nanogels is slow and no burst release was observed (Figure 4-9).

To confirm the structure and activity of β -galactosidase after loading, β -galactosidase assay was conducted on the 400 μL of 5 mg/mL aqueous nanogel solution loaded with β -gal. The amount of encapsulation calculated by BCA assay was found to be 0.7 μL β -galactosidase i.e 35% encapsulation. Figure S4 (Appendix 2) shows the change in colour of nanogel when ONPG is hydrolyzed to o-nitrophenol (yellow) and galactose by β -galactosidase. The activity of protein in supernatant and nanogel was calculated to be 1384 mU/mg and 4642 mU/mg respectively. It was therefore found that the protein was present in its native form after encapsulation and retained its catalytic activity.

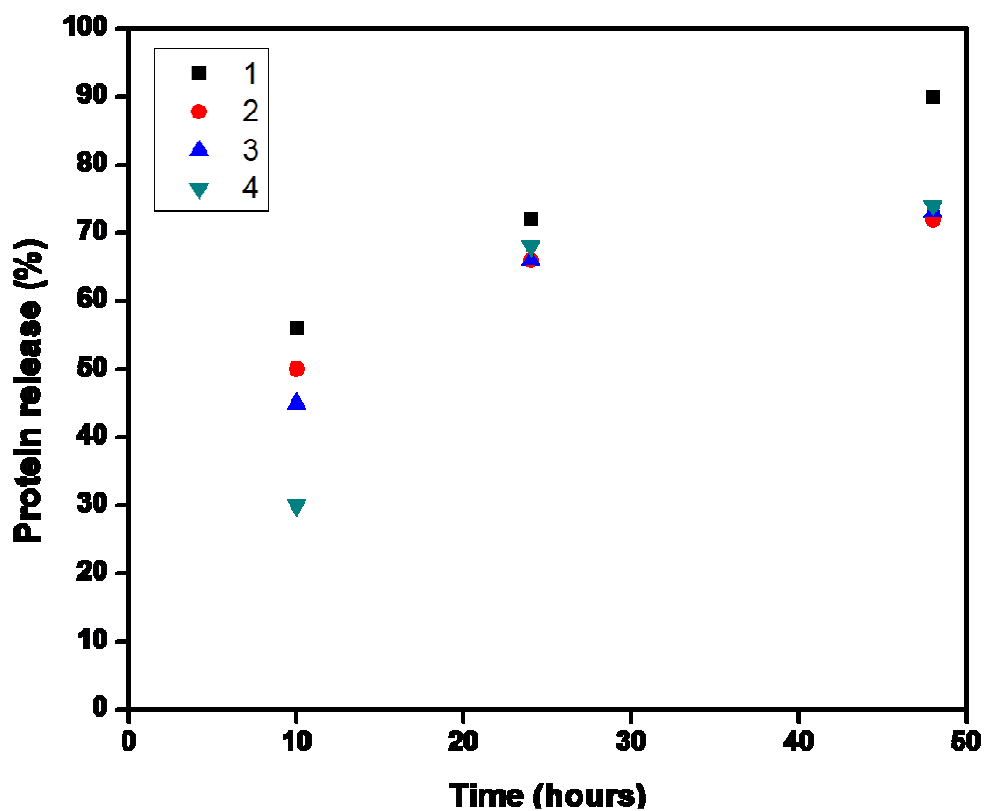


Figure 4-9: Cumulative release profile of insulin from nanogel solution of varying cross-linker concentrations: 1) 15% cross-linker concentration at pH 4.8; 2) 20% cross-linker concentration at pH 4.8; 3) 15% cross-linker concentration at pH 6.4 and 4) 20% cross-linker concentration at pH 6.4

4.4 References:

- [1] Oh, J.; Drumright, R.; Siegwart, D.; Matyjaszewski, K., *Prog. Polym. Sci.* **2008**, *33*, 448-477
- [2] Graham, N.B.; Cameron, A., *Pure Appl. Chem.* **1998**, *70*, 1271-1275
- [3] Kuckling, D.; Vo, C.D.; Wohlrab, S.E., *Langmuir* **2002**, *18*, 4263-4269
- [4] Koul, V.; Mohamed, R.; Kuckling, D.; Adler, H.J. P.; Choudhary, V., *Colloids Surf. B Biointerfaces* **2011**, *83*, 204-213
- [5] Kim, Y.; Thapa, M.; Hua, D. H.; Chang, K.O., *Antiviral Res.* **2011**, *89*, 165-173
- [6] Sahiner, N.; Godbey, W. T.; McPherson, G. L.; John, V. T., *Colloid Polym. Sci.* **2006**, *284*, 1121-1129
- [7] Sisson, A. L.; Haag, R., *Soft Matter.* **2010**, *6*, 4968-4975
- [8] Harris, J. M.; Chess, R. B., *Nat. Rev. Drug Discov.* **2003**, *2*, 214-221
- [9] Heyden, K. V.; Babooram, K.; Ahmed, M.; Narain, R., *Eur. Polymer J.* **2009**, *45*, 1689-1697
- [10] Risbud, M. V.; Hardikar, A. A.; Bhat, S. V.; Bhonde, R. R., *J. Control Release.* **2000**, *68*, 23-30
- [11] Prevot, M.; Déjugnat, C.; Möhwald, H.; Sukhorukov, G. B., *ChemPhysChem.* **2006**, *7*, 2497-2502
- [12] Goh, C.C.; Stöver, D. H., *Macromolecules* **2002**, *35*, 9983-9989
- [13] Lutz, J.F.; Akdemir, O.; Hoth, A., *J. Am. Chem. Soc.* **2006**, *128*, 13046-13047

- [14] Hu, T.; You, Y.; Pan, C.; Wu, C., *J. Phys. Chem. B.* **2002**, *106*, 6659-6662
- [15] Chen, Y.; Zheng, X.; Qian, H.; Mao, Z.; Ding, D.; Jiang, X., *Appl. Mater. Interfaces.* **2010**, *2*, 3532-3538
- [16] Tan J.P.K.; Tan M.B.H.; Tam, M., *Local Reg. Anesth.* **2010**, *3*, 93-100
- [17] Oh, J. K.; Perineau, F.; Matyjaszewski, K., *Macromolecules.* **2006**, *39*, 8003-8010
- [18] Smulders, W.; Monteiro, M. J., *Macromolecules.* **2004**, *37*, 4474-4483
- [19] Murthy, K. S.; Ma, Q.; Remsen, E. E.; Kowalewski, T.; Wooley, K. L., *J. Mater. Chem.* **2003**, *13*, 2785-2795
- [20] Arotçaréna, M.; Heise, B.; Ishaya, S.; Laschewsky, A., *J. Am. Chem. Soc.* **2002**, *124*, 3787-3793
- [21] Weaver, J. V. M.; Tang, Y.; Liu, S.; Iddon, P. D.; Grigg, R.; Billingham, N. C.; Armes, S. P.; Hunter, R.; Rannard, S. P., *Angew. Chem. Int. Ed.* **2004**, *116*, 1413-1416
- [22] Alarcon, C. de l H.; Pennadam, S.; Alexander, C., *Chem. Soc. Rev.* **2005**, *34*, 276-285
- [23] Sciannamea, V.; Jérôme, R.; Detrembleur, C., *Chem. Rev.* **2008**, *108*, 1104-26
- [24] Tsarevsky, N. V.; Matyjaszewski, K., *Chem. Rev.* **2007**, *107*, 2270-99
- [25] Moad, G.; Rizzardo, E.; Thang, S. H., *Acc. Chem. Res.* **2008**, *41*, 1133-1142

- [26] Chiefari, J.; Chong, Y.K.B.; Ercole, F.; Krstina, J.; Jeffery, J.; Le, T. P. T.; Mayadunne, R. T. A.; Meijs, G. F.; Moad, C. L.; Moad, G.; Rizzardo, E.; Thang, S.H, *Macromolecules*. **1998**, *31*, 5559–5562
- [27] Loppinet, B.; Sigel, R.; Larsen, A.; Fytas, G.; Vlassopoulos, D.; Liu, G., *Langmuir*. **2000**, *16*, 6480-6484
- [28] Stewart, S.; Liu, G., *Chem. Mater.* **1999**, *11*, 1048-1054
- [29] Saito, R.; Ishizu, K.; Fukutomi, T., *Polymer*. **1990**, *31*, 679-683
- [30] Butun, V.; Billingham, N. C.; Armes, S. P., *J. Am. Chem. Soc.* **1998**, *120*, 12135-12136
- [31] Henselwood, F.; Liu, G. J., *Macromolecules*. **1997**, *30*, 488-493
- [32] Zhang, L.; Liu, W.; Lin, L.; Chen, D.; Stenzel, M. H. *Biomacromolecules*. **2008**, *9*, 3321-3331
- [33] Zhang, L.; Bernard, J.; Davis, T. P.; Barner-Kowollik, C.; Stenzel, M., *Macromol. Rapid Commun.* **2008**, *28*, 123-129
- [34] Hales, M.; Barner-Kowollik, C.; Davis, T. P.; Stenzel, M., *Langmuir*. **2004**, *20*, 10809-10817
- [35] Kikuchi, A.; Okano, T., *Adv. Drug Delivery Rev.* **2002**, *54*, 53-77
- [36] Kim, B.; Flamme, K.L.; Peppas, N., *J. Appl. Polym. Sci.* **2003**, *89*, 1606-1613
- [37] Cai, C.; Bakowsky, U.; Rytting, E.; Schaper, A. K.; Kissel, T., *Eur. J. Pharm. Biopharm.* **2008**, *69*, 31-42
- [38] Soppimath, K.S.; Aminabhavi, T.M; Kulkarni, A.R.; Rudzinski, W. E., *J. Control. Release.* **2001**, *70*, 1-20

- [39] Panyam, J.; Labhasetwar, V., *Adv. Drug Delivery Rev.* **2003**, *55*, 329-347
- [40] Smith, M. H.; South, A. B.; Gaulding, J. C.; Lyon, L. A., *Anal. Chem.* **2010**, *82*, 523-530
- [41] Kang, Y.; Wang, Q.; Liu, Y.-C.; Shen, J.W.; Wu, T., *J. Phys. Chem. B.* **2010**, *114*, 2869-2875
- [42] Hirakura, T.; Yasugi, K.; Nemoto, T.; Sato, M.; Shimoboji, T.; Aso, Y.; Morimoto, N.; Akiyoshi, K., *J. Control. Release.* **2010**, *142*, 483-489
- [43] Blanco, D.; Alonso, M. J., *Eur. J. Pharm. Biopharm.* **1998**, *45*, 285-294
- [44] Weert, M.; Hof, R.; Weerd, J.; Heeren, R.M.A.; Posthuma, G.; Hennink, W.E.; Crommelin, D.J.A., *J. Control Release.* **2000**, *68*, 31-40
- [45] Cadée, J.; Groot, C. J. de; Jiskoot, W.; Otter, W. den; Hennink, W. E., *J. Control Release.* **2002**, *78*, 1-13
- [46] Ramkisson-Ganorkar, C.; Liu, F.; Baudys, M.; Kim, S. W., *J. Control Release.* **1999**, *59*, 287-298
- [47] Kyomoto, M.; Moro, T.; Takatori, Y.; Kawaguchi, H.; Nakamura, K.; Ishihara, K., *Biomaterials.* **2010**, *31*, 1017-1024
- [48] Nakabayashi, N.; Iwasaki, Y., *Biomed. Mater. Eng.* **2004**, *14*, 345-354
- [49] Katakura, O.; Morimoto, N.; Iwasaki, Y.; Akiyoshi, K.; Kasugai, S., *J. Med. Dent. Sci.* **2005**, 115-121
- [50] Ishihara K.; Ueda T.; Nakabayashi, N., *Polym. J.* **1990**, *22*, 355-360
- [51] Deng, Z.; Bouchékif, H.; Babooram, K.; Housni, A.; Choytun, N.; Narain, R., *J. Polym. Sci. Part A: Polym. Chem.* **2008**, *46*, 4984-4996

- [52] Mitsukami, Y.; Donovan, M. S.; Lowe, A. B.; McCormick, C. L., *Macromolecules*. **2001**, *34*, 2248-2256
- [53] Lai, J. T.; Filla, D.; Shea, R., *Macromolecules*. **2002**, *35*, 6754-6756
- [54] Roberts, D. L.; Ma, Y.; Bowles, S. E.; Janczak, C. M.; Pyun, J.; Saavedra, S. S.; Aspinwall, C. A., *Langmuir*. **2009**, *25*, 1908–1910
- [55] Bhuchar, N.; Deng, Z.; Ishihara, K.; Narain, R., *J. Polym. Chem.* **2011**, *2*, 632-639
- [56] Zheng, G.; Zheng, Q.; Pan, C. *Macromol. Chem. Phys.* **2006**, *207*, 216-223
- [57] Yan, L.; Tao, W., *Polymer*. **2010**, *51*, 2161-2167
- [58] Rapoport, N., *Colloids Surf. B Biointerfaces*. **1999**, *16*, 93-111
- [59] Jiang, X.; Liu, S.; Narain, R., *Langmuir*. **2009**, *25*, 13344-13350
- [60] Fournier, D.; Hoogenboom, R.; Thijs, H. M. L.; Paulus, R. M.; Schubert, U. S., *Macromolecules*. **2007**, *40*, 915-920
- [61] Schönhoff, M.; Larsson, A.; Welzel, P. B.; Kuckling, D., *J. Phys. Chem. B*. **2002**, *106*, 7800-7808
- [62] Kabanov, A. V.; Vinogradov, S. V., *Angew. Chem. Int. Ed.* **2009**, *48*, 5418-5429

5 Conclusion and Future Work

The thesis focuses on the synthesis of 2-methacryloyloxyethyl phosphorylcholine (MPC) homopolymers, copolymers and nanogels using reversible addition fragmentation chain transfer (RAFT) polymerization. RAFT, which is a type of living radical polymerization (LRP), is a well controlled polymerization technique that ensures low polydispersities in the resulting polymers. MPC is a biocompatible monomer and therefore MPC based materials can be used for bioapplications. MPC based copolymers with cationic groups for instance can be utilized for DNA conjugation. MPC-based nanogels have potential applications in encapsulation and *in vitro* release of drugs.

5.1 RAFT polymerization of MPC:

This first part of the thesis presents a detailed study of the reverse addition fragmentation chain transfer (RAFT) polymerization of MPC. Methanol proved to be a better solvent for dissolution of CTP and ACVA than water. An ideal narrow polydispersity ($M_w/M_n < 1.2$) of poly(MPC) could be obtained up to $M_n = 2.9 \times 10^4$ g/mol using methanol as solvent. The rate of RAFT polymerizations of MPC in methanol strongly depended on the initiator concentration (for a constant CTP concentration). In the acceptable range of viscosity, copolymerizations were found to perform with good control a higher monomer concentration and the polydispersity of resulting self-blocking MPC polymer was slightly lower when higher ratio of CTP to ACVA was used in the preparation of macro-CTA. The

poly(MPC)-based macro-CTP was successfully applied in the synthesis of block-type copolymer with various monomers. The diblock copolymers prepared via sequential monomer addition were synthesized with high yields and low polydispersities. Ongoing work in our laboratory will focus on the cytotoxicity studies of statistical and diblock copolymers composed of the poly(MPC) segment and the cationic polymer segment. These functionalized polymers may be used as a carrier of drug and gene to the cells.

5.2 Synthesis of acid degradable and thermo-responsive core-crosslinked nanogels:

In the later part of the thesis, we have successfully synthesized stable thermo-responsive and acid degradable poly(MeODEGM-AEMA) core-cross-linked micelles via RAFT polymerization using poly(MPC) macro RAFT agent. Sizes of these nanogels could be tuned accordingly by changing the cross-linker concentration and MeODEGM chain length. AEMA provided cationic character to the nanogel core, which facilitated the encapsulation of oppositely charged proteins such as, insulin, BSA and β -Galactosidase. The loading efficiency of these proteins largely depended on the pore size of nanogels, the cationic component and the size of protein. The degradation profile of acid-degradable nanogels containing entrapped proteins was studied at varying acidic pH and a controlled release profile of protein was observed. These MPC-*b*-(MeODEGM-*stat*-AEMA-*stat*-CL) nanogels therefore have promising applications as smart carriers for targeted drug delivery systems.

Future Work: We have also synthesized NIPAM-MPC core-shell nanogels using the acid degradable cross-linker. NIPAM, however, is not a biocompatible polymer, but has been studied intensively because of its thermo-responsivity. PNIPAM constituted the shrinking gel and MPC was cross-linked in the core. Nanogel sizes and protein encapsulation efficiency can be compared for various proteins with the previously synthesized MeODEGM based nanogels. It will be interesting to study the effect of a zwitterionic polymer in the core on encapsulation of both cationic and anionic proteins.

6 Appendix 1

Block Copolymerization of 2-Methacryloyloxyethyl Phosphorylcholine:

Self-Chain Extension of 2-Methacryloyloxyethyl Phosphorylcholine:

MPC based macro-CTAs were first polymerized with different CTP/ACVA ratios (typically CTP/ACVA = 2:1) and the polymerization was stopped at 60% conversion by quenching in liquid nitrogen and exposure to air. The resulting polymers were precipitated in acetone and then washed with 12.5 vol% methanol in acetone to remove any traces of monomer. Subsequently, the prepared macro-CTA with additional MPC monomer and ACVA were dissolved in different volume of methanol to conduct the self-chain extension experiments. In a typical protocol, poly(MPC) (0.30 g, 0.032 mmol, $M_n = 9.3 \times 10^3$ g/mol, $M_w/M_n = 1.07$), MPC (0.30 g, 1.0 mmol) and ACVA(0.0020 g, 0.0070 mmol) were dissolved in 2.0 mL methanol. After degassing via four freeze-thaw cycles, the flask was placed in a preheated oil bath for 18 hours at 60 °C. At the end of polymerization process, the polymer was recovered by precipitating in acetone. poly(MPC-*b*-MPC) molecular weight M_n was found to be around 1.7×10^4 g/mol and the polydispersity index M_w/M_n was shown by GPC as 1.2.

Table S1 : Evolution of molecular weight of MPC homopolymer was measured by Gel Permeation Chromatography

Code	Reaction Time (min)	Conv.% (NMR)	M_n (Theory) g/mol ($\times 10^4$)	M_n (GPC) g/mol ($\times 10^4$)	M_w/M_n (GPC)
S1.1	120	10	0.21	0.42	1.06
S1.2	165	25	0.49	0.59	1.08
S1.3	210	41	0.79	0.79	1.03
S1.4	300	67	1.28	1.11	1.04
S1.5	405	80	1.52	1.26	1.04
S1.6	540	91	1.72	1.27	1.08
S1.7	660	92	1.74	1.29	1.08
S1.8	1320	-	-	1.39	1.09

Table S2 : Effect of CTP/ACVA ratio on synthesis of poly(MPC) macroCTA and consequent effect of monomer concentration on self chain extension of MPC

Code	Macro-CTA (Trail 1)				Self-Chain Extension (Trail 2)			
	[CTP]/ [ACVA]	Conv. %	M_n g/mol	M_w/M_n	[Monomer]	Conv. %	M_n g/mol (10^4)	M_w/M_n
S2.1	1.0	83	1.07×10^4	1.11	0.20 M	N/A	1.94	1.44
S2.2(a)	2.0	65	9.40×10^3	1.09	0.20 M	95	1.45	1.29
S2.2(b)	2.0	65	9.40×10^3	1.09	0.50 M	99	1.67	1.21
S2.3	5.0	63	9.30×10^3	1.07	0.50 M	98	1.67	1.16

Table S3 : Molecular weights and molecular weight distribution of di-block copolymers of MPC:

Code	Di-block Copolymers of MPC	M_n (Theory) g/mol ($\times 10^4$)	M_n (GPC) g/mol ($\times 10^4$)	M_w/M_n (GPC)
S3.1	Poly(MPC ₅₄ - <i>b</i> -LAEMA ₆₄)	4.5	4.6	1.17
S3.2	Poly(MPC ₅₄ - <i>b</i> -GAEMA ₅₅)	3.6	3.3	1.26
S3.3	Poly(MPC ₅₄ - <i>b</i> -GAMA ₇₈)	3.61	4.0	1.11
S3.4	Poly(MPC ₅₄ - <i>b</i> -AEMA ₅₄)	2.7	2.5	1.31

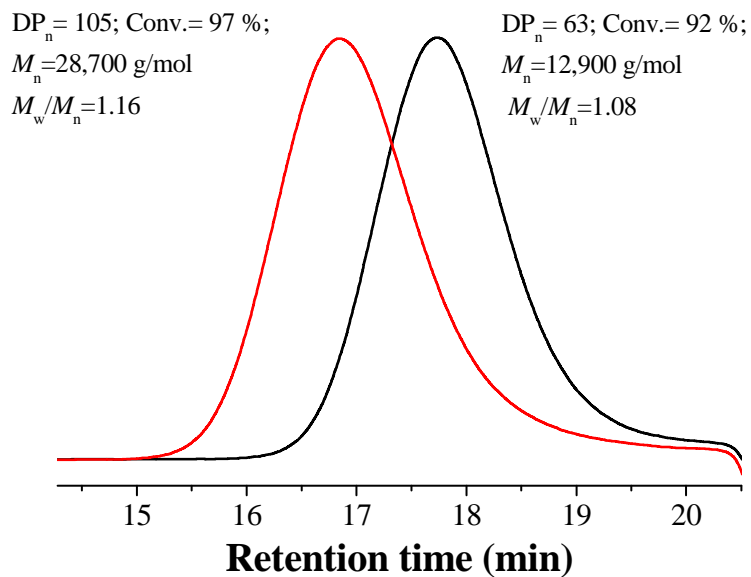


Figure S1 : GPC traces of MPC homopolymers of low as well as high molecular weights with controlled molecular weights

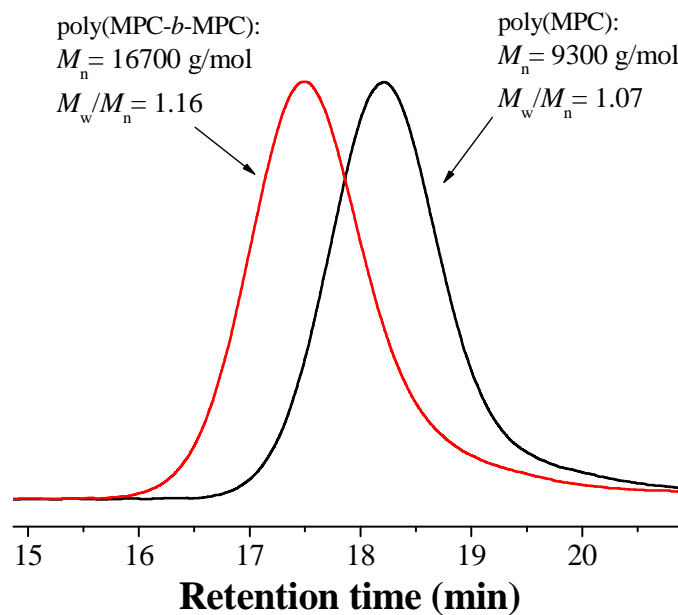


Figure S2 : GPC traces of p(MPC) macroCTA and self chain extension reaction with a CTP/ACVA = 5.0 at 60 °C in methanol.

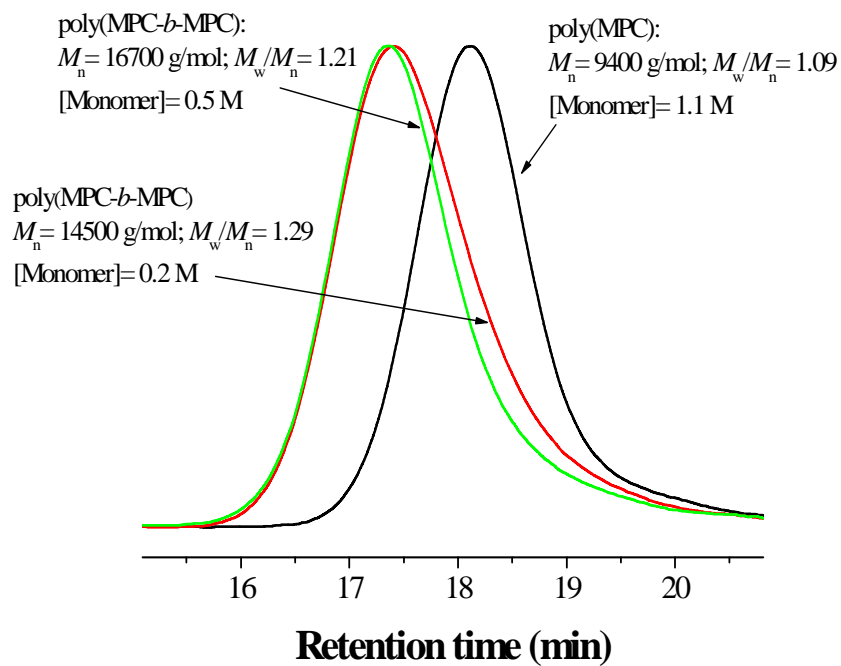


Figure S3 : GPC traces showing the effect of monomer concentration on self chain extension of MPC).

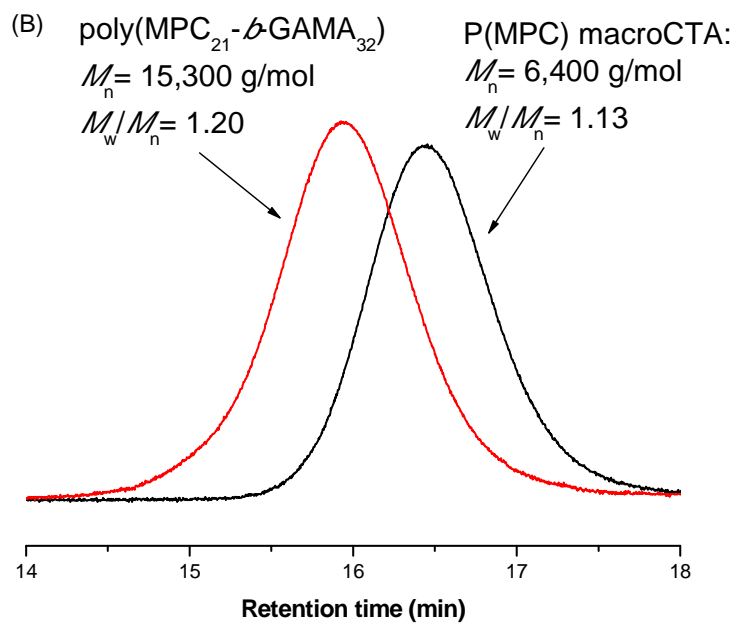
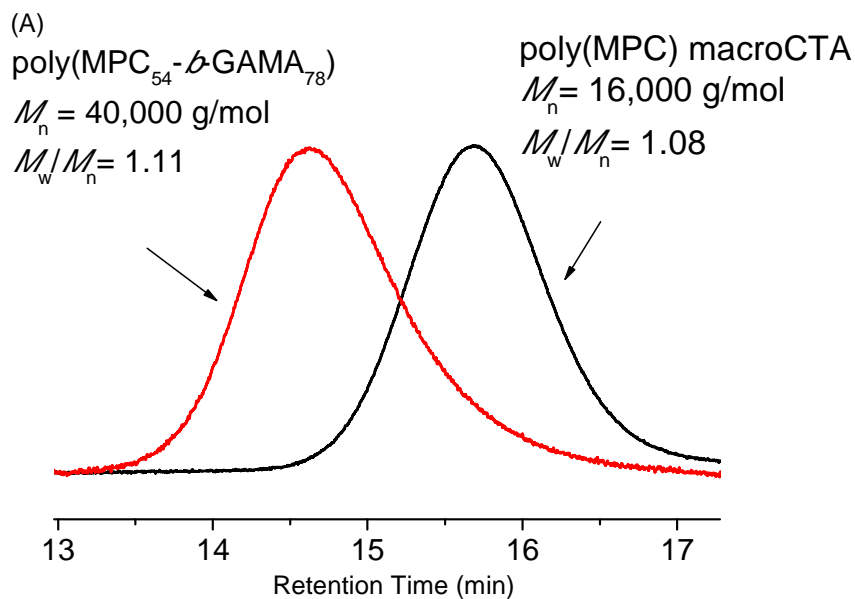


Figure S4 : Diblock copolymerization of GAMA with MPC using sequential monomer addition, forming (A) poly(MPC₅₄-*b*-GAMA₇₈) and (B) poly(MPC₂₁-*b*-GAMA₃₂)

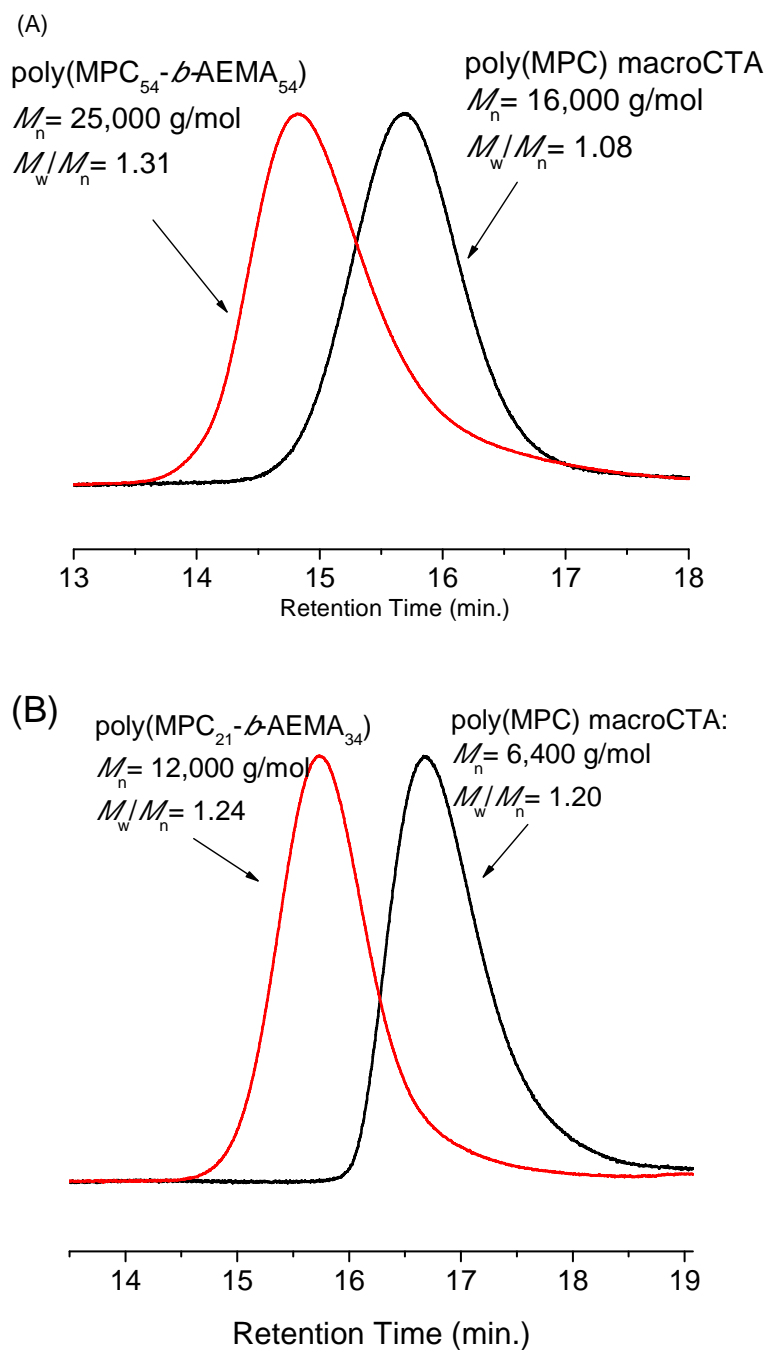


Figure S5 : Diblock copolymerization of AEMA with MPC using sequential monomer addition, forming (A) poly(MPC₅₄-*b*-AEMA₅₄) (B) poly(MPC₂₁-*b*-AEMA₃₄)

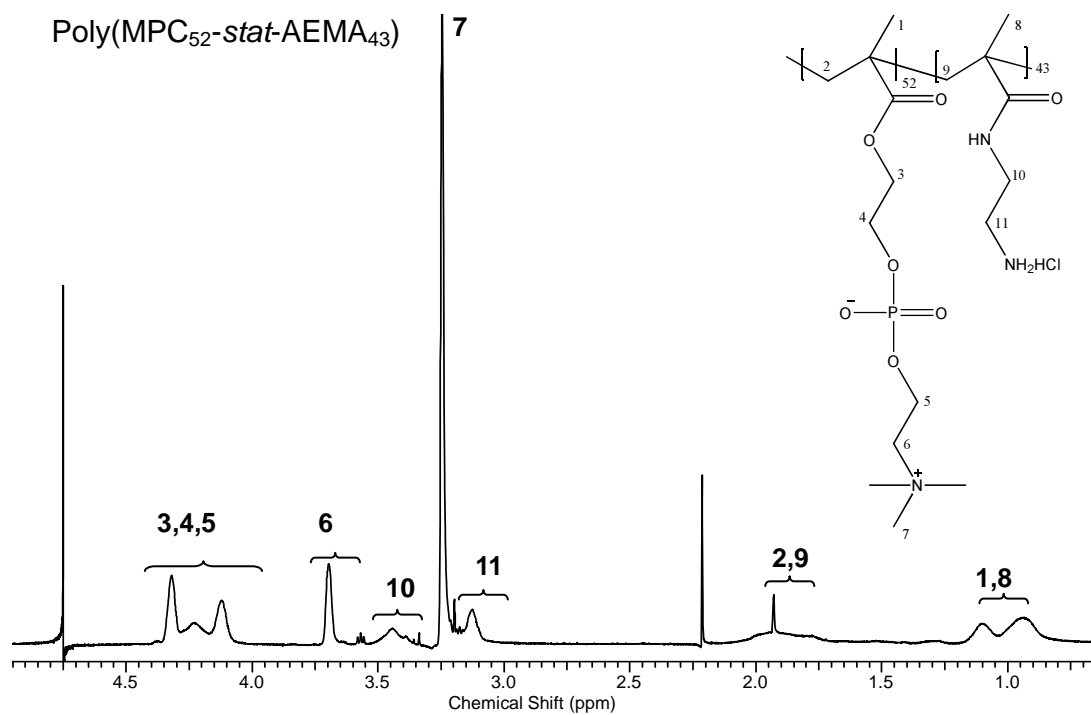


Figure S6 : Assigned ¹H NMR spectra for poly(MPC₅₂-stat-AEMA₄₃)

7 Appendix 2

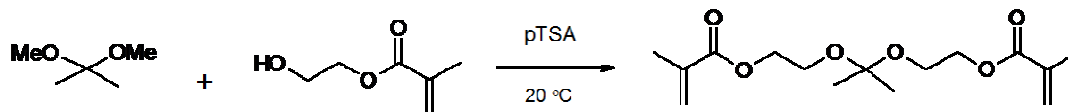


Figure S 1 : Synthesis of acid degradable cross-linker 2,2-Dimethacroyloxy-1-ethoxypropane, by reaction between Di-methoxy-propane and HEMA at 20 °C, in the presence of pTSA.

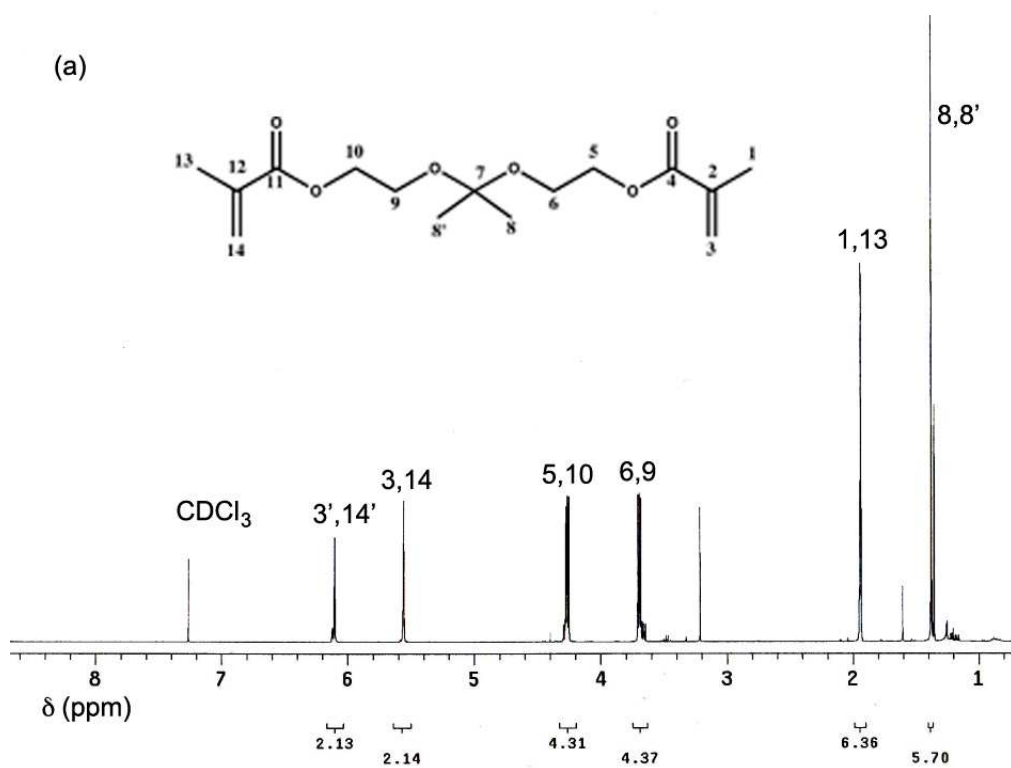


Figure S2 : ¹H NMR of acid degradable cross-linker (2,2-Dimethacroyloxy-1-ethoxypropane) in CDCl₃

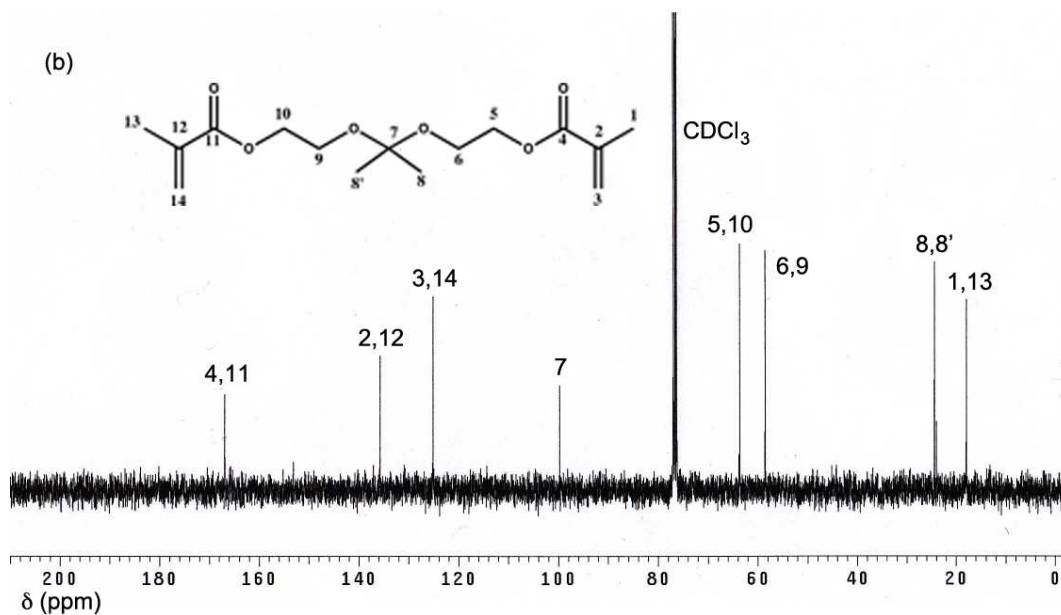


Figure S3 : ^{13}C NMR spectra of acid degradable cross-linker (2,2-Dimethacryloxy-1-ethoxypropane) in CDCl_3

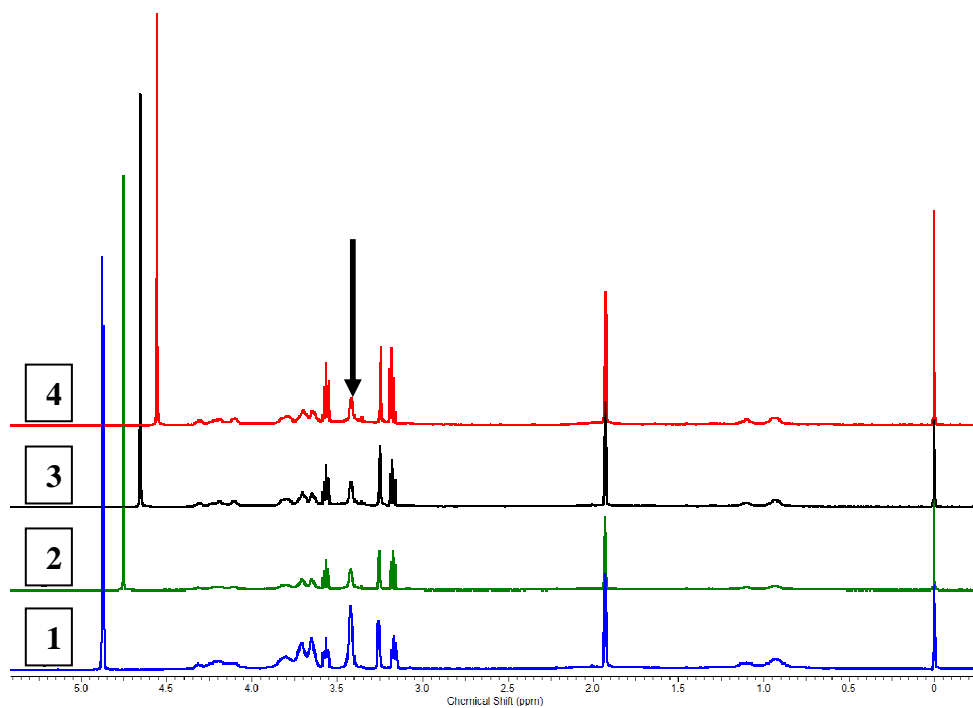


Figure S4 : VT-NMR peaks of poly($\text{MPC}_{43}\text{-}b\text{-(MeODEGM-}stat\text{-AEMA-}stat\text{-CL)}_{400}$) at temperatures below and above LCST showing the change in peak intensities of MeODEGM peaks at 1)15 °C, 2) 25°C, 3) 35 °C and 4)45 °C.

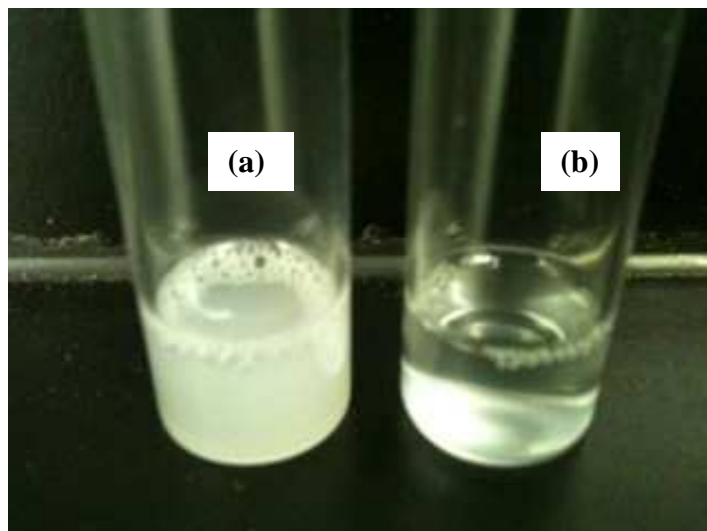


Figure S 5 : Digital photograph of 20 mg/mL aqueous solution of nanogel a) on heating above LCST and b) cooling below LCST

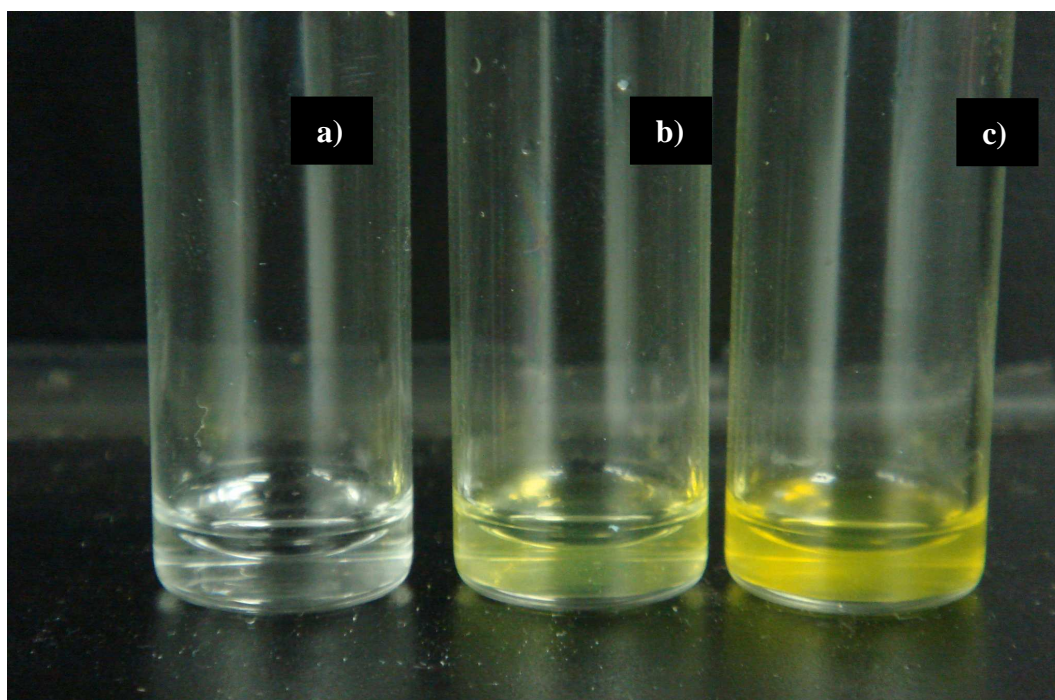


Figure S6 : Digital photograph of β -galactosidase assay conducted on aqueous solution of nanogel (Sample B) after incubation with ONPG for 4 hours showing a) negative control, b) supernatant and c) nanogel